TECHNISCHE UNIVERSITÄT MÜNCHEN

TUM School of Life Sciences

Lehrstuhl für Lebensmittel- und Bio-Prozesstechnik

A New Route for Analyzing of Casein/Hydrocolloids Interaction and Formation of Casein-based Microparticles

Yu Zhuang

Vollständiger Abdruck der von der TUM School of Life Sciences der Technischen Universität München zur Erlangung des akademischen Grades eines

Doktors der Naturwissenschaften (Dr. rer. nat.)

genehmigten Dissertation.

Vorsitzender: Prof. Dr. Michael Rychlik

Prüfende der Dissertation:

1. Prof. Dr.-Ing. Ulrich Kulozik
2. Prof. Dr. Ronald Gebhardt (RWTH Aachen)

Die Dissertation wurde am 17.02.2021 bei der Technischen Universität München eingereicht und durch die TUM School of Life Sciences am 07.09.2021 angenommen.

For improving life

Acknowledgement

I wish to express my gratitude toward all who have been involved, partially or fully, in this work during my time as a scientific researcher at the Chair of Food and Bio Process Engineering led by Prof. Dr.-Ing Ulrich Kulozik at the Technical University of Munich.

To begin with, I sincerely thank Prof. Dr. Kulozik for his unfailing faith in the project all along the course of this research. His scientific and technical guidance as well as the constructive advices on this work is greatly appreciated.

Secondly, Prof. Dr. Ronald Gebhardt, should be honored as the partner who gave birth to the success of this work. I am deeply grateful for his efforts in initiating the project, and then, providing assistance throughout the path. His extremely knowledgeable, and yet critical, supervision over the project while rendering me all the necessary freedom to explore without being lost was invaluable to say the least. Thank you, also, Prof. Gebhardt for your open-door policy to allow long discussions!

I wish to thank for everyone at the Chair of Food and Bio Process Engineering, present and past, for creating a friendly and engaging atmosphere. Without that, I could never have developed a career in science. Especially, I'd like to thank all the lab and technical colleagues, Claudia Hengst, Ilona Hager, Heidi Wohlschläger, Annette Brümmer-Rolf, Evelyn Dachmann, Michael Reitmaier and Günther Unterbuchberger, for their supports on the practical and experimental needs of this work. My thanks also go to the Werkstatt team, Christian Ederer, Franz Fraunhofer and Erich Schneider, for their excellent help on prototyping, as well as for their cordial friendship. Sabine Grabbe, Sabine Becker and Friederike Schöpflin, thank you very much for lending hand on the administrative and IT matters. Special thanks are due for my past fellow students in their uplifting moral support and team spirit.

I also would like to thank my former office colleagues, Mirjana Stulac Wolfgang Holzmüller, Seronei Chelulei Cheison, Elisabeth Eschlbeck and Joseph Dumpler, for creating a friendly and motivative atmosphere during these years. Jannika Dombrowski, Daniel Saalfeld and Tim Steinhauer, thank you for sharing your specialties in protein/separation technology.

For being physically fit, I must thank my jogging mates, Magdalena Wolz and Yuhong Mao. They kept me going!

I am grateful to Julia Sterr from Fraunhofer Institute IVV for our collaboration on the Raman spectroscopy. Julia was always willing and ready to pitch in and answer my questions.

Also, I am very grateful for the friends I have made during the years at Freising/Munich, as well as those whom I do not list for the fear of forgetting someone. Nevertheless, my big thanks for everything!

Likewise, my biggest thanks should go to my parents among many unsung heroes behind the scene. They lovingly raised, nurtured and supported me along the way, including studying abroad and developing my career. It is because of their sacrifice and love that I can now proudly stand on the podium to continue taking steps for reaching my ideals.

Last but not least, Kun, THANK YOU for entering my life building a warm relationship together. I deeply appreciated your patience, selflessness and wisdom at the time when we faced challenges in life. I feel enormously fortunate for being partners with you to move toward hand-in-hand for a delightful future.

Contents

Abbreviations and symbols

A_2	$mol \cdot L^2/g^2$	second virial coefficient
AFM	/	atomic force microscopy
AMD	/	acidified milk drinks
ATR	/	attenuated total reflection
ß	/	coherence factor
ß-Lg	/	ß-lactoglobulin
Γ	s^{-1}	decay rate (decay constant)
c	mg/mL	concentration
c_p	mg/mL	protein concentration
CCP	/	colloidal calcium phosphates
CM	/	casein micelle
CMC	/	carboxymethyl cellulose
Δc/Δx	/	concentration gradient
d	mm	diameter
D	m^2/s	diffusion coefficient
DE	/	esterification degree
D_{eff}	m^2/s	effective diffusion coefficient
DLS	/	dynamic light scattering
4-DPS	/	4,4´-dithiodipyridine
FT-IR	/	Fourier-transform infrared spectroscopy
G	J	Gibbs free energy
GMP	/	glycomacropeptide
GISAXS	/	Grazing-Incidence Small-Angle X-ray Scattering
H	J	enthalpy

HM	/	high-methoxyl
HPLC	/	High-performance liquid chromatography
E	J	energy input
E_v	J	energy density
I	/	Intensity of scattered light
IEP	/	isoelectric point
η	Pa·s	viscosity of medium
θ	°	scattering angle
K	/	optical constant
k_B	$m^2 \cdot kg/K \cdot s^2$	Boltzmann constant
kD	/	kilo Dalton
λ	mm	Wavelength
LM	/	low-methoxyl
M_w	g/mol	molecular weight
n	rev/s	rotational speed
n_0	/	refractive index
N_A	/	Avogadro's number
ρ	g/cm^3	density
p	Pa	pressure
R_g	nm	radius of gyration
R_H	nm	hydrodynamic radius
R_T	cm^{-1}	Rayleight ratio for toluene
RP-HPLC	/	Reversed Phase High Performance Liquid Chromatography
q	1/Å	scattering vector
S	J/(K·mol)	specific entropy

T	°C	temperature
t	s	time
τ	s	delay time
SEM	/	scanning electron microscope
SLS	/	static light scattering
W/W	/	water-in-water
ω	rad/s	angular velocity

1 General introduction

Investigation on the structure of milk proteins becomes attractive in recent years because of the easy accessibility and unique functional properties of the material for novel food or pharmaceutical innovations. Milk proteins consist of various components such as caseins, whey proteins, lactoferrin, and serum albumin. Caseins, a major protein in milk, has been extensively studied as sterically stabilized association colloids in the past. Its micellar form, casein micelle (CM), has unique physiochemical functionalities which could be used for various applications in the food or pharmaceutical products as building blocks or an encapsulation carrier. Common processes including heating, gelation, drying and/or membranes separation can trigger the interactions between CM and other colloidal polymers (e.g., other milk proteins or carbohydrates). From which promising new structures could be generated.

CM can form either associative or segregative complexes with other polymers depending on the pre-defined pH and ionic concentration in the colloidal system. Co-polymers type, pH, polymers, and salt concentration are among the key factors contributing to unique properties of the newly formed structure, which leads to different applications (Belitz et al., 2009). For example, the firmness of yoghurt gels is associated with the ß-lactoglobulin denaturation, as the covalent bonding to the CM surface decreases with its hydrophobicity (Belitz et al., 2009).

1.1 Caseins

Caseins are the major phosphoproteins (approximately 80%) in milk that assemble into a micellar state known as CM (Dalgleish, 1998; Dalgleish & Corredig, 2012; Holt & Horne, 1996). CM consists of α_{S1}-, α_{S2}-, β- and κ-caseins (Dalgleish, 2011; Fox & Brodkorb, 2008). Their proportions in the native CM vary in an approximate ratio of 4:1:4:1 by weight (Schmidt, 1982). In a CM, κ-casein is found mainly on the surface of a hairy-like layer denominated by glycomacropeptide (GMP). Its brush structure consists of negatively charged polyelectrolyte (de Kruif & Zhulina, 1996) attributing the CM stability through steric and electrostatic interactions. Colloidal calcium phosphates (CCP) also play an important role in holding CM together (Horne, 2006). Different in properties and compositions, casein fractions can be readily separated using SDS-PAGE or HPLC (Fox & Brodkorb, 2008; Veloso, et al., 2002).

The size of a native CM in milk ranges from 100 nm to 200 nm averaging 140 nm (Belitz et al., 2009). The size depends strongly on the mass of casein monomers, especially the amount of κ-casein (Dalgleish & Corredig, 2012). The proportion of the casein monomers in CM is greatly affected by milk source or micellar sizes. Tab.1-1 shows the ratio as a function of centrifugation time. Smaller CMs resulted from longer centrifugation times had lower α_{S1}- to α_{S2}-casein ratios but higher ß-casein proportions.

Tab. 1-1. Proportion and size of CM isolated by centrifugation (Belitz et al., 2009).

Centrifugation time (min)[a]	Composition of the sediment (%)			
	α_{S1}-casein	α_{S2}-casein	β-casein	κ-caseins
0[b]	50	32	15	3
0-7.5	47	34	16	3
7.5-15	46	32	18	4
15-30	45	31	20	4
39-60	42	29	26	3
Serum casein	39	23	33	5

[a] centrifugation speed 10^5 x g

[b] Isoelectric casein

Soluble caseins assemble themselves into CM via hydrophobic interaction, electrostatic interactions, and hydrogen bonds (Horne, 2002). Fig. 1-1 displays a CM image under a high-resolution field-emission SEM.

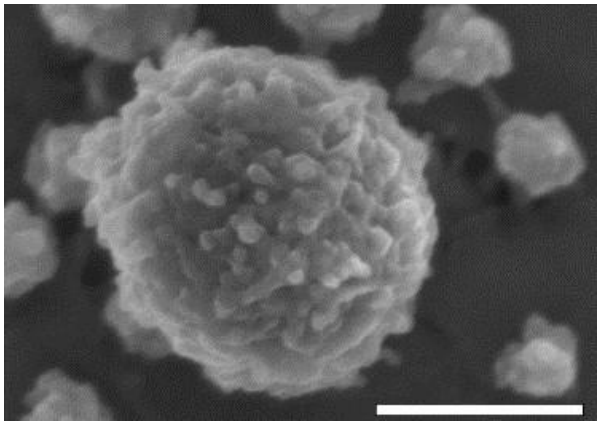

Fig. 1-1: CM under SEM. Scale bar: 200 nm (Dalgleish et al., 2004).

Although individual caseins vary on solubility and stability in aqueous environment, CMs generally remain in a sterically stable colloidal state in native milk (Bingham, 1971; Dalgleish, 2011). Upon disturbance by external factors such as temperature, pH, ionic strength and enzymatic changes, the micellar structure of a CM may dissociate and

release individual caseins to form gels (Dalgleish & Law, 1988; 1989; Dalgleish & Parker, 1980; Dalgleish et al., 1981; Horne, 1998; Salvatore et al., 2011). And that is the theory of formation for solid products, e.g., cheese and yogurt, made from milk.

1.1.1 Structure of casein micelle

Without a universally accepted definition on the structure of CM in place, numerous models were proposed (Bouchoux et al., 2010; de Kruif & Holt, 2003; Holt et al., 2003; Horne, 1998).

The very first CM model, known as Coat-Core model, was reported in 1965 by Waugh and Nobel. It emphasizes a caseinate core formed with α_{S1}- and ß-casein after aggregation at presence of calcium ions and followed by an evenly spreading κ-casein monomers on the surface to prevent caseinate precipitation. The model suggests that the size of CM is determined by the availability of κ-casein which can explain the lyophilic properties of casein colloids and the accessibility of κ-casein to chymosin (Jenness et al., 1988).

Later studies proposed a ‘sub-micelle’ model which theorizes CM to be composited of spherical subunits (or sub-micelles) ranging from 12 to 15 nm. The hydrophobicity between proteins and calcium phosphate linkages plays a key role in binding the sub-micelles together into a larger micelle (Fox, 1989; Jenness et al., 1988; Walstra, 1999). Fig. 1-2 schematically illustrates a sub-micelle model with protruding c-terminals of κ-casein chain.

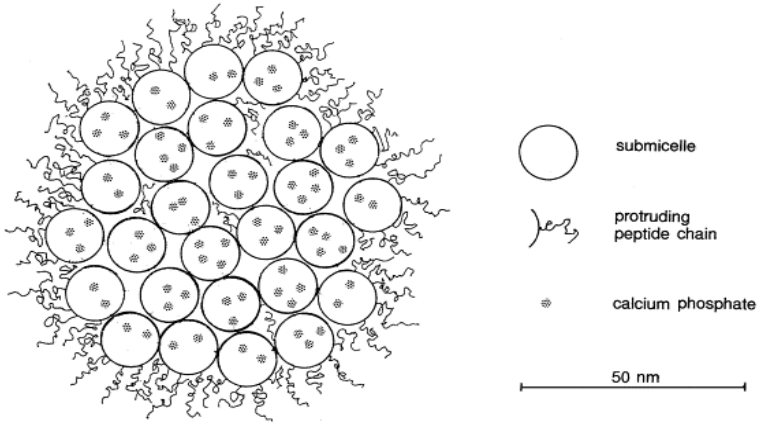

Fig. 1-2: Sub-micelle model of a CM (Walstra, 1999).

The ‘sub-micelle’ model dominated the discussion on CM structure until a new model was proposed and reported in the 1990s which reveals in detail the internal structure

of CM (Holt & Horne, 1996; Horne, 1998). The latest ‘nanocluster’ model and its later promoted ‘dual binding model’ describe the α_{S1}-, α_{S2}-, ß-casein and κ-casein to be self-associated attributing for the most part to the hydrophobic interaction and electrostatic repulsion among CMs. In it, the hydrophobic interaction between various caseins is the driving force for the CM formation via linkage between casein monomers and CCP. On the other hand, the electrostatic repulsion exerts major impacts on the sizes of CM as κ-casein forms a hairy layer on the surface of CM (Horne, 1998). Fig. 1-3 shows a representation of the nanocluster model.

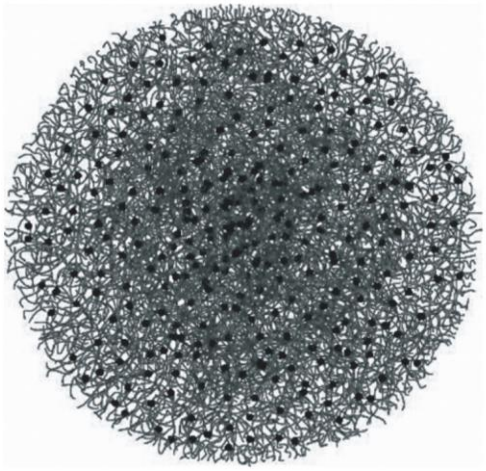

Fig. 1-3: Schematic representation of nanocluster model for CM. The casein monomers are thread-like and dark circles are calcium phosphate nanoclusters (de Kruif & Holt, 2003; Qi, 2007).

Additionally, the nanocluster model recognizes casein monomers as amphiphilic block copolymers consisting of blocks with high levels of hydrophobic or hydrophilic amino acid residues (Horne, 2002), as well as the surface behavior of casein monomers and the hydrophobic interactions between proteins that are critical for the CM formation (Holt et al., 2003).

Based on above theories, a ‘sponge’ model was developed to refine the structure by introducing voids in CM interior (Bouchoux et al., 2010; Dalgleish & Corredig, 2012). CMs are generally considered soft matters deformable by compressive force such as the osmotic stress presented in a concentration or filtration process. ß-casein molecules are associated with CCP and hydrophobically bonded to other caseins, while κ-casein and other casein macropeptide chains situate on the surface of CM. The parts consisting of these proteins and CCPs are resistant to deformation constituting the

'hard' region, while the other regions compressible with 'voids' in a micelle. A sponge model of CM with 200 nm in diameter, as shown in Fig. 1-4, depicts the structure formed by caseins/calcium-phosphate hard regions and voids filled by water or solvent (Bouchoux et al., 2010). This model helps to explain the porosity of CM and the impact of osmotic stress on the CM structure.

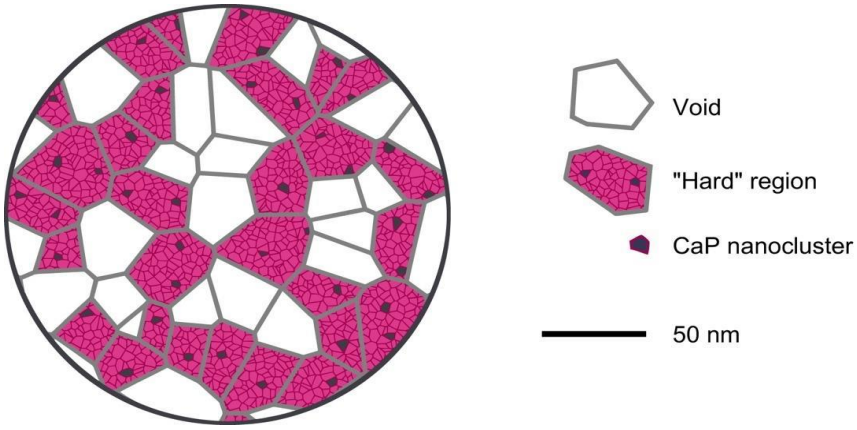

Fig. 1-4: Schematic diagram of a CM containing of protein-rich regions (purple), calcium phosphate nanoclusters (black), and voids filled by water or solvent (white) (Bouchoux et al., 2010).

1.1.2 Effect of pH on casein micelle stability

In general, CM is a colloid complex remains stable when exposed to minor heat or pH changes, as compared to other milk proteins (Walstra, 1990). The hydrophobic interactions and CCPs play a key role in holding the caseins together in a micellar state. On the exterior, κ-casein and surface electro-steric charges help maintain a distance between micelles preventing aggregation of the CMs (Horne, 1998; Walstra, 1990; Qi, 2007). Altered environmental conditions may cause CMs to lose their integrity due to collapse of the κ-casein 'hairy layer' leading to aggregations (i.e., formation of gel) by electro-steric attraction (de Kruif, 1999; Tuinier & de Kruif, 2002; Walstra, 1990).

The surface of CM is negatively charged at pH 6.7, as the isoelectric point (IEP) of CM is pH 4.6 (Fox, 1989). Thus, lowering pH close to its IEP will result in instability of CM (Fox, 2003; Walstra, 1990). Fig. 1-5 demonstrates the structural changes of CM as pH decreases from 6.8 to 5.0 (Kirchmeier, 1973). At first, the decrease in pH results in reduction of net negative charge on CMs leading to a decline on the electrostatic repulsion between CMs. At this stage, only a small amount of CCP is dissolved above

pH 6.0 allowing the internal structure of CMs remain largely intact (e.g., size) (Kirchmeier, 1973; Tuinier & de Kruif, 2002). However, further lowering in pH begins to cause collapse of the κ-casein 'hairy layer' (de Kruif & Holt, 2003) contributing to the declines in electrostatic repulsion and steric stabilization. Meanwhile, CCP within the CMs starts dissolving at pH 5.0 (Dalgleish & Law, 1988). Below pH 5.0, the net charge of CMs is close to 0, and as pH approaches IEP the van der Waals force between the micelles increases (Dalgleish et al., 2004). Once the steric distance between CMs for maintaining the structural stability is much shortened, reduction in electrostatic repulsion can cause aggregation.

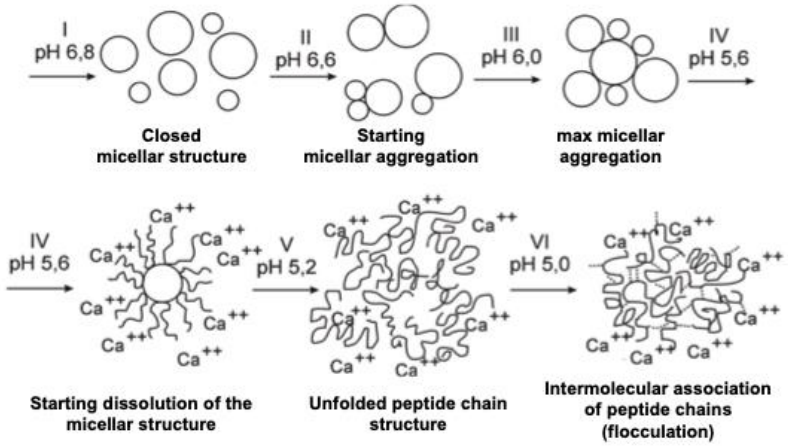

Fig. 1-5: Structural changes on CMs induced by gradual acidification of surrounding solution (reproduced from Kirchmeier, 1973).

Aggregation of caseins is an irreversible process. A constituted 3D gel network is formed by the cluster of aggregated strands. Upon further lowering pH to IEP, intermolecular linkage between peptide chains increases the hydrodynamic radius of CM (Liu & Guo, 2008). Fig. 1-6 schematically shows the impact of pH on the structure of CM (Gonzalez-Jordan et al., 2015).

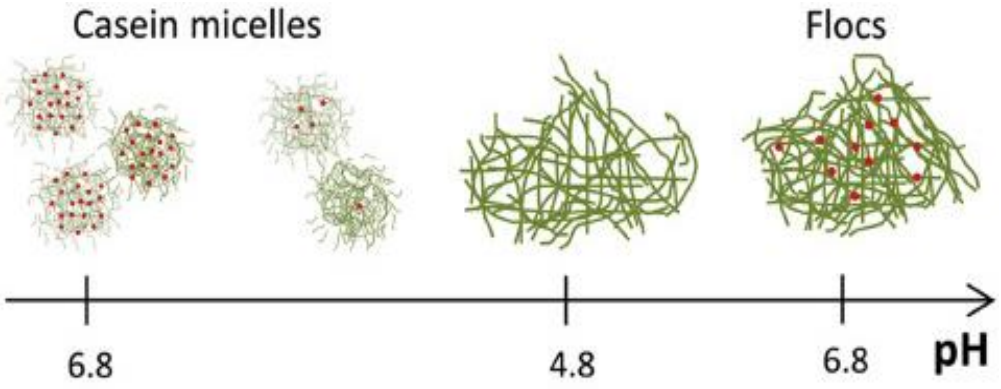

Fig. 1-6: Schematic representation of structural changes of CMs when pH is altered. Caseins (green threads) form micelle with CCP clusters (red dots). Lowering pH to 4.6 dissociates the micellar structure and releases CCP from CMs. Flocculation is formed at pH=4.8, and remain in system after pH returns to 6.8 (Gonzalez-Jordan et al., 2015).

Before an acidified condition is reached, adding hydrocolloids, e.g., anionic polysaccharides such as, pectin, carboxymethyl cellulose (CMC) or sodium alginate, could prevent the formation of aggregation and stabilize the colloidal system (Delben & Stefancich, 1997; Maroziene & de Kruif, 2000; Ntazinda et al., 2014; Tuinier & de Kruif, 2002; Wu et al., 2013). The mechanisms of stabilizing behaviors will be discussed in detail in Chapter 1.1.5.

1.1.3 Effect of calcium concentration on casein micelle stability

Individual caseins (α_{S1}-, α_{S2}- and ß-casein) are held together by calcium phosphate linkages in native milk. Despite the insensitivity to soluble calcium, κ-casein interacts with other caseins and forms a stable colloidal micellar state (Qi, 2007). Changing calcium concentration leads to disintegration (at low Ca^{2+} concentration) or large aggregates (at high Ca^{2+} concentration) of CM (Holt, 1992; Horne, 1998; Knoop et al., 1979; Lin et al., 2002). Grimley and co-worker evaluated CM stability at a reduced calcium level of skimmed milk down to 51% using ion-exchange resin (Grimley et al., 2010). Diameter of CM increases with calcium removal from skimmed milk while ethanol stability increases to nearly 100%. This process is reversible after calcium is added back to solution resulting in restoration of CM diameter (Grimley et al., 2010). In another study, Philippe and co-worker examined the effect of calcium concentration increase together with other cations in milk. It revealed that most of the added calcium is linked to CMs, and at the same time, the inorganic phosphate and citrate ions also begin to associate with CMs causing a decreased heat stability (Philippe et al., 2005).

The presence of calcium also modifies structural properties and interactions among CMs. A GISAXS and AFM study on the thin film containing CM indicated that the calcium addition weakens the stabilizing effect of κ-casein and reinforces the attraction between the neighboring CMs. This is consistent with the observation in solution where the association of CM and formation of large aggregates occurs when calcium is added (Muller-Buschbaum et al., 2007). Nevertheless, other environmental factors such as temperature, acidification or addition of cations also exert influences on the CM stability through ionic or micellar calcium concentration changes (Gaucheron, 2005).

1.1.4 Interactions of casein and hydrocolloids

1.1.4.1 Casein and ß-lactoglobulin (protein-protein) interaction

As major proteins in milk, CM and ß-lactoglobulin (ß-Lg) attribute the functional properties of milk products in various applications. Under certain circumstances (e.g., heat), CM and ß-Lg interact and alter the physiochemical properties of the material containing them.

Molecular structure of ß-lactoglobulin

ß-Lg, one of the major whey proteins in globular form, constitutes approximately 10% of total milk protein (Boland, 2011; Korhonen, 2011). Commonly, ß-Lg consists of 162 residues with a M_w of approx. 18.4 kDa (Lozano et al., 2008). It exists in both dimeric and monomeric forms depending on the surrounding pH. The dimeric form is dominantly found between pH 5.2 (i.e., IEP) and pH 7.5, while the monomers extensively under extremely acidic (below pH 3) or alkali (above pH 8) conditions (Apenten et al., 2002). Previous studies indicated ß-Lg to be a highly structured protein with orderly secondary structures, such as α-helix and ß-sheets, as well as some helicoidal turns in between pH 2 and 6 (Fox, 2008; Lametti et al., 1998; Manderson et al., 1999). And, thermal treatment can introduce intermolecular disulfide bonds in a ß-Lg-rich whey protein solution creating aggregation or gelation (Livney et al., 2003). Processing temperature and protein concentration are critical in the aggregation kinetics while pH on the structure and properties of a heat-denatured ß-Lg gel (Ikeda & Morris, 2002; Irene Boye et al., 2000; la Fuente et al., 2002; Schokker et al., 1999; Vittayanont et al., 2002).

Hence, the biological role of ß-Lg in human nutrition is attributed mainly to its binding capability of retinol or fatty acids. For example, ß-Lg is able to protect and deliver

retinol (i.e., vitamin A) to the small intestines for transferring to other retinol-binding proteins with such binding property (Fox, 2008). On the other hand, due to its high allergenic potential in humans, some proteolysis approaches produced ß-Lg-free products for infant formulas (Mao et al., 2018; Selo et al., 1999).

Structural interaction between casein and ß-lactoglobulin

The interactions between CM and ß-Lg were generally studied under heat treatment. Heat-denatured ß-Lg forms a complex with CM mainly through disulfide bonds. Moderate heating at a temperature ranging from 75 to 90°C triggers the formation of CM/ß-Lg complexes through binding of κ-casein and ß-Lg (Dalgleish et al., 1997). ß-Lg concentration in solution is crucial for such interaction because sufficient sites are essential for disulfide formation. pH, on the other hand, also affects the association between ß-Lg and CM, as indicated by the quantitative polyacrylamide gel electrophoresis studies (Oldfield et al., 2000). Reduced pH mitigates the activation energy of ß-Lg which invariably limits the CM/ß-Lg complex formation (Oldfield et al., 2000).

Consequently, salts or ionic strength in solution exerts strong impact on the association of CM/ß-Lg complex induced by heat. Increased calcium in solution reduces the amount of heat-dissociated κ-casein resulting in fewer complexes formed between CM and ß-Lg (Singh & Fox, 1987). Any change in concentration of calcium ions affects the integrity of CM. Furthermore, the interaction of the solubilized caseins with ß-Lg is enhanced mainly by the preferential binding between them through the release of calcium phosphate clusters in CM (Pouliot et al., 1989).

1.1.4.2 Casein and pectin (protein-carbohydrate) interaction

Pectin is a main component in plant cell walls. Generally extracted from apple pomace and citrus peels, commercial pectin products are classified by degree of esterification (DE) (BeMiller, 2009). Pectin is routinely used in food processing as a gelling, stabilizing or thickening agent (BeMiller, 2009; Lam et al., 2007). Associated with CM, it can deter undesired protein aggregation and stabilize acidified beverages formulated with milk (Maroziene & de Kruif, 2000).

Molecular structure of pectin

A linear chain polysaccharide, pectin consists of α-(1-4) linked D-galacturonic acid units with hydrophobic side chains of occasional neutral sugar residues (rhamnose)

(Endreß & Christensen, 2009). As shown in Fig. 1-7, pectin is capable of connecting carboxylic and hydroxylic groups. DE of pectin is defined as the ratio of esterified galacturonic acid groups to total galacturonic acid groups. Accordingly, the industrial suppliers classify pectin products into high-methoxyl (HM) -pectin (i.e., esterified carboxyl groups > 50%), or low-methoxyl (LM) -pectin (i.e., esterified carboxyl groups < 50%) (BeMiller, 2009; Endreß & Christensen, 2009; Flutto, 2003).

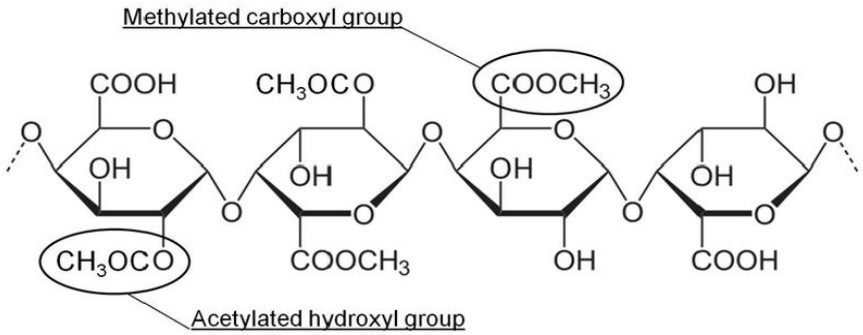

Fig. 1-7: A pectin molecule with attached methyl and acetyl groups (Schmidt, 2015).

Being a member of anionic polysaccharide family, pectin is often used as a stabilizer in acidified milk drinks (Endreß & Christensen, 2009). It prevents flocculation of milk proteins and maintains the desirable characteristics of the products (Maroziene & de Kruif, 2000). There are successful examples showing the stabilizing effect of pectin in low-fat yoghurt, stirred yogurt, and the flavored acidified milk drinks with fruits (BeMiller, 2009; Jensen et al., 2010; Laurent & Boulenguer, 2003). HM-pectin is more efficient in stabilizing protein solution than LM-pectin (Lam et al., 2007). A possible explanation for the result is that HM-pectin had a relatively low affinity to the surface of protein particles due to the high degree of methyl esterification. Blocking these low affinity areas on HM-pectin that may protrude from the protein surface as loops and dangling tails created a mechanism termed as ‘steric stabilization’ (BeMiller, 2009; Flutto, 2003; Lam et al., 2007).

Most recent studies suggested pectin be mixed with other ingredients to improve flavor, texture and other sensory perceptions for various food products (Lam et al., 2007; Mao et al., 2014; Mao et al., 2013; Sirijariyawat et al., 2012; Van Buggenhout et al., 2009).

Pectinase, an enzyme extracted from *Aspergillus niger*, can break down polysaccharide structure of pectin. It consists of pectin methylesterase, which demethylates pectin, and polygalacturonase, which hydrolyzes α-D-1,4-galacturonide. Pectinase is commonly used in fruit juice or wine production to reduce viscosity and turbidity of the

liquid material (Endreß & Christensen, 2009; Flutto, 2003). The optimum of pectinase activity is pH 2.5-3.5 at 40-55°C.

Functional properties of pectin

A well-known feature of pectin is its gel-forming in the presence of acid and/or sugar as in making jams or preserves (Flutto, 2003). DE is the key factor in pectin gel formation. The intramolecular interactions including electrostatic, van der Waals and hydrogen bonding play key roles in the establishment of the complex gel network (Endreß & Christensen, 2009; Flutto, 2003). In particular, the electrostatic interaction between cations and negatively charged cavities formed by pectin polymer chains is critical in the gel formation (BeMiller, 2009).

Besides DE, the location of ester group on a pectin chain also determines the functionality of the product (Endreß & Christensen, 2009). Varying processing conditions such as ionic strength, pH and temperature affects the intermolecular interactions as well (Fraeye et al., 2007; 2009). For instance, pH greatly influences the surface charge distribution on the ester methyl unit, and temperature on the intramolecular hydrophobic interactions and hydrogen bonding (Oakenfull & Scott, 1984; Thakur et al., 2009). Pectin is negatively charged in between pH 7.0 and 3.0. At low pH, the ionization of carboxylate groups is suppressed resulting in a reduction on the hydration of carboxylic acid. This, hence, leads to diminished electrostatic repulsion between pectin molecules (Flutto, 2003; Oakenfull, 1991; Sriamornsak, 2003) with gelation as a result (Sriamornsak, 2003). Depending on DE, the molecular structure of pectin is most stable at around pH 4. Heating at neutral pH or alkaline condition can start degradation of the pectin structure (Rolin, 1993; Sriamornsak, 2003).

Thermodynamic interaction between casein micelle and pectin

Protein-polysaccharide interactions are normally subject to the thermodynamics of the system and directly govern the stability and rheology of a food product made with a designed purpose based on them (Dickinson & McClements, 1996).

Mixing proteins and polysaccharides in a solution triggers either the segregative or associative interaction between the two biopolymers (Dickinson & McClements, 1996; Syrbe et al., 1998). Either of the interactions can bring about three possible outcomes: co-solubility (i.e., miscibility), incompatibility (i.e., segregates interactions), or complex coacervation (i.e., complex or associative interaction) on the system (de Kruif & Tuinier,

2001; Doublier et al., 2000; Syrbe et al., 1998). The protein-polysaccharide complex can become soluble or be led to an aggregative phase separation. On the other hand, if the protein and the polysaccharide carry a same charge, the thermodynamic incompatibility on the system can result in phase separation (Dickinson & McClements, 1996).

Compatibility/incompatibility between proteins and polysaccharides is mainly determined by the difference between the entropic and enthalpic contributions in a biopolymer mixture (de Kruif & Tuinier, 2001; Doublier et al., 2000). An associative phase separation is commonly found in a binary polymer system that favors a protein-polysaccharide association over a polymer-solvent interaction. This normally occurs when the protein and polysaccharide are oppositely charged, and the complexes can be formed either remaining soluble in a solvent or in an aggregative phase separation. In an aggregative phase separation, the system known as coacervate is composed of a solvent-rich phase with a few polymers and a biopolymer-rich phase (Clark, 2000; Doublier et al., 2000). Fig. 1-8 shows two kinds of phase separations between two biopolymers.

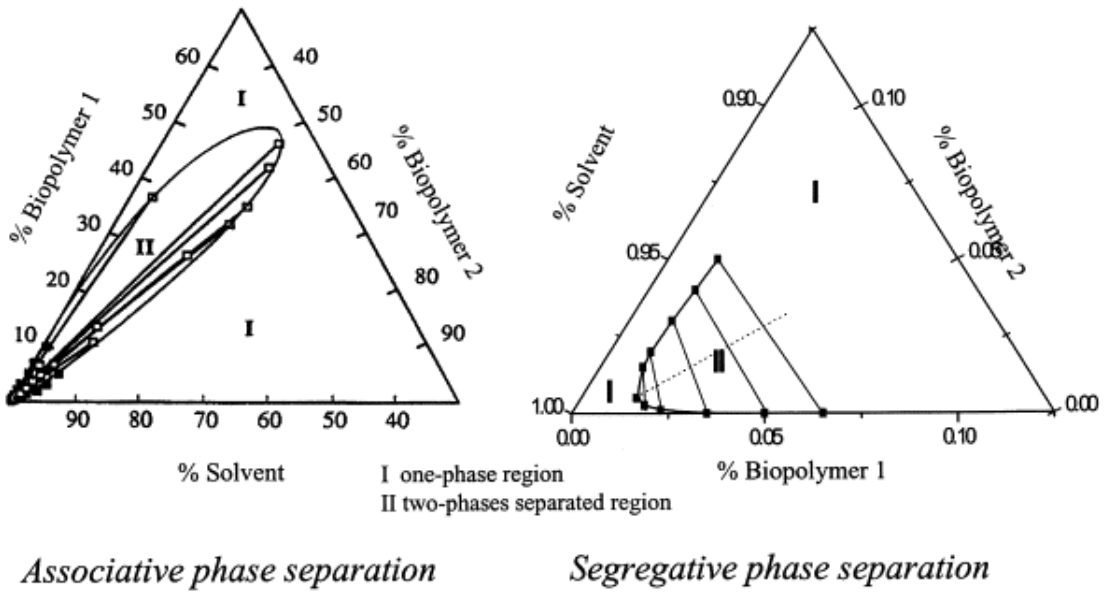

Fig. 1-8: Schematic associative and segregative phase separations of two biopolymers (protein/polysaccharide) (Doublier et al., 2000).

Thermodynamic incompatibility (or segregative phase separation) of a mixture takes place when two mixed biopolymers repulse each other. If one polymer (protein or polysaccharide) is in favor of the solvent, a two-phase system enriched with one polymer

in each phase is formed (Doublier et al., 2000). Thermodynamic incompatibility generally happens when the protein and polysaccharide in a system carrying same charges (de Kruif & Tuinier, 2001; Doublier et al., 2000).

The miscibility of a polymer with another substance is determined by the combination of an enthalpic and an entropic factor in the following formula:

$$\Delta G_m = \Delta H_m - T\Delta S_m \quad (1)$$

Where, ΔG_m is the Gibbs free energy; ΔH_m, the enthalpy of the two mixing components; and, $T\Delta S_m$, the entropy of mixing ΔS_m at temperature T (Clark, 2000). In a binary system, the formation of biopolymer-biopolymer complex take places spontaneously when ΔG_m decreases, i.e., $\Delta G_m<0$ (Clark, 2000). Changes in ΔG_m also link to system stability. In particular, the complex formation between the weakly charged polyelectrolytes is driven by negative ΔH_m due to electrostatic attraction with the oppositely charged ions while entropy release plays only a minor role. On the other hand, weak energy interactions, especially hydrogen bonding and hydrophobic interactions, can also significantly contribute to the complex formation between the oppositely charged biopolymers (Clark, 2000; Doublier et al., 2000). The same reasons were used to explain the segregative and associative phase separations based on entropy and enthalpy considerations in a casein/pectin system (Maroziene & de Kruif, 2000; Tuinier & de Kruif, 2002). Thermodynamic incompatibility was identified as the driving force leading to the phase separation of CM/pectin at neutral pH when both polymers are negatively charged (de Kruif & Tuinier, 2001; Maroziene & de Kruif, 2000).

The stability of a biopolymer complex also relies on the balance between the attractive (i.e., covalent bonds, van der Waals interaction, hydrophobic interactions, and hydrogen bonds) and the repulsive forces (i.e., steric, electrostatic, and hydrophilic repulsions).

Concentration of biopolymers significantly determines the form of thermodynamic incompatibility. Protein and polysaccharide may coexist in a single phase (miscibility) in domains in which they mutually exclude each other, or segregate into different phases when polymer the concentration exceeds the critical threshold (Doublier et al., 2000; Maroziene & de Kruif, 2000). The conditions that trigger thermodynamic incompatibility (eventually lead to phase separation) vary by the types of biopolymer. It depends greatly on specific structural and compositional features, such as molecular weight,

electrostatic charges and molecular conformation of the biomolecules (Grinberg & Tolstoguzov, 1997).

On polymers dissimilar in shape and structure, the segregative interaction reduces their concentration near the interface, as so-called depletion interaction (de Kruif & Tuinier, 2001; Maroziene & de Kruif, 2000). The concept was first introduced in early 50s (Asakura & Oosawa, 1954). It indicated that two parallel plates attract each other when immersed in a polymer solution containing non-adsorbing polymers causing by the expulsion of polysaccharides from the interstitial space between colloidal particles due to the restricted volume and osmotic pressures. The authors further proposed two possible mechanisms: 1) addition of molecules reduced the configurational entropy when polymer penetrates the space between the interacting surfaces, and 2) segments of added polymer interacted with segments of another polymer chains that belonged to the granular molecules leading to an increase in the local 'osmotic pressure'. Fig. 1-9 illustrates the depletion interaction mechanism on globular proteins and polysaccharide molecules in solution.

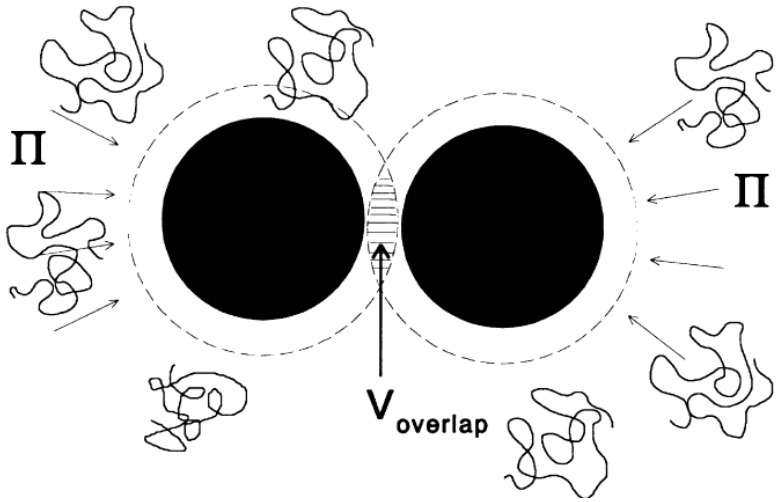

Fig. 1-9: Schematic diagram of depletion interaction between two globular proteins and polysaccharide molecules in solution (Maroziene & de Kruif, 2000).

No specific molecular interaction occurs in the excluded volume from the spherical protein surface. This is also called an effective excluded (depletion) layer, where the osmotic pressure, ∏, generated by the polymer segments is smaller than the one in the bulk solution. Two spherical particles share the depletion volume ($V_{overlap}$) when Brownian motion brings about the contact among these molecules. An increase on

$V_{overlap}$ is associated with the lowering of free energy in the system by $\Delta G = -\prod V_{overlap}$. Therefore, a collection of phase separated biomolecules is entropically advantageous (de Kruif & Tuinier, 2001; Maroziene & de Kruif, 2000). For pectin and CM, pectin does not adsorb onto the CMs at a neutral pH because of the electrostatic repulsion which results in a segregative phase separation and creation of a depletion layer around CM. Depletion interactions lead to flocculation of CM forming sediment in the solution leaving pectin in the supernatant (Maroziene & de Kruif, 2000).

Segregative phase separations are commonly observed in mixtures of hydrophilic biopolymers. Recent studies expended this phenomenon as a base for formation of water-in-water (W/W) emulsions (Capron et al., 2001; Esquena, 2016; Kasapis et al.,1993). A W/W emulsion consists of droplets of two aqueous phase. Of which, one disperses into the other that contains incompatible hydrophilic polymers (Esquena, 2016). Studies on W/W emulsions attract substantial interests for scientific research and new technology development (Antonov & Moldenaers, 2011; Antonov et al., 1996; Cesi et al., 1996; Fang et al., 2006). Mixing or mechanical agitation is generally required in a W/W emulsion preparation (Esquena, 2016). However, a major challenge for the system lies in a lasting stability. The suspended particles are susceptible to rapid coalescence or flocculation causing irreversible phase separation (Capron et al., 2001; Esquena, 2016). By enhancing or maintaining the adsorption of particles at the water-water interface, a secure colloidal system can be obtained (Firoozmand et al., 2009; Nicolai & Murray, 2017; Poortinga, 2008). In addition, adding other functional particles, including ß-Lg microgels as an effective surfactant, can also improve the long-term stability of a W/W emulsion (de Freitas et al., 2016). W/W emulsions are of interest for separating or purifying biomacromolecules in a complex biological system as well (Norton et al., 2015). Another attractive potential application of W/W emulsions is in designing encapsulated carriers with food-grade biopolymers (Sagis, 2008a; 2008b).

1.1.5 Colloidal system as carriers for encapsulation of bio-functional substances

In food and pharmaceutical industry, encapsulation of functional compounds, such as probiotics, prebiotics, vitamins and flavors, adds enormous values to the commodities

due to the improved nutritional quality in them and/or increased cost efficiency in processing and storage. Microencapsulation is a concept in which bioactive compounds in minute particle or droplet form are contained and encircled within a coated matrix. The mechanism of microencapsulation is based on the affinity of the encapsulated component to the hydrophobicity or hydrophilicity nature of the carrier. Various colloid particles or their gel/particle form are considered a popular matrix to embed biomass (Champagne & Fustier, 2007). For example, milk proteins have been proven to be served as natural vehicles for biological substances (Livney, 2010). Given excellence gelation properties, casein has been widely considered to encapsulate probiotic bacteria or drugs (Heidebach et al., 2009; Rodrigues et al., 2009). However, the process often requires energy inputs (e.g., heat treatment) or chemical/enzymatic cross-linking for the production of protein-based carrier particles (Luo et al., 2015; Puthli & Vavua, 2008).

In addition, pectin or alginate beads exhibit a capacity of high encapsulation efficiency for nutraceutical compounds (Champagne, 2006; Sriamornsak, 1999). In a study, kafirin microparticles, ranging from 1 to 10 μm in diameter, were shown to encapsulate catechin and sorghum condensed tannins for controlled release. These microparticles are spherical or irregular in shape with a rough, porous surface with numerous holes to provide an enlarged surface area for absolving antioxidants (Taylor et al., 2009a).

Most recently, studies highlighted a structure for a microencapsulated particle called “colloidosome.” It was a hollow, elastic capsule with a size ranging from micrometers to millimeters, with easily adjustable and highly controllable permeability and elasticity (Thompson et al., 2015). In other reports, the capsule surface was formed by a close-packed layer of colloidal particles covering an emulsion droplet, which acted as a core containing a continuous-phase fluid (Dinsmore et al., 2002; Shilpi et al., 2007). The major advantage of the “colloidosome” concept lies on the colloidal shell that can control the pore size and extensively increase physical stability of the structure (Shilpi et al., 2007). They could act as a carrier for both hydrophobic and hydrophilic substances. For example, a recent report indicated the polymeric colloidosomes containing a calcium alginate gel capsule to be used in encapsulating live probiotic bacterial cells. A high encapsulation efficiency, approximately 98%, of the lactic acid bacteria was achieved by the study as reported (Keen et al., 2012).

1.2 Process and sample preparation

1.2.1 Film as medium for structural analysis

Food polymers, such as globular proteins or polysaccharides, are potential candidates for film forming. These films could be widely used as edible coating material or wrapping for food to prevent spoilage or extent shelf life (Otoni et al., 2017; Pavlath & Orts, 2009). Hence, colloid-based films also allow direct investigation on 3-dimensional structure of colloids in dry states with surface sensitive techniques. Some researchers utilized methods including grazing-incidence small-angle x-ray scattering (GISAXS), atomic-force microscopy (AFM) and electron microscopy (EM) to reveal the highly ordered CM structure as a film on membrane or a solid surface (Gebhardt & Kulozik, 2014).

Different approaches have been used to form colloidal films. They include spin coating, Langmuir-Boldgett techniques, and solution casting. Spin coating or Langmuir-Blodgett techniques enables the preparation of thin films by structuring biomolecules into an ordered array (Erokhin, 2002; Hall et al., 2004). In the spin coating process, a liquid droplet falls onto a surface and is spanned to form a thin layer over the substrate. It allows a non-equilibrium conformation and extends the area of accessible structures (Hall et al., 2004). On the other hand, the Langmuir-Blodgett process calls for a transfer of compressed protein thin film from a subphase surface to a substrate (Erokhin, 2002). However, the acting surface tension increases the risk of protein denaturation because it owns equal magnitude as the forces which induce protein folding. Therefore, a modification on a likewise method is needed to produce a highly ordered protein monolayer for a fast crystal growth of the protein.

Solution casting is an easy way to prepare polymer films that is driven by the solvent evaporation at a liquid-gas interface (Sano, 1992). Usually a solution containing colloidal polymer, e.g., proteins or polysaccharides, is poured on a hard support. And, the suspension is dried in a defined temperature/humidity environment for a long time until the film is formed (Li et al., 2012; Wu & Zhang, 2001). Although time-consuming, the solution casting can produce thicker films than the spin coating or Langmuir-Blodgett method with a lower investment on equipment.

1.2.2 Centrifugation

Centrifugation is a classic mechanical process to separate particles. In nature, separation of particles in a mixture is normally realized by sedimentation via gravity. Centrifugation step boots this process by introducing centrifugal forces (Price, 1982; Schachman, 1959; Williams, 1972). It separates individual (or multiple) components in a mixed solution based on the differences of the size, shape, form, viscosity of the parts in medium under specified speed of rotor (Marziali, 2000; Taulbee & Mercedes Maroto-Valer, 2000). The technology is widely applied in food/dairy industry. For example, separating milk components into whey and casein, quark from whey, and impurities or unfavorable microorganisms from product (Berk, 2018; Farkye, 2017; Kessler, 2002; Sant'Ana, 2014; Wieking, 2002). Depending on the rotational speed and purpose of application, centrifugation could be classified into microcentrifuge (angular speeds of 12,000 to 13,000 rpm), high speed centrifuge (angular speeds of 30,000 rpm), and ultracentrifuge (angular speeds up to 70,000 rpm).

In a natural gravitational field, gravity and resisting force impose on the spherical particles (e.g., fat globule or protein). The particles sink (or rise) when their density is greater (or smaller) than the surrounding medium, while remain steady when equal to that of the medium (Kessler, 2002). The equilibrium between gravity and resisting force determines the settling or rising velocity, w. Sedimentation speed of a spherical particle is accelerated by applying centrifugal field (Kessler, 2002).

The centrifugal acceleration is:

$$\omega^2 \cdot R = \frac{w_U^2}{R} \qquad (2)$$

where w_U is peripheral velocity in m/s, R is radius of the orbital path in m, ω is angular velocity in radians per second (rad/s).

The centrifugal constant Z is expressed as a multiple of gravitational force, where g = 9.807 m/s^2:

$$\mathrm{Z} = \frac{\omega^2 \cdot R}{g} = \frac{w_U^2}{R \cdot g} \qquad (3)$$

If n is in term of number of revolutions per second (rps), then:

$$w_U = 2 \cdot \pi \cdot R \cdot n \text{ and } \mathrm{Z} = \frac{(2 \cdot \pi \cdot n)^2 \cdot R}{g} \qquad (4)$$

where n is expressed in revolution per minute (rpm), then:

$$\mathrm{Z} = \frac{R \cdot n^2}{894} \quad (5)$$

The velocity of particles in the centrifugal field w_Z is Z-times greater than in the gravitational field:

$$w_\mathrm{Z} = \frac{d^2 \cdot (\rho_s - \rho_l)}{18 \cdot \mu} \cdot g \cdot \mathrm{Z} \quad (6)$$

where ρ_s is the density of the spherical particle, ρ_l is the density of the medium and μ is absolute viscosity (Kessler, 2002).

By using centrifuge, radial force is expressed relative to gravitational force and named as relative centrifugal force (RCF) or 'g' force. The g force is governed by the rotational speed of rotor and axis of rotation (Berk, 2018; Burdon et al., 1988).

RCF could be expressed in the following equation:

$$RCF = 11.18 \cdot r \cdot \left(\frac{n}{1000}\right)^2 \quad (7)$$

where n is the revolution per minute (rpm) and r is the distance of the particle from the center of rotation in cm (Rickwood et al., 1994).

Ultracentrifugation is also used to separate protein fractions, such as CMs of different sizes (Huppertz et al., 2018; Marchin et al., 2007). Applying consecutive centrifugation steps defining by centrifugal force, native CMs can be segregated into size clusters narrowing the size distribution within a cluster as shown in Tab. 1-2 (Marchin et al., 2007). Thereby, similar protein property can be expected for CMs resuspended in a serum solution.

Tab. 1-2 Centrifugation procedure to separate and fractionate native CM from skim milk at 25°C according to Marchin et al., 2007.

	rpm	rcf (g)	Time (min)
CM	31,000	70,714	60
size fraction I	12,000	10,596	15
size fraction II	15,000	16,556	15
size fraction III	20,000	29,434	15
size fraction IV	25,000	45,990	15
size fraction V	29,000	61,884	15
size fraction VI	31,000	70,714	60

1.2.3 Enzymatic hydrolysis of pectin by pectinase

Pectin is a structural polysaccharide group containing mainly α-1,4-linked D-galacturonic acid as backbone. Homogalacturonan, galacturonan with side chains and rhamnogalacturonan are the major building elements for pectin molecules (Belitz et al., 2009). Pectinase is produced by various microorganisms in plants. It is a collection of different enzymes that degrade pectin into monogalacturonic acid via breaking glycosidic linkages. The process is widely applied for juice extraction from fruits via softening the cell wall (Mojsov, 2016). Commercialized pectinase consist of hydrolases (to hydrolyze pectic acid), lyases (to degrade pectic acid), and esterase (to break down methyl ester bonds in pectin) (Mojsov, 2016). Fig. 1-10 illustrates the enzymatic hydrolysis of pectin by pectinases.

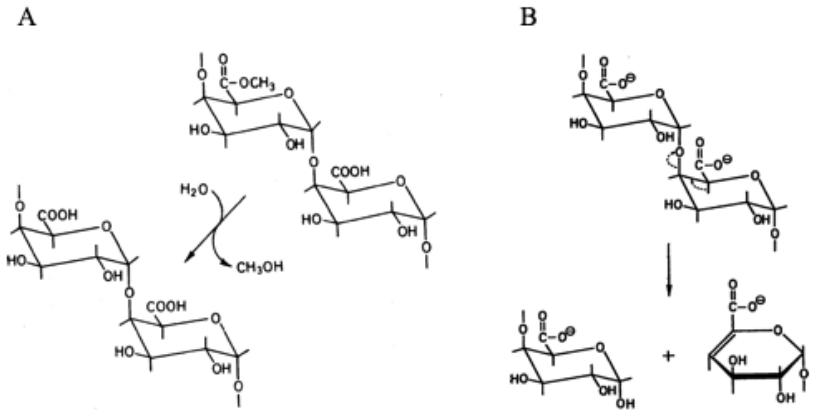

Fig. 1-10: Illustration of A) pectin esterase demethylates pectin into pectic acid and B) pectin hydrolases and lyases catalyze a trans-elimination degradation of pectic acid (Belitz et al., 2009).

Process conditions (e.g., pH, temperature, and treatment time) for pectinase hydrolysis vary in a wide range mainly depending on pectin sources. For example, pH of the treatment is varied from pH 2 to 6 and treatment time ranges between 5 min and 6 h (Croak & Corredig, 2006; Singh & Gupta, 2004; Soares et al., 2001). Hydrolysis temperature is usually maintained at below 50°C to ensure sufficient enzyme activity. Depending on the substrate, the enzyme dosage could be up to 0.135% v/w, as reported in studies (Dang et al., 2012; Singh & Gupta, 2004).

1.3 Analytical methods

1.3.1 Scanning electron microscope (SEM)

SEM produces characteristic images of a sample by scanning on its surface using a focused high energy electron beam. The interaction between electron and samples produces signals that can be further translated into information about surface topography, crystalline structure, chemical composition and crystal orientation for the scanned samples (McMullan, 2006). When electrons interact with samples, secondary electrons, backscattered electrons and characteristic x-ray signals are produced (Goldstein et al., 1981; Reimer, 1998). Coupled detectors collect these signals over a defined area of the sample surface to generate a 2-dimensional image with showing spatial variations (McMullan, 2006). The resolution of SEM can be better than 1 nm with a magnification ranging from 20x to 30,000x (Goldstein et al., 1981).

SEM is widely and routinely used in material and structural analysis because it provides images with high resolution (Cardell & Guerra, 2016; Holmér et al., 2018; Lenthe et al., 2018; Madadlou et al., 2018; Shi et al., 2018). It allows visualization of samples in nano- and micro-scale (Amidon et al., 2017; Goldstein et al., 1981; McMullan, 2006; Roth et al., 2018). In addition to the nano-scale image of single CM as shown in Fig. 1-1, Fig. 1-11 also shows examples of SEM images of particle formed by hydrocolloids at micron level in recent studies.

Although SEM provides detail structural information of sample, there are some limitations requiring special sample preparation (Clarke & Eberhardt, 2002; Egerton, 2005; Goldstein et al., 2003). For example, a sample must be solid and fit into the vacuum chamber. Thickness of the sample is generally limited and normally not to exceed 40 mm. Certain ‘wet’ samples such as coal or other organic materials are not suitable for conventional SEM due to likely outgas in vacuum environment. Specialized equipment, like low vacuum or environmental SEM, is required for this kind of purpose (Clarke & Eberhardt, 2002; Egerton, 2005; Goldstein et al., 2003).

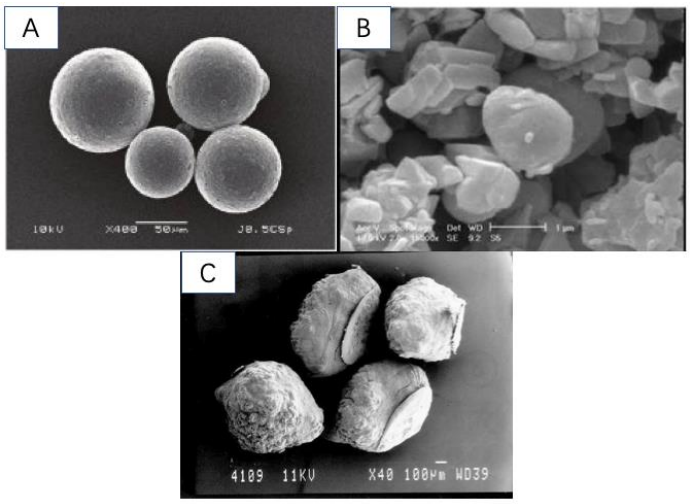

Fig. 1-11: A) the SEM image of non-cross-linked chitosan microparticle at a scale of 50μm (Takka & Acarturk, 1999); B) the SEM photograph of spray dried microparticles containing mannitol at a scale of 1 μm (Sadegh Pourshahab et al., 2011); C) The SEM photograph of alginate/chitosan microparticles at a scale of 100 μm (Karnchanajindanun et al., 2010).

1.3.2 Static and dynamic light scattering for biological material

Light scattering (static and dynamic) is a popular and useful method to characterize the diffusion behavior of particles in solution (Stetefeld et al., 2016). Tyndall reported one of the earliest light scattering in colloidal suspensions and followed by several major theoretical establishment by Rayleigh, Mie, Sutherland, Debye and Einstein (Debye, 1915; Einstein, 1905; 1906; 1910; Mie, 1908; Sutherland, 2009; Tyndall, 1869). Modern light-scatter theories are established after Zimm's modification to RGD equations (Zimm, 1945; 1948). With that, size, shape and molecular weight of molecules in solution can be estimated (Zimm, 1945; 1948). Thereafter, various approaches were developed to define the diffusion coefficient of molecules in solution, which contributes to the final development of modern dynamic light-scattering (DLS) instrument (Finsy et al., 2004; Foord et al., 1970; Koppel, 1972; Livesey et al., 1986; Morrison et al., 1985; Nyeo & Chu, 1989; Pecora, 1964).

Static light scattering (SLS) measures the absolute molecular weight utilizing the relationship between scattered light intensity by a molecule and its molecular weight (M_w) and size (Zimm, 1945; 1948). Zimm equation is the most common approach to measure the weight-average molecular weight (M_w) in response to various concentrations:

$$\frac{\mathrm{K}_c}{\Delta R(\theta,c)} = \frac{1}{M_w} \cdot (1 + \frac{q^2 \cdot R_g^2}{3}) + 2A_2 \cdot c \quad (8)$$

where A_2 is second virial coefficient indicating interaction between molecules, and R_g radius of gyration.

K is optical constant describing polymer property:

$$\mathrm{K} = \frac{4 \cdot \pi^2 \cdot n_0^2 \cdot (\frac{\partial n}{\partial c})}{N_A \cdot \lambda^4} \quad (9)$$

The refractive index increment of $\frac{dn}{dc} = 0.185$ mL/g is applied (Anema & Li, 2003).

And R is Rayleigh ratio:

$$R(\theta) = \frac{I_A(\theta) \cdot n_0^2}{I_T(\theta) n_T^2} \cdot \frac{R_T}{N(\theta)} \quad (10)$$

with

$$\Delta R(\theta, c) = R_A(\theta) - R_0(\theta) \quad (11)$$

and q is the scattering vector for polarized light:

$$q = \frac{4 \cdot \pi \cdot n_0 \cdot \sin\frac{\theta}{2}}{\lambda} \quad (12)$$

where n_0 is refractive index from solvent; λ, wavelength of the light; N_A, Avogadro's number ($N_A = 6.022 \times 10^3$); c, solution concentration; $I_A(\theta)$, light intensity of analyte (A) at measure angle θ; $I_T(\theta)$, light intensity of toluene at measure angle θ with a Rayleight ratio of toluene ($R_T = 1.35 \times 10^{-5}\ cm^{-1}$ for a HeNe laser).

A Zimm plot can be built with a double extrapolation to zero angle and zero concentration to derive the R_g, M_w, and second virial coefficient (A_2), which provides structural information of molecules in solvent.

In dynamic light scattering, the motion of molecules is a result of evaluating the correlation of intensity fluctuations:

$$g^2(\tau) = \frac{\langle (I(t) \cdot I(t+\tau)) \rangle_t}{\langle I(t) \rangle^2} \quad (13)$$

where $g^2(\tau)$ is second order autocorrelation function at wave vector q; τ, delay time; *I*, intensity of the scattered light; the angular brackets ⟨ ⟩, averaging over all t.

The second order autocorrelation, $g^2(\tau)$, and first order autocorrelation, $g^1(\tau)$, can be related via Siegert relation which represents the relationship between the electric field correlation function and intensity correlation function:

$$g^2(\tau) = 1 + \beta \cdot |g^1(\tau)|^2 \quad (14)$$

For monodisperse particles, the electric field correlation function, $g^1(\tau)$, decays exponentially:

$$g^1(\tau) = e^{-\Gamma\tau} \quad (15)$$

where Γ, is the decay constant.

The second order autocorrelation function can be rewritten as:

$$g^2(\tau) = 1 + \beta \cdot e^{-2\Gamma\tau} \quad (16)$$

where β is coherence factor that depends on detector area, optical alignment, and scattering properties of macromolecules. Average decay rate $\langle\Gamma\rangle$ and variance are determined by second order cumulant fitting of the field correlation function.

The decay constant, Γ, is related to the diffusion behavior of macromolecules, diffusion coefficient (D) as expressed in the following equation:

$$\Gamma = -D \cdot q^2 \quad (17)$$

where q is the scattering vector which is proportional to the solvent refractive index n as in eq.12 (Harding, 1999).

Thereafter, hydrodynamic radius (R_H) of macromolecules is calculated from Stokes-Einstein relation (Pusey, 1972):

$$R_H = \frac{k_B T}{6\pi\eta D} \quad (18)$$

Where D is the translational diffusion coefficient (m^2/s)， k_B is the Boltzmann constant (m^2 kg/K s^2), T is the temperature (K) and η is the viscosity of medium (Pa·s).

Light scattering, as a non-invasive method, reports detailed biophysical properties of biological samples such as size, mass, shape, and charge (Gast & Fiedler, 2012; Jachimska et al., 2008; Miller et al.,1991; Ware & Flygare, 1971). For milk proteins, DLS is one of the earliest methods to determine the distribution of their particle sizes (Dalgleish & Hallett, 1995). Dalgleish and Horne leveraged DLS to demonstrate the relationship between polydispersity and molecular sizes of isolated CM fractions after

separation process (i.e., centrifugation and chromatography) (Dewan et al., 1974; Griffin & Anderson, 1983; Horne & Dalgleish, 1985; Lin et al., 2002; McGann et al., 1980). In other study, SLS was applied to monitor the molecular interaction of CM during rehydration process (Mimouni et al., 2009). Light scattering could also couple with in-situ apparatus to analyze changes in morphology and size distribution of polymers (Gebhardt & Kulozik, 2011d; Saveyn et al., 2006).

1.3.3 High-performance liquid chromatography (HPLC) for protein analysis

HPLC is a popular analytical technique for separation and identification as well as quantification of individual chemical components in a mixture. The stationary phase in the chromatography column contains adsorbents (such as granular solid particles with 2-50 μm in average size) which leads to the separation of individual components due to their different level of interaction with those particles in the solvent. Compared to conventional liquid chromatography that relies on gravity, HPLC is more efficient because of using a high pressure (up to 350 bar) to force the mobile phase (e.g., a solvent) to pass through the stationary phase (Forgács & Cserháti, 2003; Lozano-Sánchez et al., 2018; Moreno-Arribas & Polo, 2003). Fig 1-12 is a schematic representation of a typical HPLC unit including a sampler, a pump, and a detector. The pump generates a desired flow with components through the column and the detector (for example UV/Vis, photodiode array or based on mass spectrometry) produces a digital signal proportional to the mass of the components in order to report the concertation.

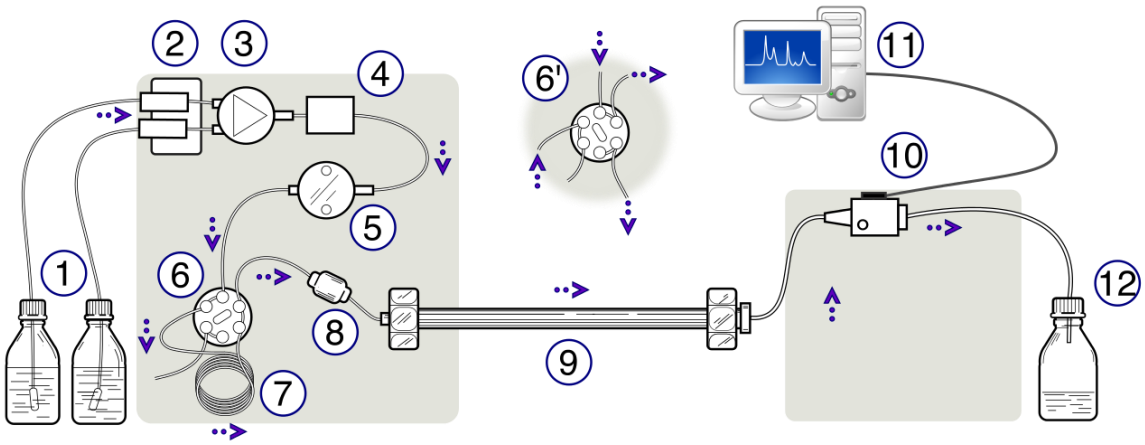

Fig. 1-12: Schematic representation of an HPLC unit. (1) Solvent reservoirs, (2) Solvent degasser, (3) Gradient valve, (4) Mixing vessel for delivery of the mobile phase, (5) High-pressure pump, (6) Switching valve in "inject position", (6') Switching valve in

"load position", (7) Sample injection loop, (8) Pre-column (guard column), (9) Analytical column, (10) Detector (i.e., IR, UV), (11) Data acquisition, (12) Waste or fraction collector (Meyer, 2004).

Several variants of HPLC exist such as partition chromatography, normal-phase chromatography, reverse-phase chromatography, and size-exclusion chromatography. The differences are mainly because of the relative polarity of the solvent and the stationary phase. For example, the normal-phase HPLC uses a column filed with polar silica particles of an average diameter of 5mm and an average length between 150 to 250 mm. The solvent used in normal-phase HPLC is typically non-polar solution. Polar compounds in the mixture interact via polar interactions on the sorbent surface (Jandera, 2013; Matés & Pérez-Gómez, 2000; Mukherjee, 2019; Robards et al., 2004). Normal-phase HPLC requires long retention time and was replaced by the reverse-phase HPLC (RP-HPLC) developed in the 1970s to improve sufficiency of the analysis. RP-HPLC equips with a non-polar stationary phase and a moderately polar mobile phase. Non-polar compounds tend to interaction with hydrocarbon groups of the molecules due to van der Waals dispersion forces. This reduces the solubility of compounds in solvent. It enables the polar molecules to travel faster through the stationary phase/column decreasing the retention time (Neue et al., 2005; Otter, 2003; Sadana, 1998). RP-HPLC is popular and the most used form of HPLC for composition and structural analysis at present.

For food research, HPLC is widely applied for composition and structural investigations on major compounds such as protein, polysaccharide or lipids (Dai et al., 2010; Douša et al., 2016; Ferreira et al., 2001; Jeschek et al.,2016; Ma et al.,2017; Meyer et al., 2001; Sturaro et al.,2016). Studies reported the use of HPLC as a precise and effective method for separation and qualification of casein and whey protein in milk (Bobe et al., 1998; Bonfatti et al., 2008; Bramanti et al., 2003; Veloso et al., 2002). Currently, new development on HPLC focuses mainly on columns of novel polymers, improved detection system, sample preparation or combinations with other devices equipment (Bonfatti et al., 2008; Dumpler et al., 2017; Pomastowski et al., 2014).

1.3.4 Fourier-transform infrared spectroscopy (FT-IR) and confocal Raman microscopy for structural analysis of colloidal polymers

Vibrational spectroscopy is a group of techniques collecting structural information of vibrational radiation from molecules. It includes infrared spectroscopy (IR), Raman spectroscopy, x-ray, and UV photoelectron spectroscopy. These methods emerged in recent years combining with imaging and on-line probing accessories to become an extremely powerful tool for structural or biological research (Gupta, 2016). Vibrational spectroscopy uses infrared or laser as exciting sources to generate vibrational modes in chemical groups. These vibrational modes can be bond stretching, bending, twisting, rocking, wagging or scissoring. Molecules interact with the exciting source creating corresponding vibration signals recorded by a spectrometer on a vibrational spectrum such as IR or Raman spectrum. It provides a unique and non-destructive means for analyzing molecular composition and structures.

Fourier Transformation-Infrared Spectroscopy (FTIR)

FT-IR spectrometer is a most often applied IR spectrometer after the interferometer was introduced. It measures all wavelengths simultaneously compared to the classic dispersive IR spectrometer, which can only measure single spectral element at one time (Schrader, 1995). It provides a faster sampling and better single to noise ratio than the classical dispersive IR instrument (Griffiths, 1983).

For biological materials, detailed assignments for individual spectral regions are studied and reported by previous studies (Baker et al., 2014; Movasaghi et al., 2008; Naumann et al., 1991). Typical spectrum referring to biomolecular peak assignment ranges from 800 to 3000 cm^{-1}. The most important spectral regions for biological samples include, such as, fingerprint regions (600-1450 cm^{-1}), Amide I and Amide II region (1500-1700 cm^{-1}) and high wavenumber regions (2550-3500 cm^{-1}) (Baker et al., 2014). Low wavenumber regions are normally referred to bending or carbon skeleton vibrations (Baker et al., 2014).

Raman spectroscopy

Raman spectroscopy has a number of advantages over the conventional techniques for studying biological systems (Huen et al., 2014; Robuschi et al., 2017; Tosato et al., 2015). Together with IR spectroscopy, the method is sensitive to various molecular

categories in visualizing their chemical structures. Comparing to IR spectroscopy, Raman spectroscopy is relatively less sensitive to water molecules allowing an easy application for studies on common biological samples containing predominantly water as a solvent (Giridhar et al., 2017).

Raman spectroscopy exploits the phenomena of inelastic scattering using monochromatic light, which is commonly available in near-IR, visible and even UV ranges (Adar, 2001). Raman scattering describes excitation of photons to virtual energy states and the resultant loss (so called Stokes) or gain (anti-Stokes) of energy that occurs because of interaction of the excitation light with vibrational modes (Herzberg & Spinks, 1939). These modes are directly associated with the chemical bonds of the sample. Raman spectroscopy observes shift in energy indicating discrete vibrational modes of polarizable molecules. Therefore, it is suitable for a qualitative analysis of chemical compositions. Raman spectroscopy can also provide quantitative information in addition to the composition if the instrument response is correctly calibrated. The peak height and area on curve are used to generate information on concentration by calculating with calibration data (Adar, 2001).

Raman spectrum normally covers the wavenumbers between 400 and 4,000 cm^{-1}. There are certain regions in Raman spectrum are of significant interests for information on biological samples. For example, 1,500 to 1,700 cm^{-1} responses to amide band vibration, which is a signature for protein. Wavenumbers between 470 to 1,200 cm^{-1} offers the backbone information for carbohydrate. Other regions, such as 980, 1090, and 1240 cm^{-1}, link to phosphate groups in DNAs and cellular biomolecules (Bunaciu et al., 2015). The peaks in high wavenumber regions between 2,700 to 3,500 cm^{-1} are associated with CH, NH or OH stretching, which are owned by lipids and proteins. All the information is the fingerprints for biological samples (Rygula et al., 2013). Assignment of Raman shifts to chemical structures is extensively reviewed in studies (Adar, 2001; Rygula et al., 2013). Tab. 1-3 shows a collection of a typical assignment of vibrational bands in proteins. Hence, Byler and his co-works has published the first study on Raman analysis of CM by 80s to understand its secondary structure. This also provides a base between assignment of vibration signals and CM's chemical structure (Byler et al., 1988).

Tab. 1-3. Assignment of typical bands in Raman spectra of proteins (reproduced from Li-Chan et al., 1994).

Band assignment	Wavenumbers (cm^{-1})
S-S stretch Cystine	510. 525, 545
C-S stretch Cystine, Methionine	630-670, 700-745
Tryptophan	760, 880, 1360
Tyrosine doublet	830/850
α-Helix	938
Phenylalanine	1005
Amide III	1235-1270
C=O stretch of COO^-, COOH	1400, 1730
C-H bend	1453
Amide I	1650-1685
S-H stretch Cysteine	2550-2580
-C-H or =C-H stretch	2880, 2930, 3060
o-H stretch	3200

Technological advancements make it possible to produce highly informative Raman images with the confocal techniques. Raman images are mapped by integrating single spectrum over large sample area with improved interpretability (Hollricher, 2010). Recently, Raman spectroscopy coupled with confocal light microscope becomes popular for material and clinical studies because it can construct visualized 3D models based on molecular chemical information (Hollricher, 2010).

Due to its high molecular specificity, Raman spectroscopy was considered an excellent technique for material investigation (Adar, 2001). By introducing the highly efficient laser sources, low-noise detector, effective Rayleigh filters as well as high-throughput optics, the applicability of Raman spectroscopy is tremendously extended to biological or food fields (Huen et al., 2014; Rygula et al., 2013). Raman spectroscopy can also be coupled with other surface analyzing tools, such as atomic force microscopy and scanning electron microscope, for further widened applications (Grodecki et al., 2016; Rygula et al., 2018).

A recent technological advancement promotes the classical Raman spectroscopy to Raman microscopy, also called confocal Raman microscopy. It combines an optical microscope with a Raman spectrometer into a single instrument providing high resolution 3D images on small samples. Fig. 1-13 is a schematic representation of a confocal Raman microscope. In brief, a confocal Raman microscope utilizes laser to enhance Raman scattering. The equipment is still equipped with an optical microscope uses normal light source to scan through samples and magnify the sample while the

Raman spectrometer scatters light and measures the excitation vibration. A beam splitter splits the incoming laser beam with the beam path reaching the sample via the objective lens. The laser beam is then split between the camera and the spectrograph after passing through a rejection filter. The light then reflects and wavelength are separated by the grating prior arriving at the detector (Giridhar et al., 2017; Gomes da Costa et al., 2019). Confocal Raman microscope is thus widely applied in structural/compositional investigations for material identification, polymer analysis and/or biological examination (Giridhar et al., 2017; Gomes da Costa et al., 2019).

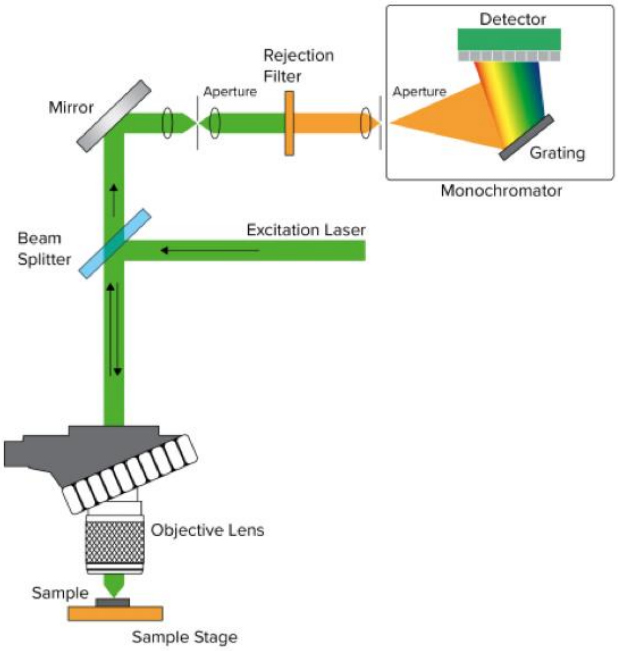

Fig. 1-13: A schematic layout of confocal Raman microscopy. (obtained from https://jascoinc.com/confocalramanmicroscopy/)

2 Motivation and objective

New insights into the structural changes of CM during interacting with other colloids are of interest to researchers despite being extensively studied in the past. Fundamental understanding of the structure of CM is essential for creating novel food products through exploration of the unique capacities of CM. Designing process conditions conducive and selecting appropriate materials to interact with CMs are being continually discovered and implemented to maximize the potential functional and health benefits of the applications. However, conventional approaches for the study can no longer answer all the questions, and new directions are in order. For instance, as reviewed and summarized before, beyond the conventional processing conditions (e.g., heating, pressurizing and/or pH modifying) it would be interesting to push the envelope by exploring less chemical-depending and energy-demanding processing technologies to achieve the desired end result based on newly unveiled properties and mechanisms on the structural changes and colloid complex formation of CMs.

One objective of this work was to decipher the fundamental of the interactions between CMs and other milk protein (e.g., ß-Lg in this study) and/or polysaccharide (e.g., pectin in this study) under conditions beyond what have previously been reported. The interaction between CMs and other colloids inspired attribution of new functional benefits to CM based new structures.

As the major proteins in milk, casein and ß-Lg have been extensively studied. The molecular interactions between the proteins induced by heat or high pressure can lead to formation of emulsions or gels. Addition of salts can alter the CM internal structure. Increased calcium in solution can result in CM aggregation, while calcium removal can destabilize CM. However, little was reported on the structural alteration of CM in a system containing the micelles with ß-Lg and salt.

The second objective of this work aimed to produce a new matrix based on the interaction between CM and polysaccharide. CM is well known for its ability to form segregative aggregates with polysaccharide at neutral pH. The matrix can retrieve its stability once the polysaccharide is removed or pH lowered. In the past, a mixture of CM and polysaccharide at neutral pH was considered ‘undesirable,’ as the segregative phase separation often occurs. This work focused on the formation and structure of

casein microparticles when pectin was added for making the film. By being a carrier of bio-functional substance, CM microparticles were incorporated with α-tocopherol (αT) in the study for demonstration.

Structural transformation of CM triggered by hydrocolloid addition could be crucial in the attempt to broaden food and pharmaceutical applications of CM.

3 Results

3.1 Influence of ß-Lactoglobulin and calcium chloride on the molecular structure and interactions of casein micelles

Summary and Contribution of the Doctoral Candidate

Caseins are natively unfolded proteins that form CM in aqueous solution. β-Lg is a well-folded globular protein, which takes up approximately 0.3 wt% in cow's milk. Little is known about the interactions between CM and β-Lg in solution without thermal treatment. Multiangle laser light scattering and differential refractometer is a powerful non-invasive analytical tool for characterizing the structure including size and morphology of heat-induced CM/β-Lg aggregates.

The structure of CM as our study showed indicates deviations from a hard sphere model when the amount of β-Lg increased beyond the concentration found in native milk. On the other hand, CMs behaved like hard spheres at calcium concentration of 10 mM or higher, irrespective of the presence or absence of β-Lg. The structural transformation related to the changes on R_g and M_w suggested that the CMs under hard sphere conditions contained an increased proportion and were different in composition of the caseins.

Doctoral candidate made significant contributions in this manuscript. He reviewed existing literatures critically and drew the underlying hypothesis with corresponding author, Ronald Gebhardt. The doctoral candidate designed and carried out the HPLC experiments. Ikuko Ueda supported the light scattering experiments and Ronald Gebhardt initiated the research plan while majorly contributed to the data interpretation of light scattering experiments. In addition, Ulrich Kulozik contributed to the revision and proof-reading of the manuscript. Writing and revising of the manuscript was done jointly by doctoral candidate and corresponding author, Ronald Gebhardt, after discussing the results with all co-authors.

*Adapted Original Manuscript**

Influence of ß-Lactoglobulin and calcium chloride on the molecular structure and interactions of casein micelles[2]

Yu Zhuang[a*], Ikuko Ueda[a], Ulrich Kulozik[a,b], Ronald Gebhardt[c]

[a] Chair of Food and Bioprocess Engineering, Technical University of Munich, 85354 Freising-Weihenstephan, Germany

[b] ZIEL Institute for Food & Health - Section Technology, Technical University of Munich, 85354 Freising-Weihenstephan, Germany

[c] Chair of Soft Matter Process Engineering (SMP), RWTH Aachen University, 52062, Aachen, Germany

Abstract

Targeted processing of CMs requires a basic understanding of their molecular structure as well as their interactions with each other and with other components. In this study, angle- and concentration-dependent static and dynamic light scattering is applied to investigate changes in the molecular weight, size, and intermolecular interactions of CM after the addition of β-lactoglobulin (ß-Lg) and calcium chloride. In the presence of β-Lg and natural calcium chloride concentrations(10mM), the molecular weight of CM is reduced and the radius of gyration is increased. Both changes can be explained by the release of α_{S2}-casein and κ-casein, which were determined in higher concentration free in solution by High performance liquid chromatography. In contrast, the structure of CMs is not altered by the presence of β-Lg at elevated calcium chloride concentrations. The repulsive forces between the CM are stronger at elevated calcium chloride concentrations but do not show significant dependence on β-Lg for all calcium chloride concentrations tested.

---

* Adaptions refer to used abbreviations as well as figure, table and section numberings.

[2] Originally published in: International Journal of Biological Macromolecules (2018), Volume 107, page 560-566. Permission for the reuse of the article is granted by Springer.

3.1.1 Introduction

Caseins and β-lactoglobulin (β-Lg) are the most abundant proteins in cow milk and they have a range of beneficial functions. For example, they act as stabilizers of interfaces (Serfert et al., 2013), carriers of bioactive substances (Semo et al., 2007; Sobel et al., 2014), or raw materials for a number of gelled products (Ji et al.,2016; Lazidis et al., 2016; Solar & Gunasekaran, 2010). Caseins, in particular, are natively unfolded proteins that form CMs in aqueous solution. Four types of casein (α_{S1}-, α_{S2}-, ß- and κ-casein) can be distinguished because of different primary structures and solubility in solutions containing calcium ions. The α_S- and ß-caseins are calcium insoluble and located inside the micellar structure while κ-casein is calcium soluble and mostly present on the micellar surface (Dalgleish & Corredig, 2012). ß-casein mainly interacts via hydrophobic bonding and dissociates from the micelle at low temperature (Creamer et al., 1977). The highly phosphorylated α_S-caseins are cross-linked with calcium phosphate nanoclusters and show no temperature-dependent dissociation. Sedimentation experiments have characterized CM as spherical molecules with a M_W of 2.8×10^8 g/mol and a mean R_H of 77.8 nm (Morris et al., 2000). Because CM have a broad range of sizes, size-fractionated samples containing CM are often used for studies aimed at revealing their structural details (Gebhardt et al., 2011c). CM effectively behave as hard spheres at neutral pH (pH=6.7, 20°C) with repulsive (steric) interactions between them (Tuinier & de Kruif, 2002). They are highly hydrated, with a moisture content of approx. 4g water per g protein (Bloomfield & Mead, 1975; de Kruif & Holt, 2003; Farrell et al., 2013). The structure of CM is sensitive to the calcium ion concentration in the surrounding solution because calcium phosphate clusters hold the caseins together. Natural milk serum contains approx. 30mM calcium for which 10mM is diffusible and 2mM exists in ionized form (Christianson et al., 1954; Gangidi & Metzger, 2006). The remaining calcium is incorporated in phosphate clusters within CM (Holt et al., 2009). Removal of calcium leads to a release of soluble caseins and this results in CM instability (Lin et al., 2002). In combination with drying forces, elevated calcium concentrations lead to aggregation of CM as surface-sensitive X-ray measurements in casein films showed (Muller-Buschbaum et al., 2007). Recent studies used high pressure to investigate structure and stability changes of CM at different calcium concentrations (Gebhardt et al., 2011a)

β-Lg is a well-folded globular protein, which takes up approx. 0.3 wt% in cow's milk (Creamer et al., 2011; Edwards et al., 2008). It has the characteristic structural feature of a calyx made of two β-strands (Kontopidis et al., 2004). Depending on the pH, β-Lg undergoes a number of structural transitions (Taulier & Chalikian, 2001) and adopts a range of oligomeric states (Gebhardt, et al., 2012a). β-Lg is also sensitive to serum Ca^{2+} concentration as denaturation and aggregation studies showed (Petit et al., 2011; Zittle, DellaMonica et al., 1957). Heat-denatured β-Lg associates on the surface of CM or form complexes with κ-casein (Anema & Li, 2003; Dumpler, et al., 2017). It was also shown by fluorescence spectroscopy that Ca^{2+} weakly but specifically binds also to native β-Lg (Jeyarajah & Allen, 1994). In addition, ß-Lg adheres on the surface of CM during microfiltration and forms a deposit of interconnected CM with a porous mass-fractal structure on top of membranes (Steinhauer et al., 2014). Consequently, the mean specific fouling resistance of the casein layer is significantly reduced in the presence of β-Lg (Steinhauer et al., 2015).

Static and dynamic light scattering are powerful tools to extract structural information, e.g., morphology, sizes and interactions, of milk proteins (Liu et al., 2017; Mehalebi et al., 2008; Mimouni et al., 2009; Tran Le et al., 2008). A recent study reported that multiangle laser light scattering and differential refractometer could be coupled with transmission electron microscopy and asymmetrical flow field-flow fractionation to characterize the size and morphology of heat induced CM/whey protein aggregates (Loiseleux et al., 2018). However, little is known about the interaction between CM and β-Lg without thermo-treatment in solution.

This study is intended to determine whether changes in the structure and interactions of CM already occur upon the addition of a surplus of β-Lg (in native state) in solution. Hence, we analyzed the stability of CM with and without presence of ß-Lg under various calcium concentration by changing the calcium chloride concentration. To achieve this, we estimated the molecular weights, intermolecular interactions, and radii of gyration and hydration by performing angle- and concentration-dependent static and dynamic light scattering and measured the individual casein concentration by HPLC. This study expands the field of application of scattering techniques to more complex systems and could have implications for the processing of skim milk and milk protein concentrates in general.

3.1.2 Materials and Methods

3.1.2.1 Materials

WPI power (Type 895, Lot No. CT08), containing roughly equal fractions of variants A and B, was obtained from Fonterra (Auckland, New Zealand). Raw skim milk was purchased from Molkerei Weihenstephan GmbH & Co (Freising, Germany). Ultrapure water from a Millipore (Milli-Q Integral 3) water treatment plant (Darmstadt, Germany) was used for the preparation. All reagents with HPLC grade were received from Sigma Aldrich (Darmstadt, Germany) unless described otherwise.

3.1.2.2 Sample preparation

Fig. 3-1 indicates the workflow of sample preparation and analysis. Native β-Lg was obtained from WPI powder after an aggregation and membrane separation process of α-Lactalbumin following the procedure described elsewhere (Toro-Sierra et al., 2013). β-Lg concentration was adjusted to 0.5 wt% in all samples used for the later scattering experiments.

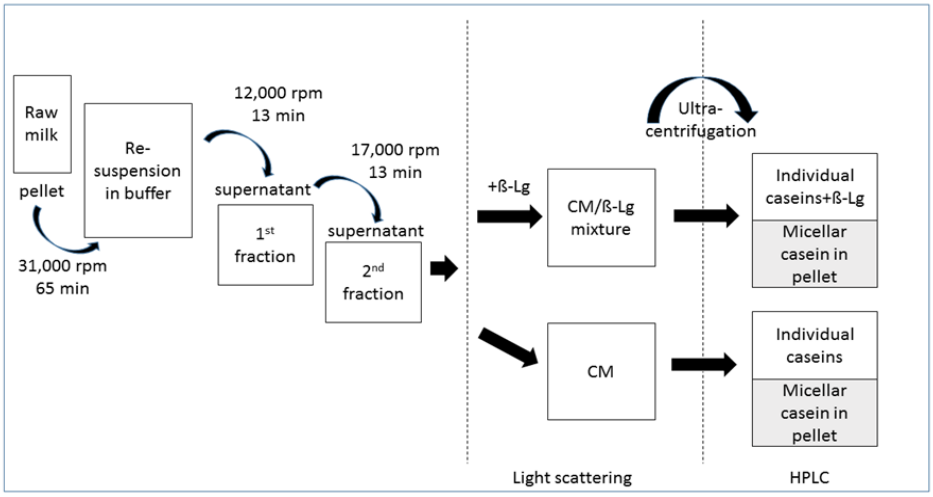

Fig. 3-1: Schematic representation of the experimental design.

CM were extracted from raw skim milk by centrifugation for 65 min at 31,000 rpm with a fixed-angle laboratory ultracentrifuge (Beckman Coulter, Germany). Centrifugation and resuspension steps were conducted at 20 °C. A Bis-Tris base buffer (50 mM Bis-Tris with 10 mM $CaCl_2$) was used to dissolve the pellets at pH 6.8.

After resuspension for 2 h, the dispersion was centrifuged at 12,000 rpm for 13 min and then the supernatant was obtained. A further centrifugation step at 17,000 rpm for 13 min resulted in a supernatant containing a second set of size-fractionated CM, which was stored to prepare casein/ß-Lg mixture.

CM and ß-Lg were mixed at 20 °C for 20 min. The concentrations of casein and ß-Lg in mixed solution were 4 and 5 mg/ml, respectively. Solutions containing casein only and casein/ß-Lg mixture were stored for light scattering experiments.

3.1.2.3 Light scattering experiments

SLS/DLS experiments were carried out with an ALV/CGS-3 Kompakt Goniometer System (ALV-Laser Vertriebsgesellschaft mbH) equipped with a 22 mW He-Ne laser source (λ = 632.8 nm) at T = 20 °C. Scattering experiments were carried out three times, at five scattering angles (θ = 20°, 30°, 40°, 50°, 60°) for 30 s each.

Zimm plot is used to analyze polymers or polymer complexes in a monodisperse nature determined by light scattering. A Zimm plot was constructed to derive the molecular parameters using eq. 19 (Petit et al., 2011):

$$\frac{KC}{R_\theta(q,c)} = \frac{1}{M_W}\left(1 + \frac{q^2 R_g^2}{3}\right) + 2A_2C \qquad (19)$$

where c is the mass concentration of the protein, q is the scattering vector, R(θ) is the Rayleigh ratio, and A_2 is the second virial coefficient.

Measured points of Zimm plot were extrapolated to zero angle and zero concentration to obtain molecular parameters, i.e., radius of gyration (R_g), molecular weight (M_w) and second virial coefficient (A_2) in eq. 19.

Arbitrary constant (K) includes all optical constants:

$$K = \frac{4\pi^2 n_0^2}{N_A \lambda_0^4}\left(\frac{dn}{dc}\right)^2 \qquad (20)$$

where n_0 is the refractive index of the solvent, dn/dc is the refractive index increment of the solute in the solvent, λ is the wavelength of the laser beam in vacuum, and N_A is Avogadro's number.

The average decay rate $\langle \Gamma \rangle$ and the variance were determined by second-order cumulant fitting of the field correlation function. The hydrodynamic radius was calculated from the Stokes-Einstein relation:

$$R_H = \frac{kT}{6\pi\eta D} \tag{21}$$

The refractive index increment of $\frac{dn}{dc} = 0.185$ mL/g was taken from the literature (Anema & Li, 2003).

3.1.2.4 HPLC determination of individual casein concentration

To analyze the stability of CM with and without mixing with ß-Lg, ultracentrifugation was used again to separate single caseins from CM in solutions with 10 mM $CaCl_2$. Due to the low stability of CM under this condition, single caseins will be released from them into supernatant upon centrifugation. The concentration of single caseins could then be detected using HPLC.

Eight samples (each of approx. 1.5 ml) were added into 8 centrifugation tubes followed by an ultracentrifugation step (31,000 rpm) at T = 20 °C for 65 min. The supernatant for each sample was then collected and stored at T = 4 °C for the determination of casein concentration using HPLC.

A total of 0.4 ml of sample was mixed with 1.6 ml of guanidine buffer (6 M guanidine-HCL, 5.37 mM trisodium citrate, 19.5 mM DTT in 0.1 M Bis-Tris buffer) in an Eppendorf reaction tubes. After a reaction time of 30 min, samples were filtered through regenerated cellulose syringe filters with a pore size of 0.45 µm and injected into HPLC vials. The concentrations of the individual caseins within the CM were determined using an Agilent 1100 series RP-HPLC system (Agilent Technologies, Germany), as described elsewhere. The chromatograms were evaluated using ChemStation (version B.04.03) for LC systems (Agilent Technologies, Germany).

3.1.2.5 Data analysis

The obtained HPLC results were analyzed with SigmaPlot (Version 12.3, Systat Inc., USA) using paired t-test for equity of variances. The significance level for all samples was set at a P-value of < 0.05.

3.1.3 Results and Discussion

3.1.3.1 Light scattering analysis on casein/ß-Lg mixture

We performed angle- and concentration-dependent scattering experiments on casein suspensions with and without added β-Lg. The filled rectangles in Fig. 3-2a are the measured scattering data plotted in the Zimm plot. The data on the nearly horizontal line correspond to one sample measured at different scattering angles, while the data along upwards directed lines represent casein suspensions of different concentrations measured at one and the same scattering angle. The lines are linear fits to the data. Filled circles correspond to data that were generated by extrapolation towards zero scattering angle (X-axis) and zero concentration (Y-axis). Values for M_W, the second virial coefficient A_2, and the radius of gyration R_g can be estimated from the fit and those for M_w and A_2 are summarized in Table 3-1.

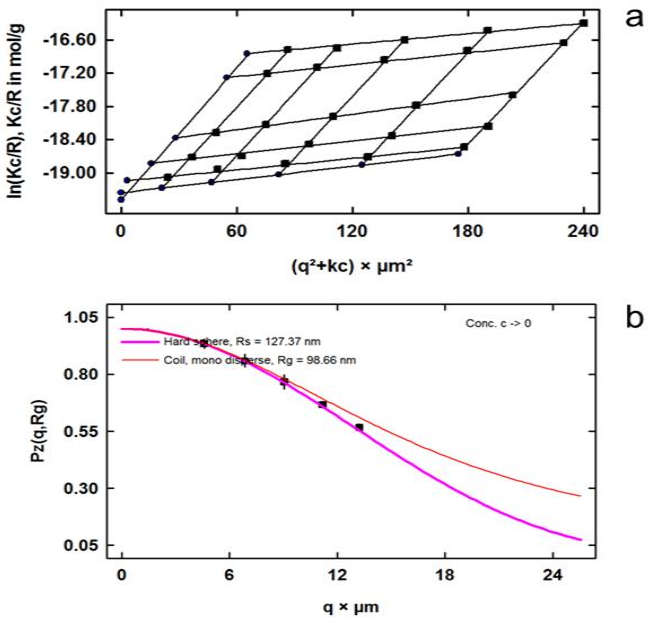

Fig. 3-2: Analysis of the static light scattering of CM. (a) Zimm plot representation of the data with lines used to extrapolate to zero angle (X-Axis) and zero concentration (Y-Axis). (b) Extrapolated scattered intensity to zero concentration as a function of the scattering vector q. The solid lines are predictions of the monodisperse hard sphere and coil models.

Tab. 3-1. Values for the molecular weight MW and second virial coefficient A_2 extracted from static light scattering on suspensions of CM and β-Lg at pH 7.2.

parameters	CM	β-Lg
M_W	2.89×10^{8} g/mol	4.57×10^{4} g/mol
A_2	2.65×10^{-10} mol·L^2/g^2	7.27×10^{-8} mol·L^2/g^2

The molecular weight of the CM is 2.89×10^8 g/mol, which is within the same range as values reported from an ultracentrifugation study (Morris et al., 2000). The second virial coefficient is very small, at 2.65×10^{-10} mol·L^2/g^2, which indicates weak repulsive interactions between the micelles. The estimated molecular weight of β-Lg corresponds roughly to the dimeric state, with 36.7 kDa (Papiz et al., 1986) expected for this pH range (Taulier & Chalikian, 2001). The repulsive interactions between the β-Lg molecules are stronger by two orders of magnitude than those between CM under the same conditions.

The scattering function of CM in Fig. 3-2b was generated from the scattering data after extrapolation towards zero concentration. The clear angular dependence is an indication of a strong contribution of the micellar form factor to the scattering intensity. The solid lines in Fig. 3-2b correspond to model fits with monodisperse hard spheres and random coils. The best fit describes the micelles as hard spheres in solution.

Furthermore, the effects of both 0.5 wt% β-Lg (with and without) and four different calcium concentrations on the structure and interactions of CM were tested. All corresponding scattering data are shown in a Debye plot in Fig. 3-3, which plotted of Kc/R as a function of casein concentration based on results obtaining from Zimm plot. The ratio of Kc/R for CM without β-Lg (open symbols) increased with an increase of casein concentration from 1 mg/mL upwards. This positive correlation indicates repulsive interactions between CM, which enlarge the distance between micelles and prevent CM from aggregation. This leads to a stable suspension. In contrast, the Kc/R ratio increase with a decrease in calcium concentration below a casein concentration of 1 mg/mL. Attractive interactions dominate between micelles at a low calcium concentration, which leads to disintegration of the internal structure of CM.

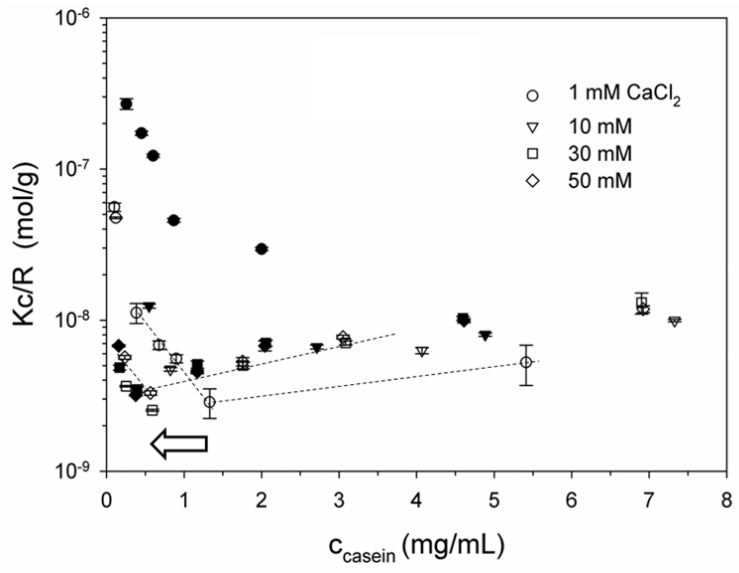

Fig. 3-3: Concentration dependence of K·c/R of CM only (open symbols) and in the presence of 0.5 wt% β-Lg (closed symbols) at four selected calcium chloride concentrations.

An arrow in the plot shown in Fig. 3-3 indicates that the addition of calcium chloride stabilizes the CM in diluted suspensions. The critical concentration c* of $CaCl_2$, indicating the point of (de-) stabilization of CM, was shifted from c* = 1.3 to 0.5 mg/mL when the calcium chloride concentration was increased from 1 to 50 mM.

Fig. 3-3 also shows how the addition of a surplus of ß-Lg (closed symbols) influenced the stabilities of casein suspensions. Disintegration occurs already at c* = 3 mg/mL, while pure CM exhibited instability only at c* = 0.2 mg/mL. A less pronounced but significant destabilizing effect of β-Lg could also be seen in the presence of 10 mM $CaCl_2$. In contrast, scattering data of CM with and without adding β-Lg did not demonstrate similar effects at 30 and 50 mM calcium chloride.

The data sets obtained at a calcium chloride concentration of 1 mM are excluded from further consideration. It is because the instability/disintegration of the CM occurs throughout nearly the entire casein concentration range in this study.

We estimated characteristic sizes for CM for the various experimental conditions, namely, using eq. (16) for determining the radius of gyration (R_g), and eq. (18) for calculating the radius of hydration (R_H). Without β-Lg, the radii of gyration for CM showed no dependence on calcium concentration and were distributed around R_g

= 100 nm (Fig. 3-4a). A difference in CM with added β-Lg only occurred when calcium chloride concentration was at 10 mM. The increased radius of gyration for CM under these conditions can be explained by the dissociation of material originating from the core of the CM, by the mere transfer of mass to the outside, or by an expansion due to the association of material. The latter can be ruled out since the corresponding radius of hydration with 10 mM calcium chloride + β-Lg did not significantly increase (compared with Fig. 3-4b). In general, the hydrodynamic radii for CM are distributed around 120 nm and show no dependence on either β-Lg or calcium chloride. To explain the increase in the radius of gyration, it is thus necessary to consider the molecular weights.

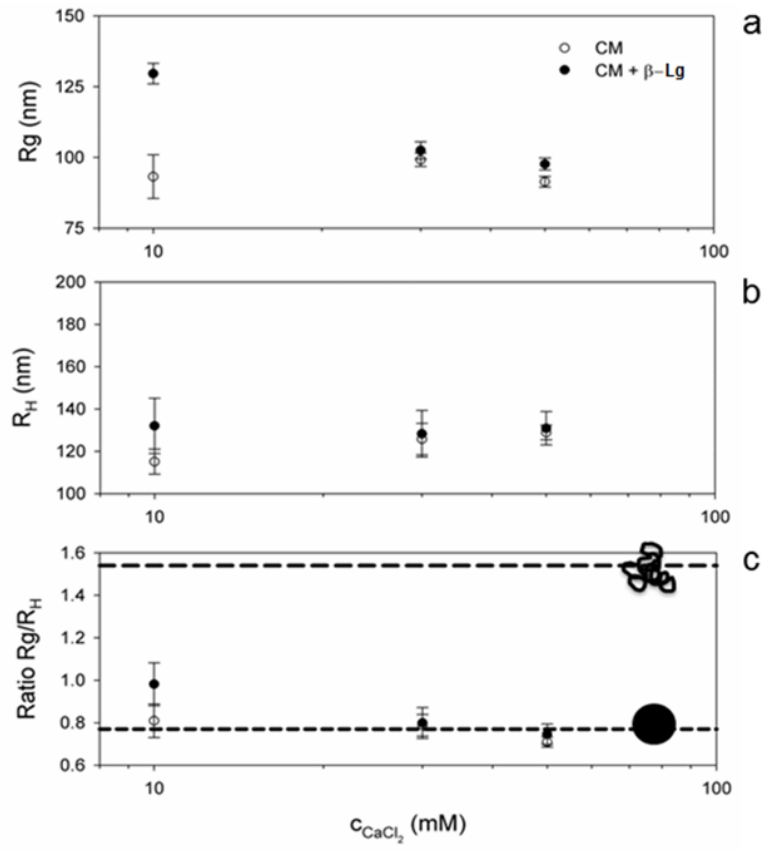

Fig. 3-4: Radii of gyration (a), radii of hydration (b), and radii ratio R_g/R_H (c) for CM (open symbols) and CM+β-Lg (closed symbols) as a function of calcium chloride concentration.

Fig. 3-5 shows the variation of the molecular weight of CM with calcium chloride concentration. Addition of β-Lg reduces the molecular weight of CM at 10 mM calcium chloride to two-thirds of its original value. This suggests that these conditions cause weakly bound caseins to dissociate from the micellar interior and disperse

into the solution. A possible reason for this is the calcium sensitivity of β-Lg (Jeyarajah & Allen, 1994), which competes with the caseins for the micellar calcium. The withdrawal of calcium leads to dissociation of caseins from the micellar interior and changes the mass distribution of CM. The resulting larger mass density near the surface results in an increase in the radius of gyration. These structural changes lead to deviations from the hard sphere model. The ratio R_g/R_H (Fig. 3-4c) does not correspond exactly to the theoretical value of a hard sphere in the presence of β-Lg and 10 mM calcium chloride concentrations in our samples and indicates a more open structure instead. Without β-Lg, an increase in salt concentration causes a slight reduction in the molecular weight. This takes place without a noticeable change in the overall size and density distribution because the radii of CM in the absence of β-Lg do not change at different calcium chloride concentration (see Fig. 3-4). High pressure experiments provide an explanation for this observation based on changes in intermolecular interactions. High pressure dissociation experiments of CM revealed a calcium-dependent transition of CM between 10 and 50 mM, which was accompanied by the formation of new intermolecular interactions, such as calcium phosphate bonds and hydrophobic contacts (Gebhardt et al., 2011b). Additionally, the more compact structure of pressure-treated CM was explained by a pressure-induced increase in the calcium concentration and a subsequent enhancement of the hydrophobic interactions (Gebhardt et al., 2006). As a result of elevated calcium concentrations, the micelles would release water that was previously bound at the protein interface or trapped in voids. Based on these considerations, $2.8 \cdot 10^6$ water molecules would separate from a single CM after the addition of 30 mM calcium chloride. These would account for approx. 40% of the bound water molecules.

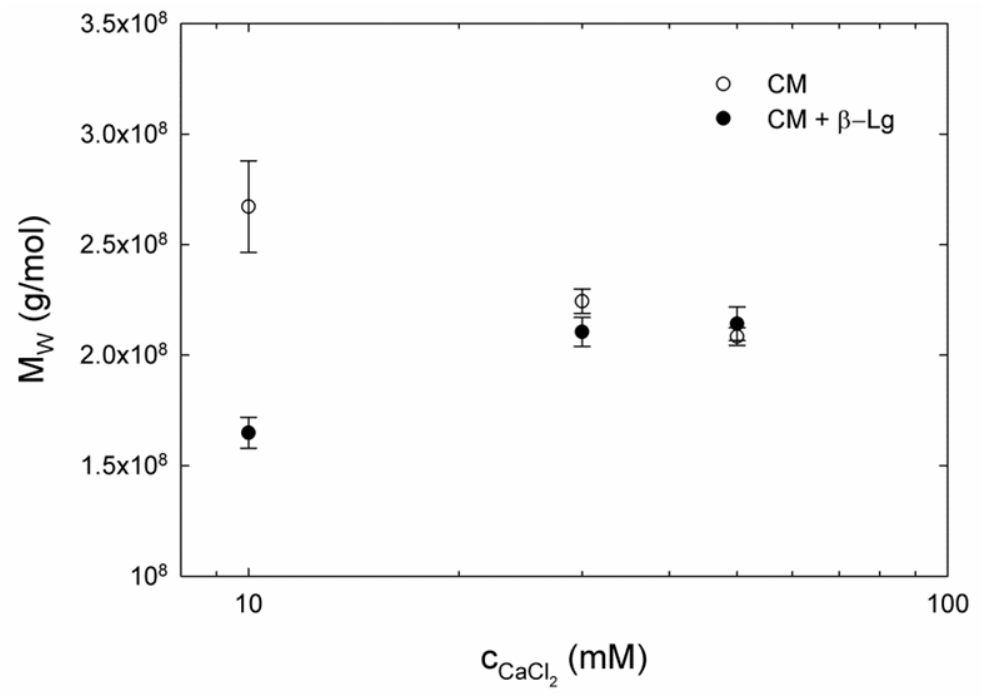

Fig. 3-5: Molecular weights for CM (open symbols) and CM+β-Lg (closed symbols) at different calcium chloride concentrations.

Fig. 3-6 shows the calcium chloride dependence of the second virial coefficient. It describes the non-ideal solution behavior and is often used to quantify the solute-solute interactions. The weak steric repulsion forces between CM show no significant dependence on β-Lg, but increase by a factor of two at elevated salt concentrations (30 and 50 mM). The latter does probably not reflect changes of the micellar interaction but is rather a consequence of contributions of protein-cosolute interactions (Alford et al., 2008; Winzor et al., 2007).

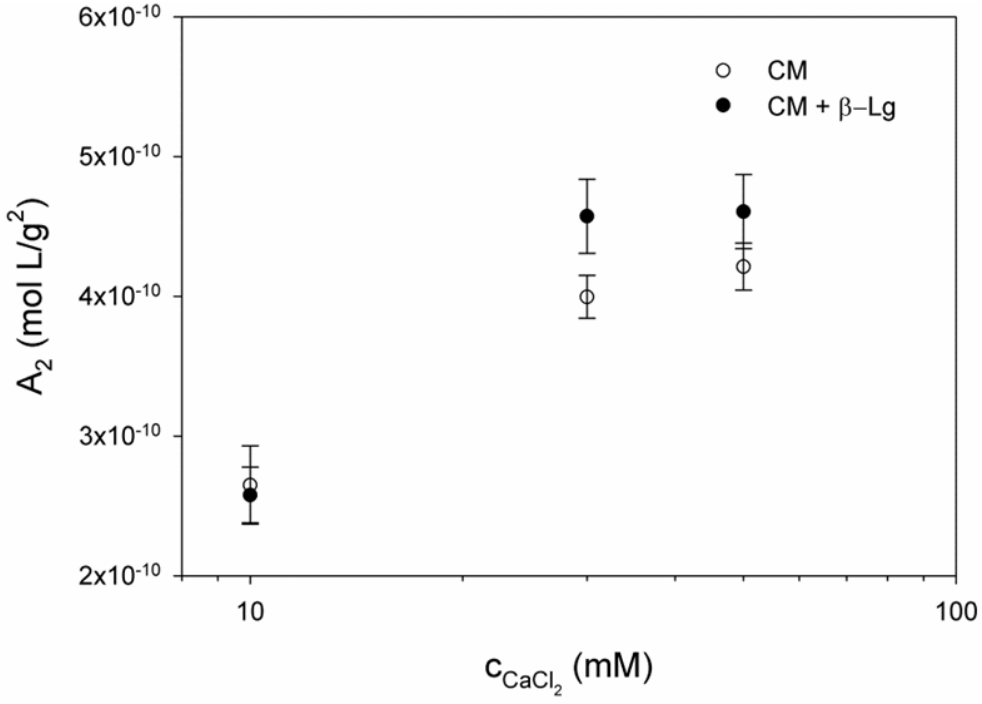

Fig. 3-6: Second virial coefficients for CM (open symbols) and CM+β-Lg (closed symbols) at different calcium chloride concentrations.

3.1.3.2 Concentration of individual caseins in casein and casein/ß-lactoglobulin mixture at natural calcium chloride concentrations

This set of experiments aims to reveal the impact of adding ß-Lg to the stability of CM at a $CaCl_2$ concentration of 10 mM as mimics of natural milk serum. Specifically, ultracentrifugation is used to induce the sedimentation of micellar caseins into a pellet and we can then determine the concentration of free residual caseins remaining in the supernatant using HPLC. Fig. 3-7a shows the concentration of individual caseins with and without the addition of ß-Lg after centrifugation in supernatant with 10 mM $CaCl_2$.

The concentrations of free κ- and α_{S2}-casein in the solution containing also β-Lg were significantly higher than the one without the addition of ß-Lg (Fig. 3-7b). Interestingly, the concentrations of two other caseins (α_{S1}- and ß-casein) remained unchanged.

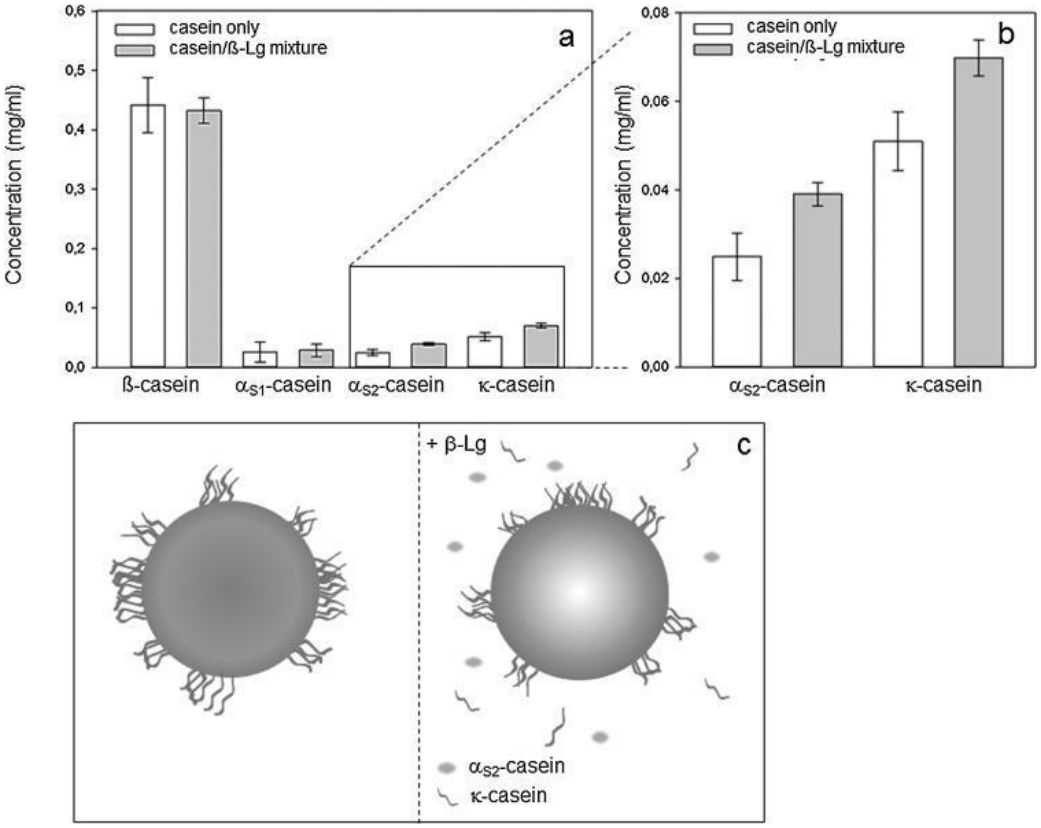

Fig. 3-7: a) Effects of ß-Lg on concentrations of non-micellar caseins at 10 mM $CaCl_2$. Changes of k-casein and α_{s2}-casein concentrations are shown in an enlarge view in b). Structural changes of CM are shown in the schematic representation under c).

We explain this observation by the reduced stability of CM due to the competition of calcium in the presence of surplus ß-Lg. It destabilized the calcium phosphate center and CM tend to lose their integrity, which results in an open structure via the release of α_{S2}-casein and κ-casein (Dalgleish, 2011). This is consistent with the lower molecular weight of CM in the presence of ß-Lg at 10 mM $CaCl_2$, as shown in Fig. 3-5 and the higher R_g/R_H ratio as shown in Fig. 3-4c. The release of both proteins in the presence of β-Lg creates an inhomogeneous inner structure (as shown in Fig. 3-7c) compared with the CM structure under native conditions and leads to a higher R_g value upon the measurement of light scattering (see Fig. 3-4a).

3.1.4 Conclusion

The structure of CM shows deviations from a hard sphere model when the amount of β-Lg is increased compared to the native concentration ratios found in milk. In

contrast, CM behave as hard spheres either in the absence of β-Lg at calcium concentration of 10mM or at an elevated calcium concentration, irrespective of whether β-Lg is present. The structural transformation involves changes in the radius of gyration and the molecular weight, suggesting that CM contain a higher proportion and a different composition of caseins under hard sphere conditions. These changes may have consequences for food processing, in which the concentrations of whey protein and calcium chloride change. For instance, these findings may be relevant to the process of producing milk concentrates using nano-filtration, where part of the ionic components present in the milk serum get lost into the permeate. Specifically, CM as deposits on a membrane are in contact with whey protein when the salt concentration is high during the filtration process. Two different mechanisms can be identified to explain the structural changes induced by β-Lg and calcium chloride. First, β-Lg competes with caseins for micellar calcium in solution. A surplus of ß-Lg weakens contacts between caseins in the micellar interior and induces the dissociation of a proportion of caseins which results in a reduction of the molecular weight of CM. Second, elevated calcium concentration induces the formation of new intermolecular interactions between caseins and the release of water from casein interfaces. The finding that the strength of the repulsive forces between CM does not change in the presence of β-Lg underlines the fact that the structural changes mainly involve the core of the micelle. Despite the release of κ-casein, the intermolecular interactions remain largely unaffected. For future studies, it would be interesting to investigate the consequences of the ß-Lg effect on the colloidal stability of CM in real milk samples.

Acknowledgments

Authors thank Ilona Hager and Claudia Hengst for their technical support on HPLC analysis. We also thank Namrata Pathak for helpful discussions.

3.2 Application of confocal Raman microscopy to investigate casein microparticles in blend casein/pectin films

Summary and Contribution of the Doctoral Candidate

Caseins (α_{s1}-, α_{s2}-, β-, and κ-caseins), the abundant protein in milk, receive an increasing attention by the food, cosmetics and pharmaceutical industries. Together with colloidal calcium phosphate, the proteins organized in micellar form as CM suspended in milk. Pectin is an anionic polysaccharide consisting of a partially methyl-esterified galacturonic acid backbone with branches of arabinose, galactose and xylose. At neutral pH, individual pectin molecules are mostly negatively charged and separated from each other due to electrostatic repulsion. In this study, casein microparticles were formed in films after addition of pectin to a solution of CM at neutral pH prior to dehydration.

Confocal Raman microscopy was applied to closely examine the spatial distribution of casein and HM-pectin in the dried films. The occurrence of casein microparticles in film matrix was explained by polymer segregation and volume exclusion as reported by complement studies on biopolymers in solution. The incompatibility between the two different polymers at neutral pH plus the concentration increase led to the formation of microparticles in film. During the formation, the particles were compressed becoming ellipsoidal in shape.

This study illustrated the microparticles formation of casein in dried films using confocal Raman microscopy. The formed particles could be isolated to be used to encapsulate bioactive substances.

Most significant contribution to this manuscript was made by the doctoral candidate. This included(i) the conception and design of experiments with critical literature review; (ii) experimental conduction on the sample preparation and characterization of casein microparticles with supports from Julia Sterr on Raman microscopy; (iii) data analysis and data interpretation. Ulrich Kulozik and Ronald Gebhardt initiated the work and reviewed the research plan. In addition, writing and revising of the manuscript was done jointly by doctoral candidate and corresponding author, Ronald Gebhardt, after discussing the results with all co-authors.

*Adapted Original Manuscript**

Application of confocal Raman microscopy to investigate casein microparticles in blend casein/pectin films[1]

Yu Zhuang[a], Julia Sterr[b], Ulrich Kulozik[c] and Ronald Gebhardt[a], *

[a] Chair of Food Process Engineering and Dairy Technology, Technische Universität München, 85354, Freising-Weihenstephan, Germany

[b] Chair of Food Packaging Technology, Technische Universität München, 85354, Freising, Germany

[c] Research Centre for Nutrition and Food Science (ZIEL) - Section Technology, Technische Universität München, 85354, Freising-Weihenstephan, Germany

Abstract

Pectin triggers formation of casein microparticles during solution casting. Confocal Raman microscopy revealed their composition and spatial dimension in resulting films. Peaks in the Raman spectra corresponded to those found in films prepared by either casein or pectin. This suggested that no conformational changes occurred after mixing. Raman images revealed incompatibility of both polymers because particles consisted of casein only and the surrounding matrix of pectin. Deformation of microparticles into an oblate shape took place during film formation. In dried films, an empty space between casein and pectin was found in lateral dimension. In contrast, casein microparticles overlapped with the pectin matrix in vertical dimension.

---

* Adaptions refer to used abbreviations as well as figure, table and section numberings.

[1] Originally published in: International Journal of Biological Macromolecules (2014), Volume 74, page 44-48. Permission for the reuse of the article is granted by Elsevier.

3.2.1 Introduction

Microparticles from protein have been of interest in numbers of applications involving carrying or releasing of bioactive compounds (Bysell et al., 2011; Huppertz & de Kruif, 2008; Santos et al., 2013). Caseins (α_{s1}-, α_{s2}-, β-, and κ- caseins), the abundant protein in milk, receive an increasing attention by the food, cosmetics and pharmaceutical industries. They are organized in micelles (CM) together with colloidal calcium phosphate (Horne, 2006). Integrity of CM is ensured by electrostatic and hydrophobic interactions (Gebhardt et al., 2011a) while steric stabilization is provided by an outer surface layer (Tuinier & de Kruif, 2002).

Addition of polysaccharides have been used to introduce new functionality in foodstuffs (Krzeminski et al., 2014; Tourrette et al., 2009). Pectin is an anionic polysaccharide, which consists of a partially methyl-esterified galacturonic acid backbone with branches of arabinose, galactose and xylose. It is commonly utilized as a stabilizer, gel former and/or viscosity enhancer in protein rich dairy products (Lam et al., 2007). High-methoxyl pectin (HMP) has a high degree of methyl-esterification (degree of methyl esters > 50 %), and is efficient in textural modification and stabilization of acidified milk dairy products (Laurent & Boulenguer, 2003; Nakamura et al., 2006).

The mechanism of complex formation between CM and HMP at various pHs has been widely discussed. At neutral pH, individual molecules are mostly negatively charged and normally separated from each other due to electrostatic repulsion (Maroziene & de Kruif, 2000). Under these conditions, pectin molecules are expelled from CM. This phenomenon is generally related to volume exclusion behavior in two component systems. Excluded volume of large polymers, i.e., CM, restricts the accessibility of small polymers, i.e., pectin. This may lead subsequently to depletion flocculation of large molecules (Hill, 1960).

When pH decreases to pH 4.6 (isoelectric point of CM), the micelles become unstable and start to form flocculated aggregates. This is because of collapse of the ‘hairy’ κ-casein layer (Walstra, 1990). At low pH, pectin is able to bind on the surface of CM. Bridging between neighboring CM occurs at low pectin concentrations

which may lead to subsequent aggregation (Maroziene & de Kruif, 2000). In contrast, a surface layer of pectin is formed at high carbohydrate concentrations preventing interconnection between CM.

Films can be used to study phase transformation (Gebhardt et al., 2009), crystal structure formation (Gebhardt et al., 2014) and deformation (Gebhardt & Kulozik, 2014) of biopolymers. It has been shown that particles rearrange and concentrate by capillary force on a substrate at the early stage of film drying (Tirumkudulu & Russel, 2004). Later, drying forces compress the particles in vertical direction leading to a deformed shape (Tirumkudulu & Russel, 2004). Thereafter, biopolymers are embedded within the dried film matrix (Gebhardt et al., 2009).

Raman microscopy is suitable to visualize the structural homogeneity or composition of biopolymer films (Wellner, 2013). Raman scattering provides information on the vibrational modes which are characteristic for chemical groups within the sample (Ronningen et al., 2014). By combining confocal Raman scattering with high resolution scans, it is possible to analyze the distribution of components in spatial dimension. Previous researchers successfully used confocal Raman microscopy to localize micro-components in cells or tissues (Baranska et al., 2011; Leroy et al., 2014; Zhang et al., 2013). Another advantage of confocal Raman spectroscopy is that it offers a possibility to look inside the samples in a non-destructive way (Deabate et al., 2008; Kavukcuoglu & Pleshko, 2011).

In this study we investigated casein microparticles in films after addition of pectin to a solution of CM prior to film formation. We used confocal Raman microscopy to explore the spatial distribution of the polymers in the film matrix. This allowed us to gain molecular information of the microparticles concerning their structure, composition and flexibility which are not easily accessible in solution.

3.2.2 Materials and methods

3.2.2.1 Materials

CM were extracted from raw skim milk (Molkerei Weihenstephan GmbH & Co, Germany) by centrifugation for 65 min at 31,000 rpm and 25 °C (Heinrich & Kulozik, 2011). A Bis-Tris base buffer (50 mM Bis-Tris with 10 mM $CaCl_2$) was used to

dissolve the pellets. After stirring for 5 h at 37 °C, dust and large casein aggregates were separated by a third centrifugation step (6000 rpm at 25 °C for 10 min). Thereafter, the solution was again centrifuged for 15 min at 12,000 rpm. The supernatant containing the size-fractionated CM was used for the structural study in a final concentration of w/w = 3 % similar to the casein concentration in conventional milk.

HM Pectin (Herbstreith & Fox KG, Germany) was dissolved in a same Bis-Tris buffer at 80 °C and adjusted to pH 6.8 for further use.

After mixing at room temperature, the protein concentration in solution was 3 % (w/w). The final ratio between casein and HM-pectin was 1:0.1 (w/w). Solutions of 0.1 M HCL and 0.1 M NaOH were used for pH adjustment. After stirring for 15 min at 20 °C, the CM/HMP mixture was stored at a cold room (4 °C) for 24 h.

3.2.2.2 Film preparation

After pH adjustment, 2 mL of the CM/HMP matrix were carefully deposited on microscope slides (VWR international, Germany). All slides were placed in an isolated box of 28.8 cm x 40.5 cm x 15.7 cm (length x width x height) at a constant temperature of 20 °C and relative humidity of 30 % for drying. Temperature and relative humidity were monitored by Almemo 2490-1 sensor for more than 36 h. Thereafter, resulting films were removed from the drying chamber and stored at room temperature for Raman measurements.

3.2.2.3 Confocal Raman measurements

Raman spectra were obtained at room temperature using a confocal Raman microscope (Alpha 500, WITec GmbH, Germany), equipped with a Nd:Yag Laser (λ = 532 nm). The polarized laser is passing through a polarization-preserving single-mode optical fiber to the microscope. At a dichroic beam splitter, the beam is deflected to a microscope objective (here: 100x Nikon objective, NA = 1.0) and focused on the sample. The laser polarization is set in x-direction. The scattered Raman radiation passes the same objective and is focused by a multi-mode fiber (here 50 µm core diameter), which is connected to a UHTS 300 spectrometer with a black-illuminated charged coupled device (CCD) camera (Newton DU970 N-BV, Andor, Inc., cooled to -59 °C) and a grating with groove density of 600 g/mm and

500 nm blaze wavelength. A typically Raman image was recorded collecting single spectra at every image pixel (80 x 80 pixel, total 6,400 spectra) with a lateral size of 60 µm x 60 µm (horizontal area scan) and 60 µm x 20 µm (vertical depth scan). The integration time was 37.02 ms per spectrum. For Raman data analysis the program WITec Project (version 2.10, WITec GmbH, Germany) was used. The Raman images showing the distribution of certain constituents were calculated by integrating the corresponding Raman band region of each spectrum in the image. The integrated value then was displayed with a special color profile, where bright colors represent high and dark colors represent low integrated values.

3.2.3 Results and discussion

We used confocal Raman microscopy to identify the spatial distribution of casein and HM-pectin in dried films. At first, we measured reference spectra by applying Raman spectroscopy to films consisting of either casein or pectin. The peaks in the spectra are assigned to characteristic vibrational modes as shown in Fig. 3-8. The Raman spectrum of CM showed strong intensities at 1669 cm^{-1}, 1454 cm^{-1} and 3065 cm^{-1} corresponding to the Amide I, II and B bands, respectively. They are typical assignments for protein backbone vibrations, as stated in literature (Schrader, 1995). For HM-pectin we assigned the peaks at 699 cm^{-1} and 1748 cm^{-1} to out-of-plane vibration of hydroxyls (ring configuration of HM-pectin) and to the C=O stretching of COOH groups, respectively (Synytsya, 2003). Intense bands between 2852 cm^{-1} and 2988 cm^{-1} are visible in both HM-pectin and casein spectra. These bands belonged to the stretching of C-H bonds and their different shapes suggested the varying contributions from CH_2 and CH_3 modes (Snyder et al., 1980). The band between 3200 cm^{-1} and 3500 cm^{-1} corresponded to the inter-molecular hydrogen bonding of the polymers (Synytsya, 2003).

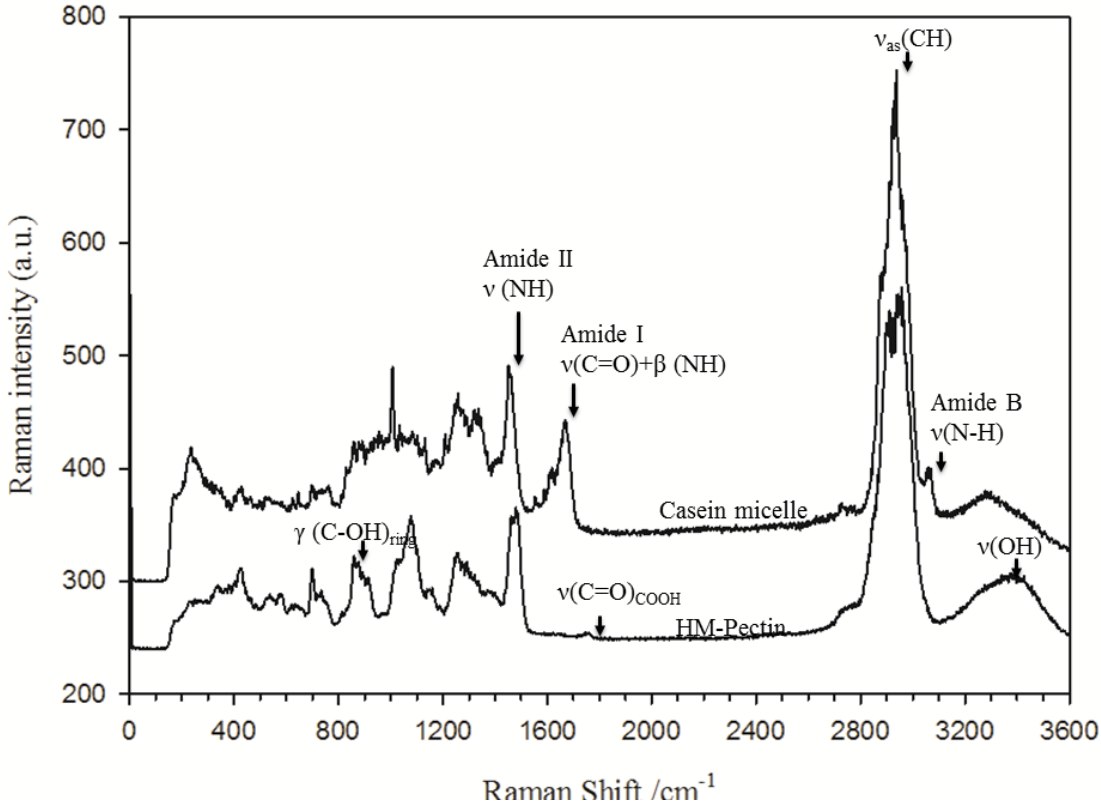

Fig. 3-8: Confocal Raman spectra of films consisting of either CM or HM-pectin.

We mixed 3% casein with HM-pectin (mixing weight ratio 1:0.1) and prepared films using solution casting. Fig. 3-9 shows the resulting film morphology at different magnification. Contrary to films consisting of casein or pectin only (see Fig 3-S.1 in supplementary notes), films of casein/pectin mixtures had a turbid appearance as the digital photograph in Fig. 3-9A shows. Optical micrographs at 10 x (Fig. 3-9B) and 100 x (Fig. 3-9C) magnifications provide a more detailed view. Spherical structures of different size are distributed throughout the film surface. We applied scanning Raman microscopy to access information about the lateral and vertical structure of three spherical objects as shown in Fig. 3-9C. A lateral scan was applied over the whole area of Fig. 3-9C. The black line in the same figure indicates where the vertical depth scan (X-Z direction) was performed.

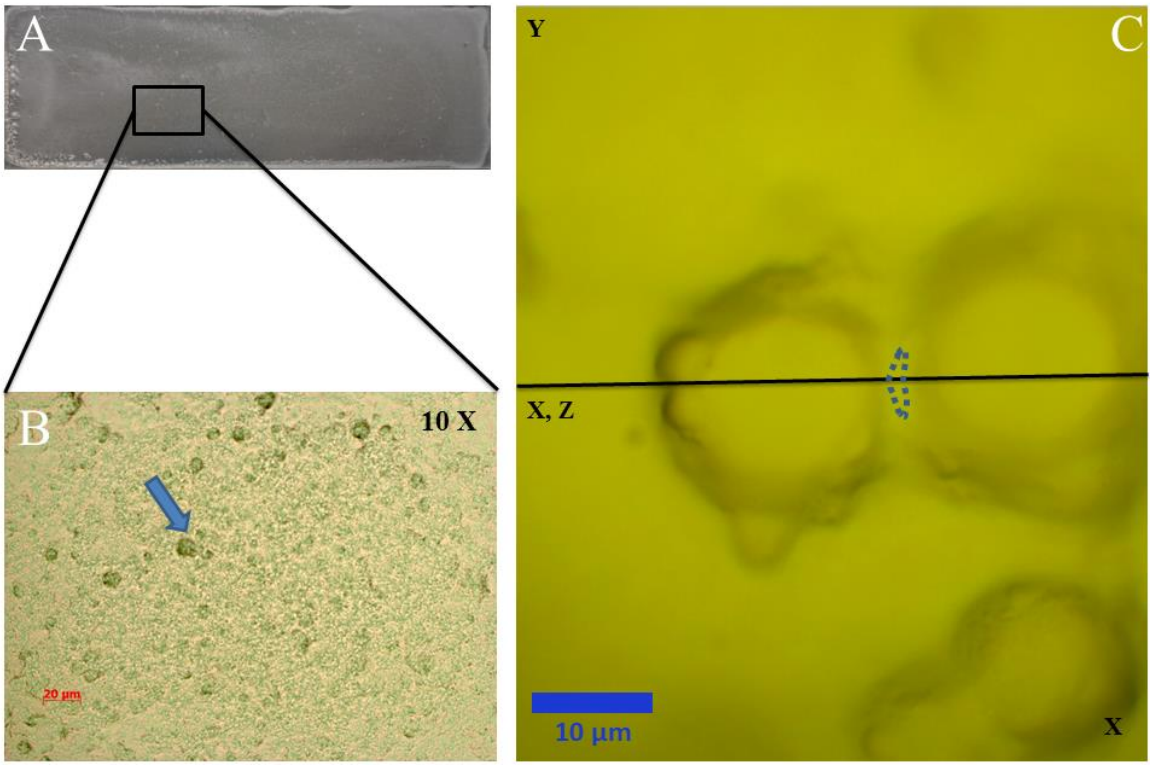

Fig. 3-9: (A) Surface of a film prepared from CM/HM-pectin mixture, (B) optical microscopy image (magnification: 10x) of film surface, (C) microscopic image showing the range where the lateral (X-Y direction) Raman scan was performed. The X-coordinates of the vertical scan (X-Z direction) are indicated by a solid line; one of the border regions is indicated by a dotted line.

We grouped the spectra of the scans into three classes: spherical structure, surrounding and border region. Fig. 3-10 shows averaged spectra of the three groups. While spectra sampled inside the spherical structures belonged to casein, those in the surrounding corresponded to pectin. The border region consisted of a mixture of both polymers at a much lower concentration as the comparison of the spectra in Fig. 3-10 indicated.

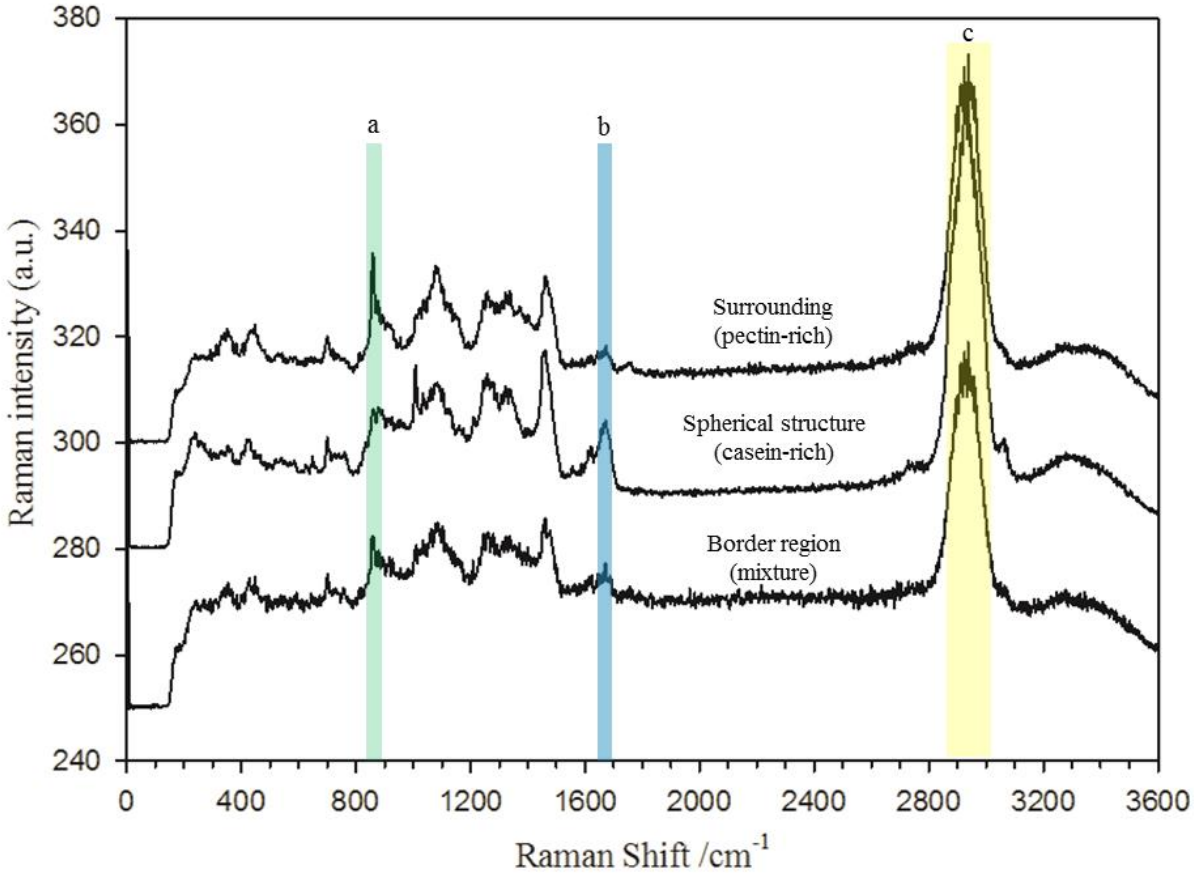

Fig. 3-10: Confocal Raman spectra collected in the spherical structures (casein-rich), surrounding (pectin-rich) and border regions (mixture of both polymers) on blended casein/pectin films. Bands in the range of (a) 837-875 cm^{-1}, (b) 1645-1687 cm^{-1} and (c) 2087-3022 cm^{-1} were the basis for Raman microscopic images shown in Fig. 4 and Fig. 6.

Compared to the spectra of casein or pectin films, those of the mixed films showed no significant shifting of bands or changes of their shapes. This indicated an absence of conformational changes. Such changes could occur for instance after associative polymer-interactions such as complex coacervation (Klemmer et al., 2012).

Both polymers showed rather segregative phase behavior as Maroziene et al. discussed on the basis of a solution study (Maroziene & de Kruif, 2000). In detail, the authors attributed the casein/pectin interactions to the thermodynamic incompatibility or depletion. The spectra taken from the border region of the spherical structures (Fig. 3-9C) showed signature peaks (Amide I and B, CH ring stretching) from

casein and pectin with very low intensities. This indicated smaller concentrations due to the depletion of the polymers in this region.

We mapped the microparticles and the distribution of casein and HM-pectin in the film on the basis of the Raman-scans. Raman images were generated by selecting characteristic bands (marked in Fig. 3-10). We used the intensities between 837-875 cm^{-1} (band a) as an indicator for the concentration of HM-pectin and band b (1645-1687 cm^{-1}) for casein, respectively.

For the Raman images we used a resolution of 0.75 µm (step size) and a beam-size of approximately 400 nm. Using this configuration, we could determine the dimension and composition of structures in the film.

We generated Raman images on the basis of lateral Raman scans. Band A was used for Fig. 11A and band b for Fig. 3-11B. Both images resolved the same round structures as found by optical microscopy (Fig. 3-8). The light green color in Fig. 3-11A (CH deformation of pectin ring configuration) suggested the presence of pectin outside the round structures. Strong intensities of Amide I in Fig. 3-11B indicated an accumulation of casein into microparticles. How do casein-microparticles form during the solution casting process? CM become concentrated during solvent evaporation. Without pectin, we found aggregation into casein microparticles only when a 10 % casein solution was used for film preparation (see supplementary notes Fig. 3-S2). In contrast, no microparticles were found with a 3 % casein solution (see supplementary notes Fig. 3-S1). However, casein-microparticles formed when HM-pectin was added. This is because pectin locally increased the amount of casein above the critical concentration for aggregation due to volume exclusion (Maroziene & de Kruif, 2000).

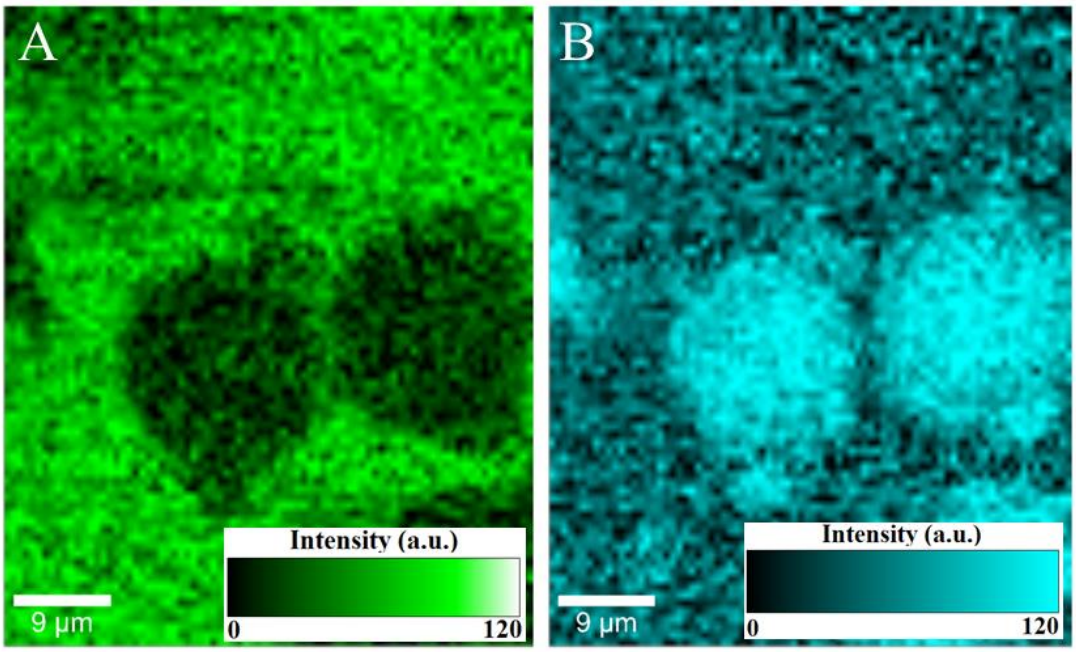

Fig. 3-11: Raman images (x-y direction) generated by integration over selected vibrational bands: (A) γ (C-OH) ring, (B) Amide I.

Fig. 3-12 shows composite Raman images generated by integration of C-OH deformation mode of carbon ring (837-875 cm^{-1}) and Amide I (1645-1687 cm^{-1}). Characteristic peaks of casein and pectin are marked in dark blue and green, respectively. Fig. 3-12A resulted from a vertical scan and provided height information of the microparticles. Yellow line shows position of lateral scan, which was performed approx. 5 µm below the film surface. Hence, both images in Fig. 3-12 show one and the same microparticles from different perspectives. A pectin-layer (green) separated from the caseins (blue) was either attached above or below the microparticles. This suggested that there was no preference of HM-pectin for deposition close to air/solid interface.

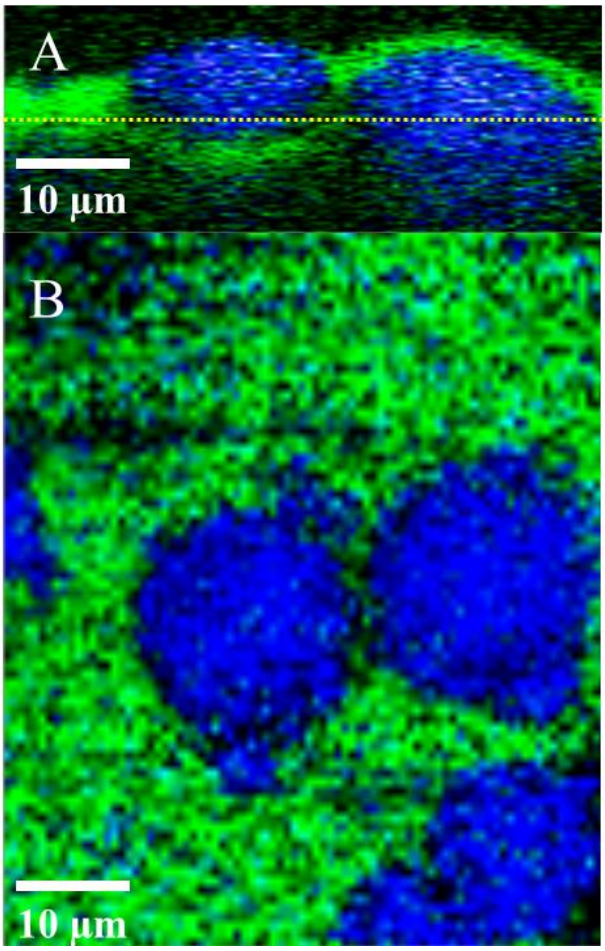

Fig. 3-12: Color-coded Raman microscopic image by integration over selected vibrational bands: (A) vertical direction, (B) horizontal direction, casein-rich region (blue), and pectin-rich region (green).

Fig. 3-12A illustrates the vertical deformation of casein aggregates. The aggregated structures were a result of the volume exclusion effects, which occurred as the solution was concentrated during film formation. In addition, capillary pressure compressed the microparticles in vertical direction. This observation is in agreement with previous studies on colloidal polymer films by König and Russel (König et al., 2008; Tirumkudulu & Russel, 2004).

We calculated the size of casein microparticles on the basis of a simple geometrical shape. The volume of the ellipsoid on the left side of Figs. 3-12A and B is approximately 298.10 μm^3 by considering the major axis as 17 µm and the minor axis as 1.97 µm. The CM in their native state had an average particle diameter of 160 nm (Maroziene & de Kruif, 2000; Tuinier & de Kruif, 2002). Under these considerations one ellipsoidal casein microparticle would contain approx. 1.3×10^5 native CM.

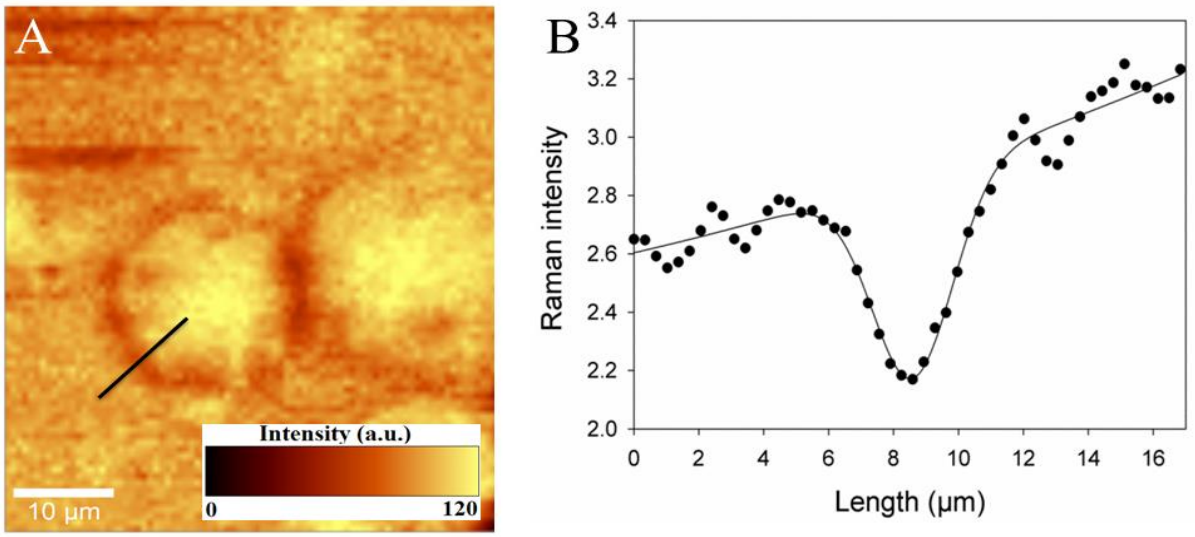

Fig. 3-13: (A): Raman image generated by integration over the CH-stretching band; (B): Height profile of a representative cross-section through Fig. 13A (marked by a black line). The negative peak corresponds to an area depleted of polymers. Peak position and width were analyzed by a Gaussian profile and a 2nd degree polynomial background.

Both polymers showed strong CH-stretching bands (compare Fig. 3-10). We used this band to map regions with low polymer concentration in the film. The space between the microparticles is clearly visible in Fig. 3-13A. We took 8 cross-sections at different positions and plotted an average height profile in Fig. 13B. A detailed analysis let to a width of the gap of 2.65 ± 0.69 µm with two standard deviations ($2 \cdot \sigma \pm 2 \cdot \delta\sigma$). The observed gaps both between casein microparticles and microparticles and the surrounding HM-pectin matrix do not only originate from the segregative phase behavior of the polymers. The distance we found was much greater than what was reported in a previous solution study. The gap width created by depletion forces was found to be in the nm scale (Jenkins & Snowden, 1996). We attributed the much larger gap (2.6 µm) in our study to the relaxation of casein microparticles during film formation. When solvent evaporates during drying, the formed liquid/air interface forces soft matter into an oblate ellipsoidal shape (Tirumkudulu & Russel, 2004). Such a deformation was recently also found for single CM in a film state (Gebhardt & Kulozik, 2014). Ellipsoidal casein microparticle as found in Fig. 3-12 has a higher surface energy compared to a spherical

shape. To minimize the energy a surface reduction takes place leading to a reduction in the lateral expansion. HM-pectin already in the film state- does not follow the retraction movements. The relaxation of the microparticles in the pectin matrix explains why the gaps were only laterally formed. In vertical direction, the ellipsoidal microparticles expand during relaxation leading to a densification of the polymers due to overlapping of caseins and pectin (see Fig. 3-S3 - supplementary notes). The gaps in lateral dimension can be considered as micro-cracks. Energy of deformation is released during relaxation of the casein microparticles. A part of the energy is invested in the creation of new surfaces which results in the formation of the cracks around the microparticles.

3.2.4 Conclusions

We applied confocal Raman microscopy to explore the spatial distribution of casein and HM-pectin in dried films. The occurrence of casein microparticles in the film matrix can be well explained by polymer segregation and volume exclusion and complement studies on biopolymers in solution. As our study demonstrates, confocal Raman microscopy is a suitable method to study the spatial distribution in mixed biopolymer films. In contrast, TEM or AFM have restriction because of limits in contrast and resolution on the surface. The incompatibility between both polymers at neutral pH and the resulting increase in local concentration led to the formation of microparticles. During film formation the particles became compressed into an ellipsoidal shape. There was a gap of several micro-meters between microparticles and pectin matrix in lateral direction while no separation was found in vertical direction. We explained this observation by the relaxation of microparticles. Elastic properties of the microparticles should be investigated in greater detail in future studies. It is also worth to study their inner structure (integrity and connectivity of CM) in order to understand formation and properties of the film structures. Polymer concentration, pH, temperature and drying conditions are crucial parameters we intend to vary in a systematic way to generate microparticles of various size and elasticity. They could be isolated in future and used as either targets to encapsulate bioactive substances or building blocks for bio-based materials. We also intend to map casein microparticles by 3-dimensional Raman scans for more detailed statements concerning their size and shape.

Acknowledgements

The authors thank Yan Yan for technical assistants in preparing films. Herbstreith & Fox KG is acknowledged for their kind donation of HM pectin. Fraunhofer Institute (IVV) is appreciated for its support of providing access to confocal Raman spectroscopy.

Supporting Information

Application of confocal Raman microscopy to investigate casein microparticles in blend casein/pectin films

Films of pure casein and pure pectin

Fig. 3-S.1 shows images of films prepared from pure casein (weight concentration: 3% w/w) (Fig. 3-S.1A) and pure HM-pectin (0.83 %) (Fig. 3-S.1B). On the contrary to mixed casein/pectin film, pure casein and pure pectin films were transparent. No turbidity or microparticles could be observed on the surface of both films. This indicated that at low concentration one polymer alone was not able to induce the formation of microparticles.

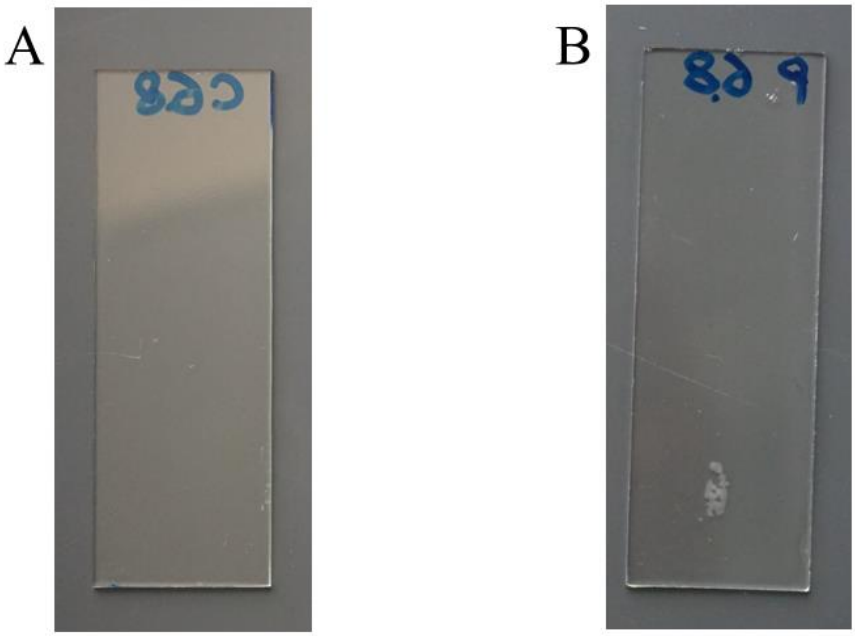

Fig. 3-S.1: Surface of films prepared (A) only from CM and (B) only from HM-pectin.

Optical and Raman microscopy images of films prepared from highly concentrated casein solution (10% w/w)

We prepared films from a 10 % casein bulk solution using solution casting. It can be clearly seen that microparticles were formed on pure casein films. Fig. 3-S.2A depicts a microscopic image of a representative single casein microparticle. The image corresponds also to the range where a lateral Raman scan was performed.

The latter was generated by integration over the Amide II band of the Raman spectra. The size of the microparticle was approx. 40 µm. Hence, it was larger than the microparticles in the casein/pectin mixed films (approx. 15-20 µm). Fig. 3-S.2B shows the Raman image which resulted from the lateral Raman scan. Since contrast is missing in films consisting of one polymer only, Raman intensities of casein are detectable throughout the whole film. A gap around the casein microparticle is visible similar to that seen in the mixed films.

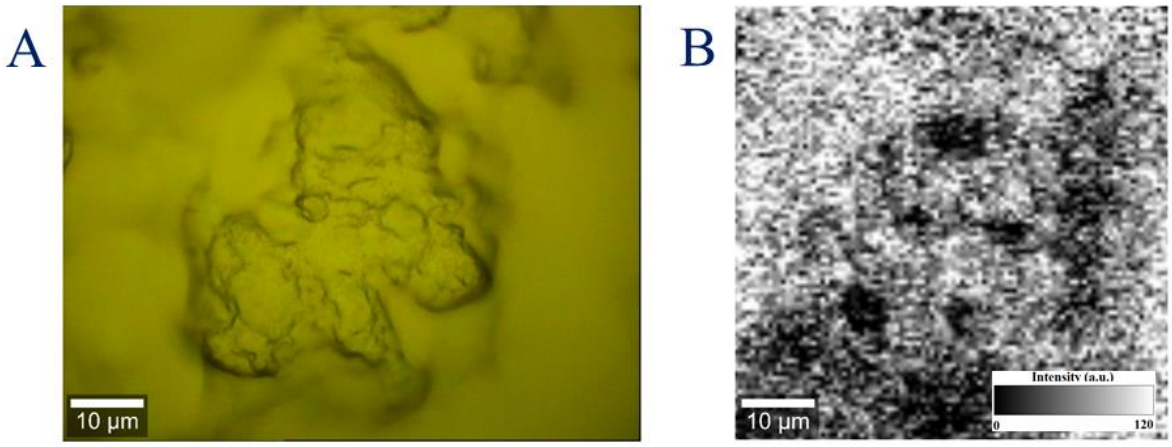

Fig. 3-S.2: A: Microscopic image (100 x) of the film prepared from 10 % casein solution; B: Raman image generated by integration over the Amide II band (1645-1687 cm^{-1}).

Overlapping of casein and pectin-rich regions as observed from composited Raman images in vertical direction (compare Fig. 3-12, main text)

Fig. 3-S.3 shows representative spectra corresponding to the spherical structure (casein-rich), surrounding area (pectin-rich) and the border area in vertical direction. The exact position of the border region is highlighted in Fig. 3-S3B. Characteristic peaks for pectin (γ $(C\text{-}OH)_{ring}$) and casein (Amide I and II) were both visible in this spectrum. In contrast to the spectra of the border region in lateral direction (Fig. 3-10), both peaks showed high Raman intensities.

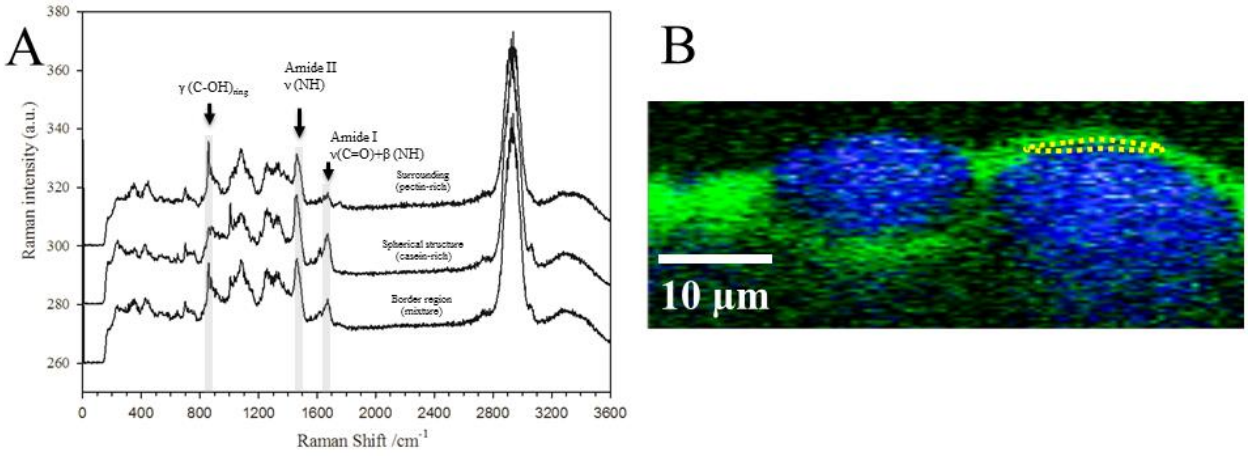

Fig. 3-S.3: A: Confocal Raman spectra sampled in the spherical structures (casein-rich), surrounding (pectin-rich) and border regions in vertical direction (mixture of both polymers) on blended casein/HM-pectin films; B: Highlighted area where spectra for the border region in vertical direction were sampled (compare Fig. 3-12A).

3.3 Casein microparticles from blend films form emulsion droplets with α-tocopherol in solution

Summary and Contribution of the Doctoral Candidate

Protein-based microparticles continued to receive increasing attention by the industry and scientists because of their utility for a variety of applications, such as encapsulation of probiotics or microorganisms and controlled release of hydrophobic bioactive substances. As consumer concerns regarding the use of synthetic materials heightened, applications utilizing edible biopolymers, e.g., milk proteins and polysaccharides, are becoming in the forefront for all.

Casein and pectin are materials widely applied in food and pharmaceutical products. Since casein microparticles are thermodynamically incompatible, pectin can further promote the formation. As a result of pectin depletion, CMs would aggregate among themselves and undergo phase separation. Casein microparticle(s) could form multilayer structures with other components to stabilize the complexes. In a previous study, casein-based microcapsules were produced to protect αT from an unfavorable environment.

For the first time, this study demonstrated a new method to prepare casein microparticles that were stable in solution for no less than three weeks. Deviations in casein composition indicated that the structure of the microparticles harvested from the dried films was differently organized in comparison to that of native CM.

The doctoral candidate made the major contribution to this manuscript. He reviewed existing literatures critically, drew the underlying hypothesis, and designed the experiments. In addition, he did most of the method establishment, carried out major parts of the analyses, interpreted the data collected with support from Julia Sterr on Raman microscopy and Alica Schulte on sample preparation. Doctoral candidate discussed and reviewed the research plan with Ulrich Kulozik and Ronald Gebhardt. Finally, the doctoral candidate wrote and revised the manuscript jointly with corresponding author, Ronald Gebhardt, after discussion with all co-authors.

*Adapted Original Manuscript**

Casein microparticles from blend films form emulsion droplets with α-tocopherol in solution[3]

Yu Zhuang[1], Julia Sterr[2], Alica Schulte[1], Ulrich Kulozik[1,3], Ronald Gebhardt[1,4,*]

[1]Chair for Food and Bioprocess Engineering, Technical University of Munich, 85354, Freising, Germany

[2]Chair for Food Packaging Technology, Technical University of Munich, 85354, Freising, Germany

[3]Institute for Food and Health (ZIEL) - Technology Unit, Technical University of Munich, 85354, Freising, Germany

[4]Institute of Bioprocess Engineering, Friedrich-Alexander-University of Erlangen-Nuremberg, 91052, Erlangen, Germany

Abstract

Microparticles continue to receive widespread attention from food professionals because of their potential use as carriers of bioactive substances. This study demonstrates a novel method to prepare casein microparticles, which co-assemble with αT into emulsion droplets. When the particles were extracted from the pectin matrix via enzymatic degradation, they remained stable in a buffer solution for at least three weeks. Optical microscopy showed that the size distribution of the microparticles is between 5 µm and 50 µm, which is in accordance with previous observations in blend films. High-performance liquid chromatography revealed that the amounts of α_{S1}- and κ-casein in the microparticles are significantly higher than those in native CMs. Confocal Raman microscopy showed that in the presence of αT, the microparticles assemble into emulsion droplets, with phenol in the core and casein in the shell. Herein, we demonstrate a new method to form casein-based emulsion droplets for potential use as carriers of bioactive substances.

---

* Adaptions refer to used abbreviations as well as figure, table and section numberings.

[3] Originally published in: Food Biophysics (2016), Volume 11, page 332-338. Permission for the reuse of the article is granted by Springer.

3.3.1 Introduction

Protein-based microparticles continued to receive increasing attention because of their utility in a variety of applications, such as the encapsulation of probiotics or microorganisms and controlled release of hydrophobic bioactive substances (Cook et al., 2012; Sağlam et al., 2014). Previously, heat-induced aggregation, application of mechanical force, or interactions with other polymers were used to produce protein microparticles (Phan-Xuan et al., 2011; Spiegel, 1999). In particular, the utilization of edible biopolymers, e.g., milk proteins and polysaccharides, became popular as consumer concerns regarding the use of synthetic materials increased (Huppertz et al., 2007; Marreto et al.,2013).

Casein and pectin are widely used in food and pharmaceutical applications (Jensen et al., 2010; Luo et al., 2015; Sedlmeyer et al., 2004). They are negatively charged and repel each other at neutral pH. In aqueous solution, α_{S1}-, α_{S2}-, κ- and β-casein are organized into CMs (de Kruif et al., 2012). The integrity of CM is strongly influenced by the balance between the hydrophobic and electrostatic forces (Horne, 1998). Since casein microparticles are thermodynamically incompatible, pectin can trigger their formation. The exclusion volumes of CM for pectin overlap when the former come close to each other. CM aggregate and undergo phase separation as a result of pectin depletion (Maroziene & de Kruif, 2000). In general, particles formed by segregative separation may subsequently become unstable. They can either dissociate from each other or form gels when the environmental conditions are altered, e.g., an increase in the ionic strength or change in pH (McClements, 2006). Drying can overcome these limitations. This was demonstrated using complexes formed between whey proteins and polysaccharides. i.e., pectin and chitosan (Bastos et al., 2012; Serfert et al., 2013) or sodium caseinate and maltodextrin (Selamat et al., 2009). In dried films, biopolymeric particles build densely packed film structures, in which their integrity is maintained (Gebhardt et al., 2014; Gebhardt et al., 2011c; Gebhardt et al., 2012b).

Caseins are commonly used for delivering bioactive hydrophobic substances and drugs (Elzoghby et al., 2011; Kimpel & Schmitt, 2015; Shapira et al., 2010). For instance, casein can be used to encapsulate vitamin D by taking advantage of the high hydrostatic pressure-induced dissociation of CM and altered solute-solvent

interactions (Menéndez-Aguirre et al., 2014). The addition of calcium induces the reassembling of CM and hence enables the encapsulation of polyunsaturated fatty acid (Semo et al., 2007; Zimet et al., 2011). Caseins can also form multilayered structures with other components in order to stabilize the emulsion (Dickinson, 2015; Hu et al., 2010). In a previous study, casein-based microcapsules were produced to protect αT from an unfavorable environment (Selamat et al., 2009).

αT is a major form of vitamin E, which is essential for human nutrition (Bastos et al., 2012). It is also used as an antioxidant in emulsions or dairy products to extend the shelf life of the products (Hernández et al., 2016; Karmowski et al., 2015). The hydrophobicity of αT hinders several direct applications in aqueous food systems. To overcome this difficulty, the incorporation of αT in a protein matrix has been widely applied, with the additional benefit of shelf life improvement (Luo et al., 2011; Somchue et al., 2009). However, little is known about the use of the particulate form of casein for the formation of droplets with αT-cores in solution.

In a previous study, we used a highly methylated pectin (HM-pectin) to form casein microparticles in a film (Zhuang et al., 2015). HM-pectin can induce casein microparticle formation in solution due to the thermodynamic incompatibility between the two polymers. The microspheres become unstable if the polysaccharides are degraded by, for example, enzymatic hydrolysis. Drying the films immobilizes the microparticles in the casein/pectin matrix. The ellipsoidal shape of the casein microparticles indicates their deformation by capillary forces. However, the microparticles' becoming embedded in a dried film limits their further application as a functional material.

The current study shows that casein microparticles (1) can be solubilized in a buffer solution after enzymatic extraction from dried casein/pectin films, and (2) can form emulsion droplets with αT in a model system. The proposed procedure enables the manufacture of casein-based microparticles with potential use in functional foods.

3.3.2 Materials and Methods

3.3.2.1 Sample preparation

CM were extracted from raw skim milk (Molkerei Weihenstephan GmbH & Co, Germany) by centrifugation at 31,000 rpm for 65 min at 20 °C. A Bis-Tris base buffer

at pH 6.8 (50 mM Bis-Tris with 10 mM $CaCl_2$) was used to dissolve the resulting pellet at 20 °C for 2 h, followed by mixing at 4 °C for 12 h, until the CM was completely hydrolyzed. The particle size distribution of the CM in buffer solution was measured using dynamic light scattering (Zetasizer Nano-Z ZEN 2600, Malvern Instruments GmbH) and compared with that in raw milk (see Supporting information S.1). No significant difference between the two distributions was observed. The buffer was used to ensure constant pH conditions during the experiments and to avoid interactions with other components in the raw milk.

HM-Pectin (Herbstreith & Fox KG, Germany) with a 75% degree of methylation was dissolved in the same Bis-Tris buffer at 20 °C for 12 h. The solution was adjusted to pH 6.8 using 0.5 M HCl.

CM and HM-pectin were mixed thoroughly at 20 °C. The final concentration of casein was 2.5% (w/w), and the casein:HM-pectin ratio was 1:0.1 (w/w). Solutions of 0.1 M HCl and 0.1 M NaOH were used for adjusting the pH to 6.8. The CM/HM-pectin mixture was stirred at 20 °C for 30 min prior to film preparation.

3.3.2.2 Microparticle formation in casein/pectin blend film

2 mL of CM/HM-pectin (mixing ratio: 1:0.1 w/w) mixture was evenly deposited on each of the 27 microscope slides with cut edges (VWR International, Germany). A drying chamber at a constant temperature of 20 °C and relative humidity of 30% was used for dehydrating the films over 24 h. The dried films were stored in a clean container at 20 °C.

3.3.2.3 Enzymatic degradation of casein/pectin blend film

Pectinase (10% w/w, > 1 U/mg) from Aspergillus niger (Sigma-Aldrich, Germany) was used to extract the casein microparticles from the films by degrading the pectin matrix. The dried films on the glass slides were deposited in vacuum tubes containing 8% (w/w) pectinase in the above-mentioned Bis-Tris buffer solution. The enzymatic hydrolysis proceeded to completion after 60 min at 47 °C and resulted in a turbid solution. The resulting solution containing casein microparticles was centrifuged at 4,000 g for 15 min to remove residual pectin and pectinase. The

pellets, retained as a precipitate in the centrifugation tubes, were collected and dissolved in Bis-Tris buffer for further investigation.

3.3.2.4 Particle sizes

An Axiovert 135 optical microscope (Zeiss, Germany) was used to measure the size of the casein microparticles in solution at 40× magnification. Measurement on 100 individual particles was conducted for each preparation, and particle size determined using the tools provided by the Axio Vision software (version 6.4x, Zeiss, Germany). The diameter of the particles was also recorded for generating a histogram with 10 classes using Sigma Plot 12.3 (Systat Software Inc, USA).

3.3.2.5 High-performance liquid chromatography (HPLC)

A mixture of 0.4 mL of sample in 1.6 mL of guanidine buffer (6 M guanidine-HCl, 5.37 mM trisodium citrate, 19.5 mM dithiothreitol (DTT) in 0.1 M Bis-Tris buffer) was placed in an Eppendorf reaction pipette for 30 min. The mixture was then filtered through a regenerated cellulose syringe filter with a membrane pore size of 0.45 µm, prior to injecting the filtrate into high-performance liquid chromatography (HPLC) vials for measurement. The concentration of individual caseins in the microparticles was determined using an Agilent 1100 series RP-HPLC system (Agilent Technologies, Germany) following the procedure described elsewhere (Bonfatti et al., 2008; Bonizzi et al., 2009). The chromatograms obtained were evaluated using ChemStation (version B.04.03) for LC systems (Agilent Technologies, Germany).

3.3.2.6 Formation of casein/α-tocopherol emulsion droplets

The synthetic αT (purity ≥ 96%) obtained from Sigma-Aldrich, Germany, appeared to be a yellow-brown viscous liquid at room temperature. 0.5 g of αT was placed at the bottom of a beaker and 5 mL of Bis-Tris buffer solution containing the casein microparticles (total casein conc. = 1 mg/mL) were added. The solution was immediately mixed at 20 °C for 60 min under mild stirring using a magnetic stirrer. Emulsion droplets were formed when the hydrophobic excess αT automatically migrated

to the liquid/air interface. Subsequently, the solution containing the casein/αT droplets was centrifuged at 5619xg at 20 °C for 20 min. The resulting pellets were dissolved in the Bis-Tris buffer for further investigation.

3.3.2.7 Confocal Raman microscopy

Raman spectra were recorded on a Witec Alpha 500 (Witec GmbH, Ulm, Germany) instrument powered by a Nd:YAG Laser (λ = 532 nm). The laser was polarized in the x-direction and deflected to a 100× Nikon objective lens (NA = 1.0). Back-scattered spectra were transferred through a multimode fiber (50 µm core diameter) to a UHTS 300 detector with a black-illuminated charged-coupled device (CCD) camera (Newton DU970 N-BV, Andor, Inc., cooled to −60 °C). The camera was equipped with 600 g/mm gratings and 500 nm blaze wavelength. All spectra were obtained with an integration time of 37.02 ms and a wavelength accuracy of 2 cm−1. The data acquisition and analysis were performed using the Witec Control and Witec Project software (version 4.10). Spectra were obtained for every pixel of the lateral area scan (60 × 60 µm2, 80 × 80 pixels). Color-coded Raman maps were acquired by integrating the bands characteristic for selected materials. Bright color values on the image represent high amounts of the corresponding material (i.e., high integral values), while dark colors correspond to low values.

3.3.3 Results and Discussion

3.3.3.1 Isolation and characterization of casein microparticles

We prepared blended casein/pectin films to obtain casein microparticles as described in a previous study (Zhuang et al., 2015). 2 mL of the casein/pectin solution on a single glass slide generated ~2 × 10^5 microparticles. The schematic in Fig. 3-14a illustrates the steps involved in the preparation of casein microparticles in solution. We used pectinase to hydrolyze the films at 47 °C for 1 h. This allowed the release of the casein microparticles into the Bis-Tris buffer solution. After centrifugation, we obtained pectin residues in the supernatant and microparticles in the pellet. Thereafter, the obtained pellet was resuspended in Bis-Tris buffer. The microparticles in solution were stable at 4 °C for at least three weeks after the formation. Drying in the film state is the decisive step in the procedure, since the

integrity of the particles in the absence of pectin is provided only by drying (see Fig. 3-S.5 in Supporting information).

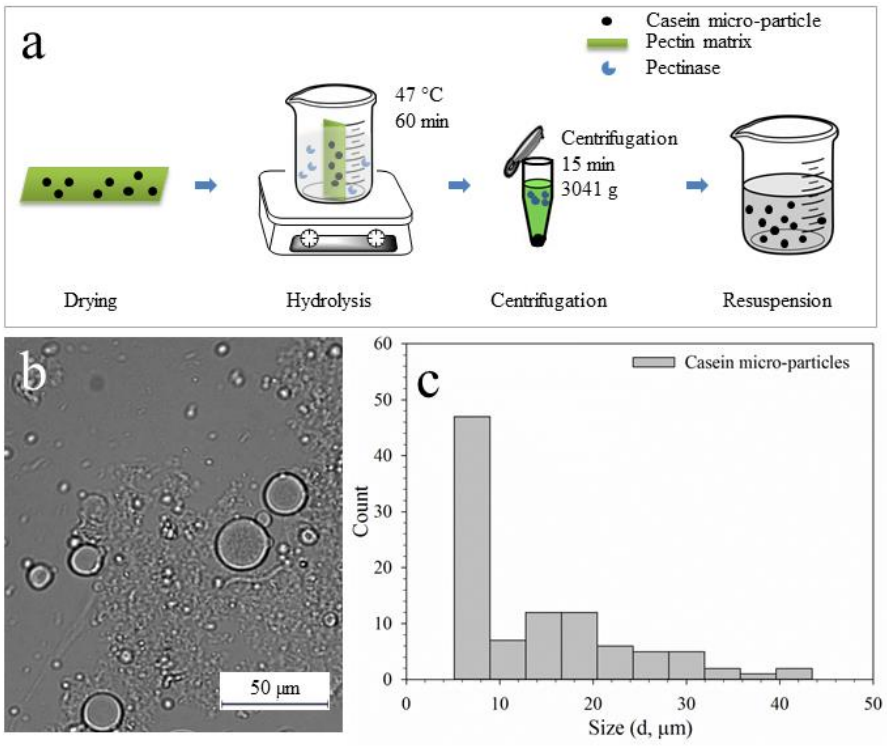

Fig. 3-14: a) Schematic of the isolation process, including enzymatic hydrolysis of pectin/casein films followed by separation of casein microparticles from pectin residues in solution; b) an optical microscopy image of representative microparticles resuspended in solution; and c) histogram of the casein microparticle size distribution in solution.

Fig. 3-14b demonstrates the round shape and homogeneous surface morphology of the particles in solution. There is no indication that the ellipsoidal form the particles adopted in the films persists. The size distribution of the particles ranges between 10 and 50 µm, as seen from Fig. 3-14c. The stability of the casein microparticles can be attributed to the deformation of the overall structure during film formation. The concomitant compaction probably led to additional internal crosslinking (hydrophobic interaction-induced non-covalent bonding) between caseins within the particles (see also Fig. 3-S.10 in Supporting information). This conclusion was arrived at from the following observations. When the particles were dissolved in different solutions, e.g., EDTA, SDS, and DTT, as shown in Fig. 3-S.8, the samples in SDS solution became less turbid compared with EDTA and DTT.

We therefore assumed that the crosslinking within the microparticles could be mainly attributed to hydrophobic interaction-induced binding.

3.3.3.2 Composition of casein microparticles

We determined the composition of the casein microparticles by HPLC (original chromatograms are shown in Fig. 3-S.6 in Supporting information). Casein microparticles have different proportions of caseins compared with CM in skim milk. The amounts of α_{S2}- and β-casein are significantly lower, whereas those of α_{S1}- and κ-casein are higher, in the microparticles (Fig. 3-15). Since HPLC is not adequate to determine the mechanism behind the compositional change, we propose two possible explanations for this observation. As the CM aggregate, the dissociation of α_{S2}- and β-casein might take place, or CM with more α_{S1}- and κ-casein preferentially assemble to form casein microparticles, resulting in the differences in composition as well as internal structure between them. Compared with natural CM, the microparticles have a different composition and altered internal structure. In a previous study, we showed that CM are mainly stabilized by hydrophobic and electrostatic interactions (Gebhardt et al., 2011b). Furthermore, it is well known that CM become unstable at pH values < 5.2 (de Kruif, 1999). Casein microparticles, however, remain stable over a broad pH range between pH 3 and 10.5 (see Fig. 3-S.8 in Supporting information). This indicates that casein microparticles are, in contrast to native CM, mainly stabilized by hydrophobic interactions. The mechanisms that govern these differences remain unclear. Our hypothesis is that a new structure forms (as indicated by the occurrence of a new Raman band) via a hydrophobic interaction during the film formation. This structure might contribute to the stability of the particles against pH changes.

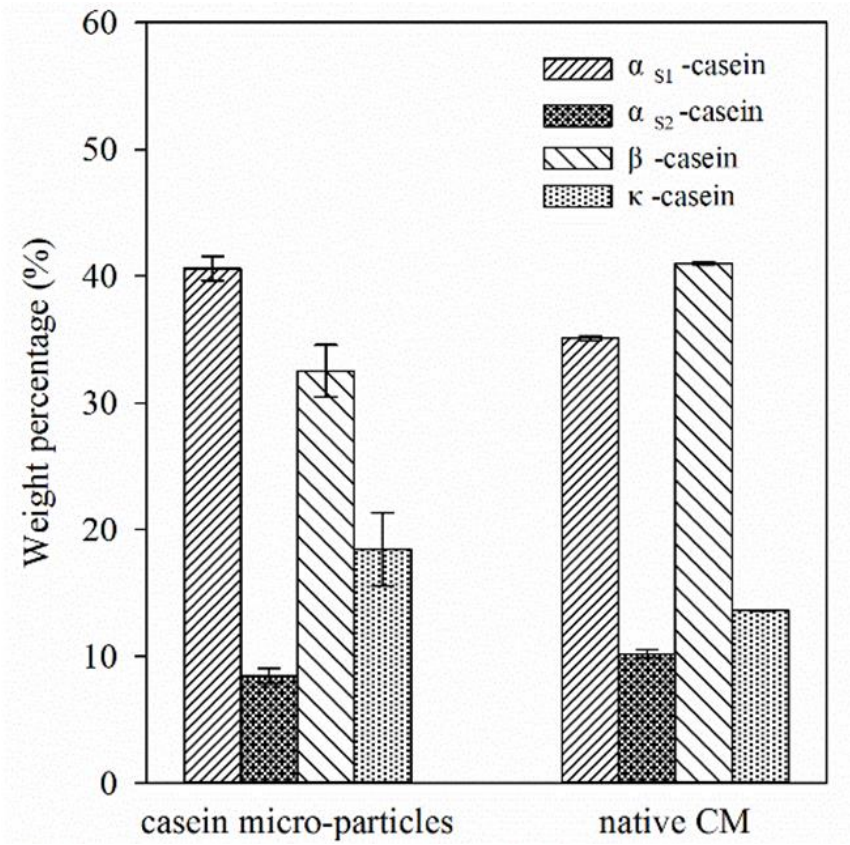

Fig. 3-15: Comparison of relative contents of caseins (weight percentage) in the microparticles and native CM.

In addition to HPLC, Raman spectroscopy was used to obtain additional information about the microparticles. The images from confocal Raman microscopy provide detailed information about the structure of a single casein microparticle. Raman intensities integrated over the Amide I band (between 1646 and 1686 cm^{-1}) were used to generate the color-coded map shown in Fig. 3-17a (for the full spectra, see Fig. 3-S.7 in Supporting information). No differences in the amide region between the Raman spectra of casein microparticles and native CM can be seen. This is because amide bands are sensitive to secondary structures, which are all random for caseins. There are, however, differences at lower wavenumbers (700 cm^{-1}), which we could not assign to any specific vibration mode in this study. The Raman maps further showed no voids, which implies that the caseins are evenly distributed within the microparticles.

3.3.3.3 Emulsion droplets made from casein microparticles and α-tocopherol

The process used for the preparation of emulsion droplets in solution using microparticles with αT is shown in Fig. 3-16a. αT was placed in a beaker and casein microparticles dissolved in Bis-Tris buffer were added such that the solution overlaid the αT. Mechanical mixing was performed to disperse the αT in the buffer solution. This increases the probability of contact between the microparticles and αT. The incorporated αT moved to the liquid/air interface and underwent phase separation because of its hydrophobic nature. The procedure used for αT incorporation caused no obvious change in the shape and morphology. However, the particle size distribution was altered (compare Figs. 3-14c and 3-16c). The frequency of particle sizes smaller than 10 µm decreased after mixing with αT while that of the larger particles increased.

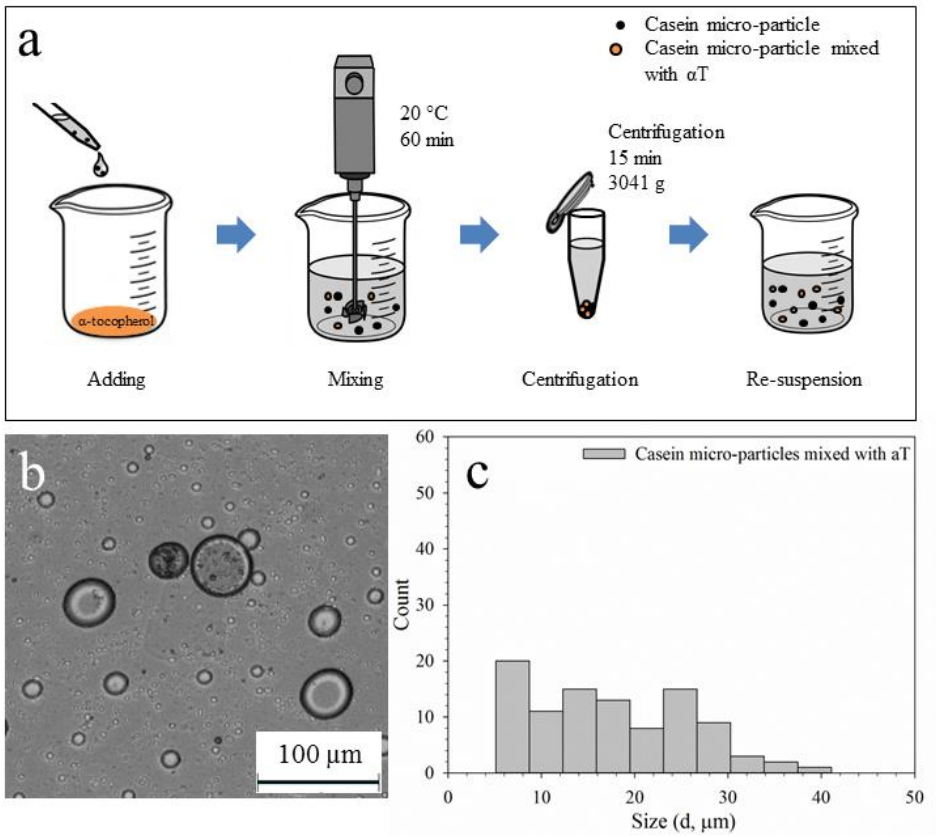

Fig. 3-16: a) Schematic of the encapsulation process. Mixing by a stirrer was followed by centrifugation to separate emulsion droplets from excess αT; b) an optical

microscopy image of a representative emulsion droplet; and c) histogram of the sizes of casein/αT emulsion droplets in solution.

ATR-FTIR measurements (see Supporting information Fig. 3-S.8) performed on washed pellets also showed that αT was incorporated in the casein microparticles. However, ATR-FTIR measurements provide spectra averaged over a large sample surface and therefore information about the microstructure of the emulsion droplets could not be obtained. For that reason, we used confocal Raman microscopy again to elucidate the structure at the single-particle level.

Compared with caseins, αT shows a significant band in the Raman absorption in the range between 1336 and 1368 cm^{-1}. This band corresponds to CH_2 twisting, as other Raman studies on αT have shown (Beattie et al., 2007; Feng et al., 2013). Fig. 3-17a shows a Raman map of a casein microparticle generated by integrating over the Amide I region. Details of the wavenumbers used to mark the components in the Raman map are provided in Fig. 3-S.10 of the Supporting information. Fig. 3-17b shows a Raman map of casein/αT droplets. The αT-rich region in the Raman map is shown in blue and the casein-rich regions in red. The αT forms the core of the emulsion droplets while caseins stabilize the interface by forming a layer to the surrounding solution. We note that not all microparticles form emulsion droplets with αT. Based on the results from the Raman, 3 out of 15 microparticles were loaded with αT and formed emulsion droplets. The rest of particles remained unchanged in their structure.

We estimated the volume of a representative emulsion droplet, shown in Fig. 3-17b, using a simple spherical model. The thickness of the casein shell is ~5 µm and the radius of the inner αT droplet is ~16 µm. Based on these values, we calculated a volume of ~21,635 $µm^3$ for the casein shell. Approximately 200 microparticles are needed to form a shell with a thickness of 5 µm, if we assume a particle diameter of 6 µm as the most frequent size for the smaller particles. Emulsion droplets are larger than the unloaded ones and contribute, with diameters of around 30 µm, to the new population in the size distribution (compare Fig. 3-16c). Emulsion droplets deviate from the structure of casein microparticles. A core formed by αT alone is surrounded by caseins, which stabilize the interface with the aqueous solution because of their amphiphilic nature. Our observation supports

previous work, which showed that colloidal particles can effectively stabilize the interfacial structure in dispersions or emulsions (Dickinson, 2015). Based on the histogram in Figs. 3-14c and 3-16c, a mechanism for the formation of the casein/αT droplet can be derived. Smaller casein particles, which occur in a higher number in Fig. 3-14c, probably move to the αT/water interface of the droplets and form a shell with a thickness of 5 µm around them.

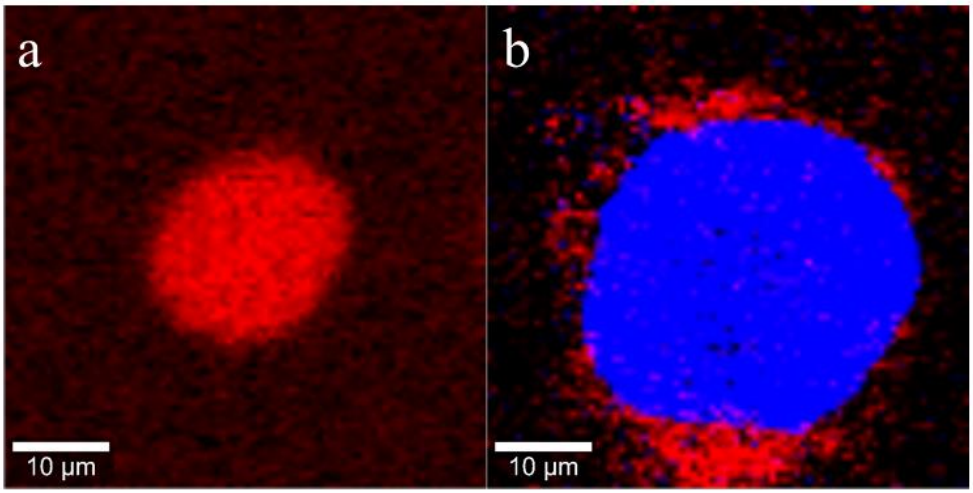

Fig. 3-17: Color-coded Raman maps of a casein microparticle (a) and a casein/αT emulsion droplet (b) generated by a lateral scan (αT-rich region is shown in blue and casein-rich regions in red).

3.3.4 Conclusions

In this study, we developed a new method to prepare casein microparticles, which are stable for at least three weeks in solution. Deviations in the casein composition indicate that the structure of the microparticles is differently organized compared with native CM. Compression during the film formation produces a compact internal structure of the protein molecules in each microparticle. The hydrophobic contacts are the dominant interactions. Electrostatic interactions play a minor role, since no acidic disintegration of the casein microparticles was observed. The microparticles encapsulate αT by mixing in a stirred solution without the use of additional processes such as enzymatic crosslinking, high pressure, or thermal treatment. This would be especially interesting if the encapsulation of heat- or pressure-sensitive substances were to be conducted without further additives, such as enzymes. Confocal Raman microscopy is a useful tool to demonstrate that casein microparticles

and αT co-assemble into an emulsion droplet. The mechanisms that make the microparticles stable at low pH are an interesting topic for future work on this subject. In the future, it will also be worthwhile to optimize the enzymatic treatment during microparticle preparation and determine the exact amount of αT within the emulsion droplets after its incorporation. Furthermore, the encapsulation efficiency could be improved by modifying process parameters. In general, this study offers a new route for the creation of microparticles with bio-functional properties.

Acknowledgements

The authors thank Yan Yan for technical assistants in preparing films. Herbstreith & Fox KG is acknowledged for their kind donation of HM pectin. Fraunhofer Institute (IVV) is appreciated for its support of providing access to confocal Raman spectroscopy.

Supporting information

Casein microparticles from blend films forming casein/α-tocopherol emulsion droplets in solution

Particle-size distribution of CMs in raw skim milk and a Bis-Tris buffer

We compared the particle size of CM in raw skim milk and in a Bis-Tris buffer system. The particle size distribution is shown in Fig. 3-S.4. No significant differences between particle sizes in the buffer system and raw milk were observed. It is considered that the CM retain their integrity in the Bis-Tris buffer upon the addition of 10 mM $CaCl_2$.

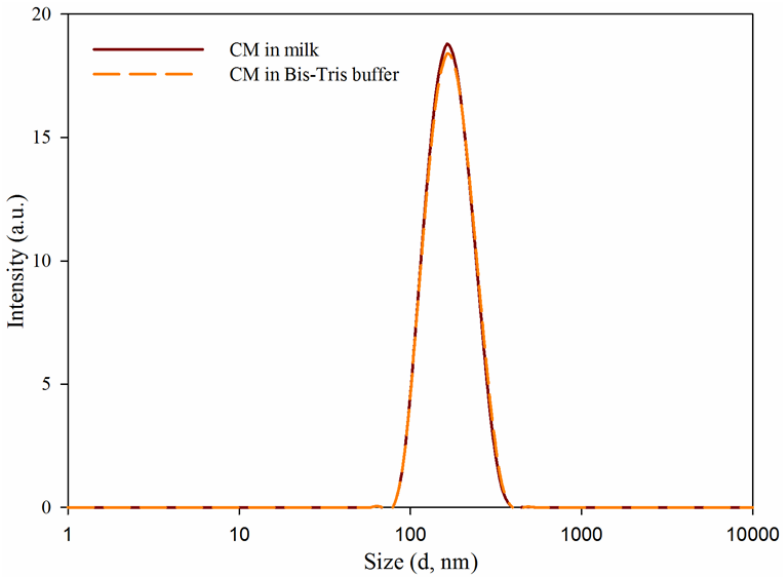

Fig. 3-S.4: Particle size distribution of CM in a Bis-Tris buffer solution and raw skim milk.

Addition of pectinase to casein microparticles in solution for bypass-film formation

This series of experiments aimed to investigate the effect of pectinase on the formation of casein microparticles in solution. We deposited a droplet of casein/pectin blend, which was prepared as mentioned in the main manuscript, on a glass slide under an optical microscope. A cover glass was carefully placed on top of the droplet. An image, shown in Fig. 3-S.5a, was recorded, which displayed the spherical casein microparticles. Meanwhile, certain microparticles began to merge and

formed rod-shaped particles. Then, a 5% pectinase solution was introduced using a syringe on the edge of the cover glass, allowing the pectinase to diffuse into the casein/pectin solution on the slide. The microparticles instantaneously disappeared upon contact with pectinase (Fig. 3-S.5b) as the pectin matrix was hydrolyzed. Within 5s, all the casein microparticles were dissolved into the liquid phase (Fig. 3-S.5c). This indicates that the electrostatic interaction between pectin and casein was ins3-ufficient to sustain the physical integrity of the particles suspended in the solution. It was the compaction of the microparticles during film drying that played an important role in preserving the particles, especially when the particles were released in the solution.

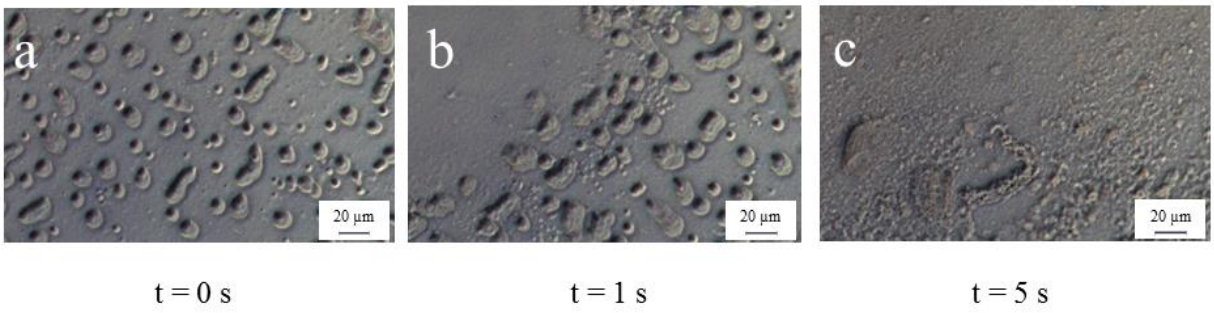

Fig. 3-S.5: Optical images of casein microparticles dissolved by pectinase solution at contact times of a. 0, b. 1, and c. 5 s.

High-performance liquid chromatography (HPLC) chromatograms of caseins in native CM in a Bis-Tris buffer and in casein microparticles in solution

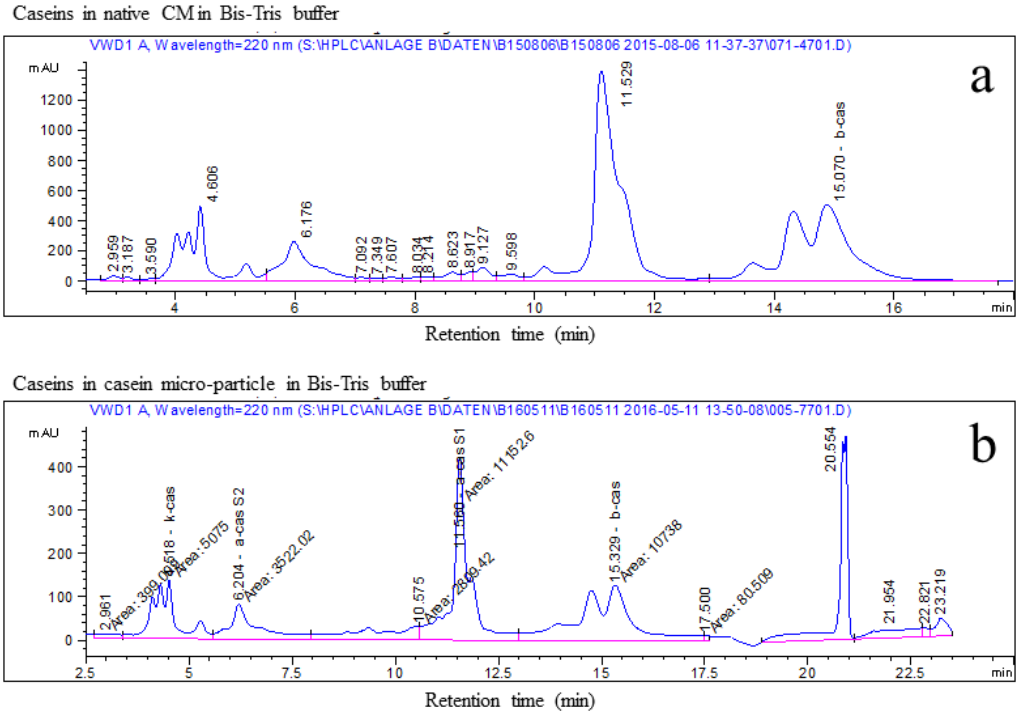

Fig. 3-S.6: High-performance liquid chromatography (HPLC) chromatograms of caseins in native CM in a Bis-Tris buffer and in casein microparticles in solution.

Raman spectra of casein microparticles in film and in solution after pectinase hydrolysis

Fig. 3-S.7 shows representative spectra corresponding to the casein microparticles in film and in solution after enzymatic hydrolysis. Characteristic peaks for casein (Amide I, II and B) are visible in the spectra. The Raman intensities of the microparticles in solution are similar in both the film and in solution.

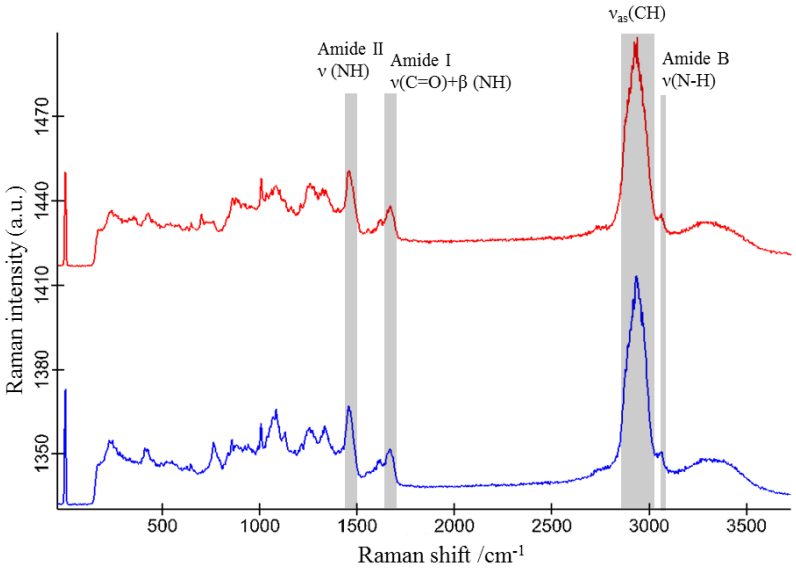

Fig. 3-S.7: Raman spectra of casein microparticles in film (red) and as sediments from solution (blue) after enzymatic hydrolysis.

Optical investigation of casein microparticles under various pH values and storage times

This set of experiments aimed to investigate the effect of pH on casein microparticles. Fig. 3-S.8 shows optical images of these particles over a broad pH range. The particles remain spherical under optical investigation. However, their sizes slightly change when the pH is altered. We attribute this observation to the changes in hydration of the casein microparticles.

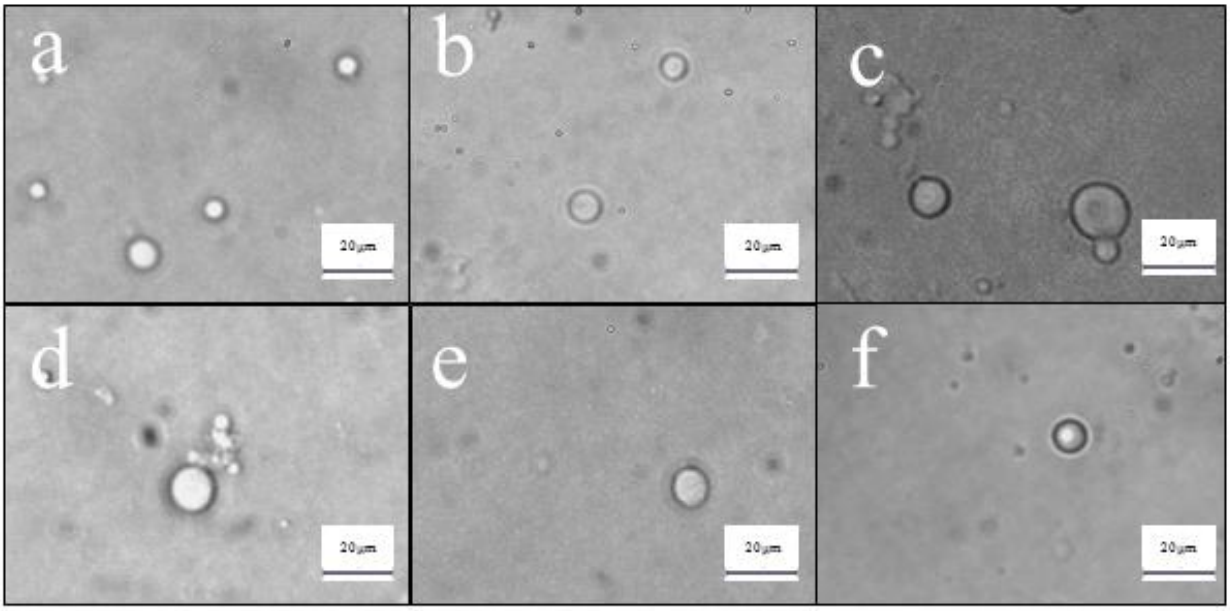

Fig. 3-S.8: Optical images of casein microparticles under a. pH = 3.2, b. pH = 4.7, c. pH = 5.2, d. pH = 8.5, e. pH = 9.5, and f. pH = 10.5.

Dissolution of casein microparticles in EDTA, DTT and SDS solution

Dissolving protein aggregates in organic solvents is an effective way to identify the specific binding between the molecules. For example, EDTA is a preservative that chelates divalent cations (e.g., Ca^{2+} or Mg^{2+}). SDS breaks up the two- and three-dimensional structure of the proteins by adding a negative charge to the amino acids. In addition, DTT is a strong reducing agent, which disrupts the tertiary and quaternary structure by reducing disulfide bonds. We mixed our microparticles in these solutions and compared their turbidity with the particles in Bis-Tris buffer. After 24 h storage, the casein dissolved in SDS shows less turbidity compared with

other solvents. Therefore, we assumed that the assembly of caseins into microparticles is primarily because of non-covalent bonding between caseins, which might be induced by hydrophobic interactions. However, we are unable to specify the nature of the binding in this study.

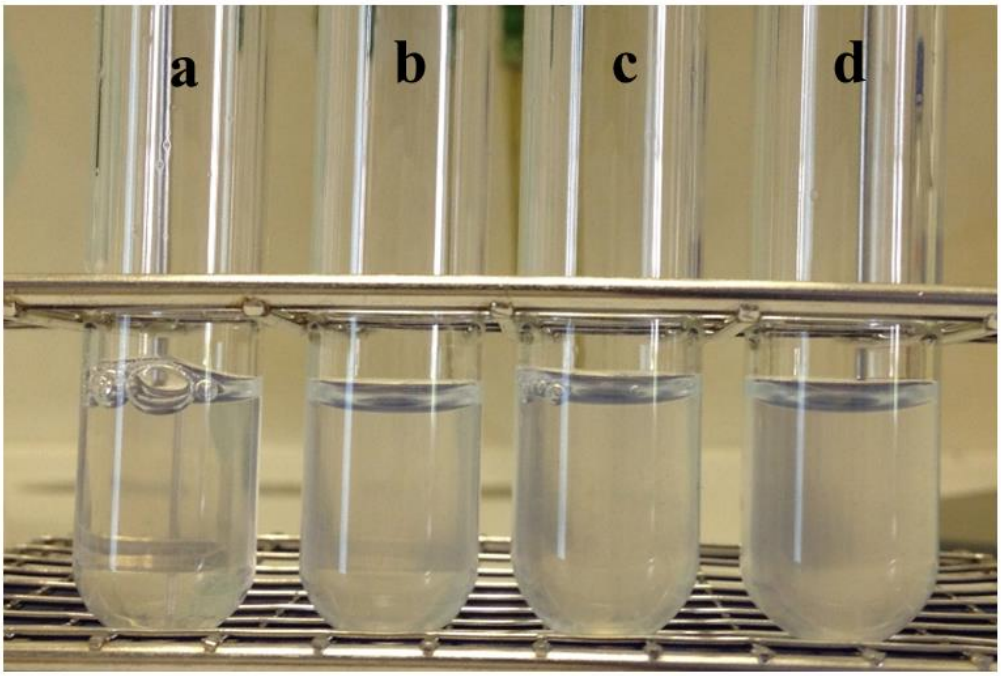

Fig. 3-S.9: Dissolution of casein microparticles in organic solutions, a. 1 mM SDS, b. 1 mM EDTA, c. 19.5 mM DTT, and d. 50 mM Bis-Tris buffer.

Fourier transform infrared spectroscopy (FT-IR)

A Tensor 27 spectrometer (Bruker Optik, Ettlingen, Germany) was used to record FT-IR spectra using a deuterated triglycine sulfate (DTGS) detector. The spectrometer was equipped with a GladiATR (single-reflection diamond-attenuated total reflectance) accessory (PIKE Technologies, Inc, Madison, USA). The spectrum of each sample was obtained by taking the average of 24 scans at a resolution of 4 cm^{-1}. It was recorded between 4,000 and 400 cm^{-1}, at a scan rate of 10 KHz and a background of 24 scans. The reference spectra were recorded using a blank ATR crystal for each sample. Casein microparticle sediments were obtained by centrifugation at 4,000 rpm for 15 min at 20 °C. They were carefully deposited on a diamond crystal and dehydrated before measurements in order to minimize the effect of free water in the sample.

Fig. 3-S.10a shows the FT-IR spectra between 2,880 and 2,960 cm^{-1} of the casein microparticles alone as sediment, those mixed with αT, and αT alone. The peak at 2,925 cm^{-1}, assigned to the CH_2 stretching, was used to identify the presence of αT. The second derivative (Fig. 3-S.10b) clearly illustrates the characteristic peak. The strong intensity indicates that αT was successfully retained in the casein microparticle sediment. However, we were unable to confirm the entrapment of αT droplets within the microparticles. Therefore, using confocal Raman microscopy, the spatial distribution of the tocopherol-loaded microparticles at the single-particle level (main text, section 3.3.2) was obtained for further study.

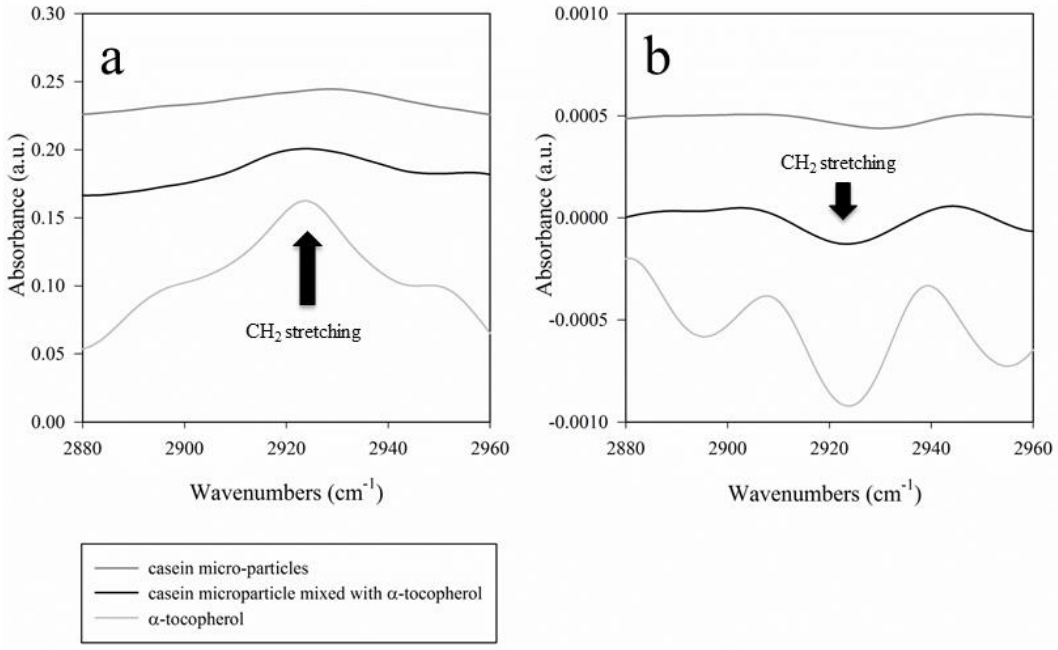

Fig. 3-S.10: a) ATR-FTIR spectra and b) second-derivative spectra of casein microparticles, those mixed with αT, and αT alone.

Raman spectra of casein/α-tocopherol emulsion droplet

Fig. 3-S.11 reveals representative spectra corresponding to the αT core and casein shell in the microparticles after the encapsulation process. We used the vibrational band between 1336 and 1368 cm^{-1} as the characteristic band for αT. This band corresponds to the CH_2 twist in tocopherol. In addition, the Amide I band is again used to identify casein.

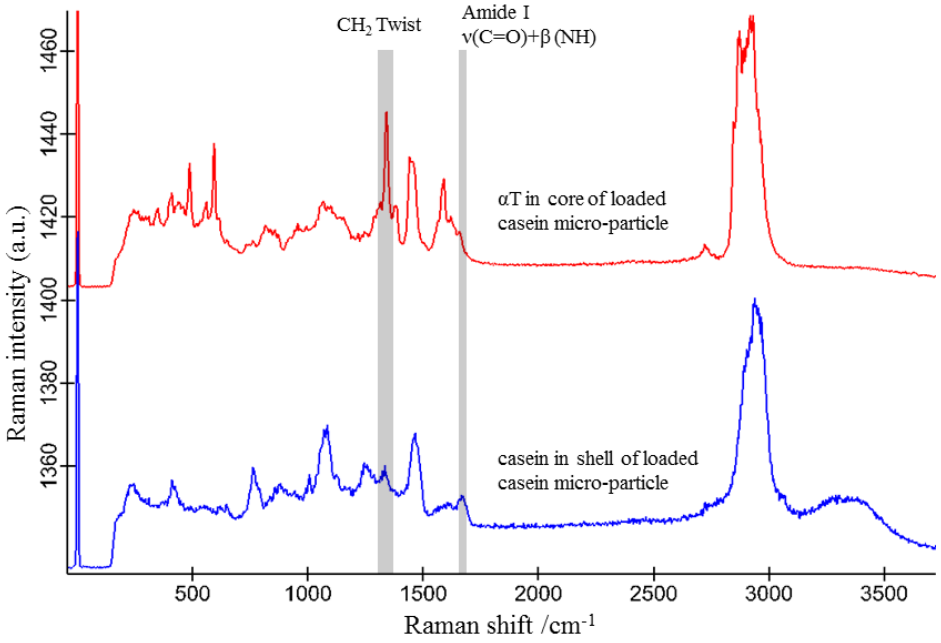

Fig. 3-S.11: Raman spectra of casein shell (blue) and αT core (red) of casein microparticles after the encapsulation process.

Scanning electron microscopy (SEM)

Casein microparticles and casein/αT emulsion droplets were suspended in Bis-Tris buffer. Approximately 40 µL of sample was spread over a glass slide (25 × 75 mm) and dried under a gentle flow of filtered air for 20 min at 20 °C. Glass slides were then sputter-coated for 80 s with gold in an argon plasma with a BAL-TEC SCD 005 sputter-coater (Bal-Tec AG, Liechtenstein). Scanning electron micrographs were obtained using a JEOL JSM-5900 LV scanning electron microscope (JEOL GmbH, Eching, Germany) at 15 kV. Further sample preparation, like fixation or exchange of solvents, was deliberately avoided. As shown in Fig. 3-S.12, we observed a particle-like structure under SEM measurement. This object is located at the edge of the film crack and shows a spherical shape. However, we were not able to identify the composition of this object from the electron microscopy study. Therefore, we used confocal Raman microscopy to reveal the structural details of the microparticles.

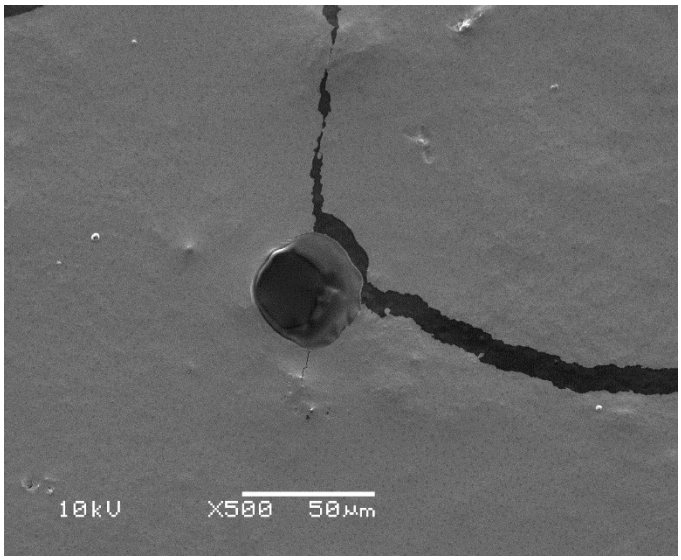

Fig. 3-S.12: SEM image of particle-like structure in film.

Phase separation of casein/pectin macroemulsion in solution after 48 h.

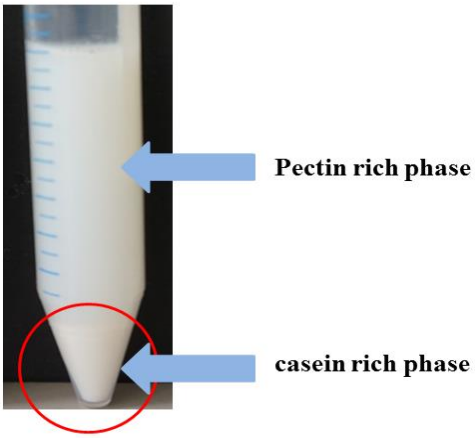

Fig. 3-S.13: An optical micrograph of the casein/pectin mixture (mixing ratio between casein and pectin = 1:0.1 (w/w)) in solution after storage for 48 h. The upper part indicates a phase rich in pectin and the lower part is a phase rich in casein.

Optical investigation of casein microparticles after a storage period of 3 weeks

We stored casein microparticles in Bis-Tris buffer solution at 4 °C for 21 days. These particles retained their spherical structures after a storage period of 14 and 21 days, as shown in Fig 3-S.14.

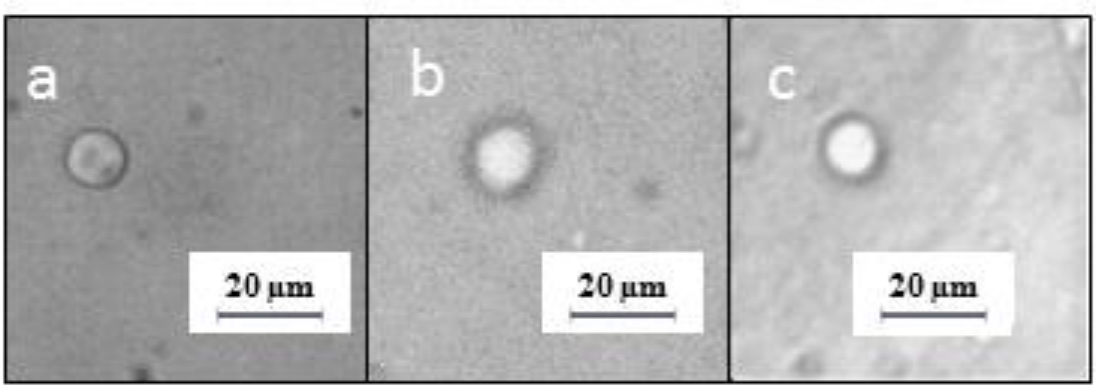

Fig. 3-S.14: Optical images of casein microparticles.

4 General discussion and outlook

Interaction between CM and hydrocolloids can lead to many useful food applications. Surrounding conditions, such as temperature, pH, shear force, and polymer concentration, play a crucial role in either forming the colloidal matrix or triggering the molecular interactions. Understanding the structural transformation induced by the molecular interactions would help to predict the behaviors of the newly formed polymeric matrix for developing novel products and applications. In the current chapter, the results are discussed integrally focusing on 3 aspects: a) structural study on the interactions between CM and hydrocolloids; b) formation and analysis of the casein microparticles afforded by CM/pectin interaction, and c) demonstration of incorporating bio-functionality on a casein microparticle.

4.1 Structural investigation of interaction of casein micelle with other hydrocolloids

Interaction between casein micelle and native ß-lactoglobulin by an elevated salt concentration in solution

Understanding the structural interactions between casein and other proteins is fundamental for process optimization and new product design involving them. Certain process conditions (e.g., temperature, pressure, etc.) can induce association of CM and ß-Lg (Bingham, 1971; Cho et al., 2003). Heating is a conventional approach to form a covalent complex of CM and ß-Lg (Mounsey et al., 2005; Oldfield et al., 1998; Smits & Brouwershaven, 1980). The covalent formation is attributed mainly to the S-S bridges or hydrophobic interaction between ß-Lg and κ-casein (Henry et al., 2002). However, the structural conformation of proteins is greatly altered under heat treatment. On the other hand, controversial results of either promote or inhibit the CM/ß-Lg complex formation were reported on the effect of the ionic interaction (Doi et al., 1981; Haque & Kinsella, 1987; Smits & Brouwershaven, 1980). Regardless, calcium concentration plays an important role in the stability of CM. Insufficient or surplus calcium can result in disintegration or aggregation of CMs (Holt, 1998; Grimley et al., 2010; Philippe et al., 2005). Nevertheless, the structural response of CM to surplus protein (such as ß-Lg in its native state) while the presence of salt (i.e., calcium) in one system requires in-depth understanding,

which could potentially shed some lights on structural interaction of proteins in real condition of milk products.

The recent work using static and dynamic light scattering revealed a structure deviation of CM from the well-known hard sphere model when concentration of ß-Lg was raised (from that in native milk). Under certain conditions, this is consistent with previous studies that indicated CM to appear as a hard sphere at the presence of calcium chloride and ß-Lg at a concentration of 10 mM or above. Since CMs are held together via CCP clusters, any surplus ß-Lg might compete with casein for the limited micellar calcium inducing new interaction between caseins. This is reflected by the changes in R_g and M_w of CM using SLS. The understanding would be helpful in processing milk concentrates by filtration, where CMs deposited on the membrane began to interact with ß-Lg while salt concentration increased.

The interaction between CM and other milk proteins is important insofar as quality of milk products is concerned. Taking advantage of the interaction could conceivably improve cheese manufacturing. Hence, the concentration increase on ß-Lg mainly occurs during cheese curdling as ß-Lg interferes the rennet coagulation. Such condition prolongs the coagulation and weakens the curd formation in cheese making ill-affecting the texture and flavor of the products.

Interaction between casein micelle and pectin during film formation

Interaction between casein and pectin was extensively discussed in the past. At present, the primary use of pectin in dairy processing is for stabilizing CMs in the acidified products such as yogurt. CMs form coacervates with pectin at low pH (Maroziene & de Kruif, 2000). At neutral pH, pectin triggers depletion flocculation of CMs which decrease the stability of the system by forming aggregations (Syrbe 1998). Two phases containing pectin and CM aggregates individually were separated by gravity which often considered as unfavorable, which limited the exploration of natural formed CM aggregates. In this work, the depletion flocculation of CMs takes place on a solid substrate (e.g., glass), the CM accumulation can be kept inside an environment containing pectin molecules avoiding formation of larger aggregates, as shown in Fig. 4-1. Naturally, these aggregates would remain dynamic and only to lose their integrity if pectin is removed from the system. This

phase separation behavior is also called ‘W/W’ emulsion by other studies that utilized caseinates and alginate (Antonov et al., 1996; Capron et al., 2001). Unfortunately, little is known to date on the phase behavior in a CM/pectin containing system to create new structures by gelation.

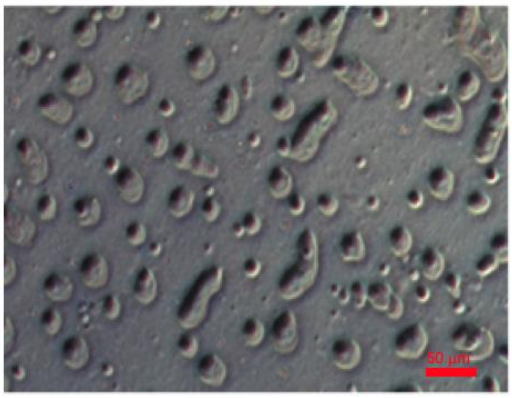

Fig. 4-1: A representative optical micrograph of CM accumulates surrounding by pectin matrix on a glass substrate.

For the first time, this work demonstrated the addition of pectin to form casein microparticles in film state, and subsequently, immobilize in a dried state. In brief, CMs and pectin were mixed in a ratio of 1:0.1 by weight in solution at neutral pH. The concentrations were close to the thresholds that can trigger a phase separation. The experiment in this study was conducted in a buffer solution using screened CM size fractions by consecutive centrifugations to exclude other elements in the native milk including unwanted proteins and/or surrounding conditions. The experimental focus was on the interaction between pectin and CMs. Centrifugation confined the CMs to a limited size distribution. As a result, these CMs had similar casein content and calcium phosphate ratio to provide similar physiochemical properties and polydispersity of the materials for testing (Dalgleish & Corredig, 2012; Marchin et al., 2007).

4.2 Formation, separation and investigation on casein microparticles

As discussed previously, CM can interact with other proteins and/or polysaccharide to initiate structural transformation or generate new formats. This work particularly focused on the interactions of CMs with polysaccharide as an example of creating novel structures. Past studies reported that individual caseins could form nano- or micro-particles to be developed into carriers for biological substances as well as

for controlled release in human stomach or duodenum with the pH-dependency of CM (Głąb & Boratyński, 2017). Majority of the reported particle formation was based on the gelation or aggregation induced by heating or enzymatic cross-linking of caseins or casinate (Huppertz et al., 2007; Huppertz et al., 2008; Panouillé et al., 2005; Thomar & Nicolai, 2016), only a few utilized native CMs as the base material to develop a new structure. Hence, the processes involved were often required additional operation or energy inputs.

For stabilizing acidified milk products, adding polysaccharide, e.g., pectin, to a casein-containing solution has been studied extensively in the past (Maroziene & de Kruif, 2000). Marreto and his co-workers demonstrated a casein-pectin coacervation under low pH to form microparticles using spray drying (Marreto et al., 2013). However, the high energy-demanding drying process can be too expensive to be practical for industrial applications. Nonetheless, no other casein-polysaccharide interaction under neutral pH was reported due to unstable aggregation. In contrast, the dried film approach could be a practical substitute for the matrix and new structure formation (Gebhardt & Kulozik, 2014; Gebhardt et al., 2012b; Gebhardt et al., 2011c). Hence, dry film was considered as an excellence substrate to investigate structural behaviors of particles using non-invasive techniques.

In this work, the accumulated CMs in solution were formed despite the instability instilled by the addition of pectin prior to deposition onto a substrate. On a hard surface, the thin polymer film limited the gravitational effect permitting the pectin matrix to isolate and form casein microparticles while preventing them from aggregating into large sizes. The subsequent evaporation of the thin film at ambient temperature immobilized the microparticles. The dehydration was indeed an essential step to enable stabilization of the CMs with the aid of pectin short of any other input or treatment. And, the surrounding temperature, air flow, and relative humility were also critical factors for an effective film formation. Thus, optimizing these parameters would facilitate and accelerate the process increasing the efficiency of the microparticle production. Moreover, in contrast to a mechanical process by grinding a dried polymeric film into fine particles (Elkharraz et al., 2003), current approach would produce the casein microparticle product considerately more homogeneous in size and shape .

Prior to releasing casein microparticles from the film matrix, the detail morphological and interior structure of the particles was examined under confocal Raman microscopy, a non-destructive microscopic method, to decipher the forming mechanisms of the microparticles. A 3D mapping technique allowed visualization of the film matrix containing casein microparticles which revealed that it was due mainly to the capillary force that changed the spherical microparticles into ellipsoidal shape during the film formation. The shape, however, could be reversible by rehydration, as the casein microparticles have inherited the physical properties of CM as a deformable soft matter (Gebhardt et al., 2012b).

As shown in Tab. 4-1, the Raman spectra of the microparticles with the signature protein peaks are similar to the vibrational signal of casein from previous study (Fontecha et al., 1993; Byler et al., 1988). It showed that the composition of casein microparticles was intact while being entrapped in the pectin matrix. There were no cross-linking or bonding formed between CMs and pectin in the solution, which agreed with the volume exclusion effect as discussed previously (Maroziene & de Kruif, 2000).

Tab. 4-1. Structural assignment of casein microparticles (Data is from Zhuang et al., 2015).

Wavenumbers (cm^{-1})	Structural assignments of casein (according to Fontecha, 1993 and Byler, 1988)
1450-1500	Amide II - ν (NH)
1650-1700	Amide I - ν (C=O) and β (NH)
2900-2950	$\nu_{as}(CH)$
3050-3100	Amide B - ν(N-H)

To determine the functionality and stability of the obtained casein microparticles, the film matrix containing pectin was enzymatically hydrolyzed to release the microparticles into solution. A buffer solution was used as the incubation medium for the enzymatic hydrolysis to avoid a kinetic different from pure water or other physiological solution (Chernova et al., 2016). After a required incubation time, at the optimal temperature pectin in the film matrix was degraded into short saccharides allowing the collection of casein microparticles for purification with several washing steps. The rinses ensured a complete removal of pectin residuals and pectinase. Further study on the microparticle structure, which might attribute to the functional

properties, was to follow. Raman microscopic images displayed the morphology and chemical properties of the microparticles. The results confirmed that the composition of the casein microparticles obtained remained unchanged from prior to the collection process. This is in line with other studies, even though different substrates were used for the film formation by assembling particles without alteration on their physio-chemical structure (Chernova et al., 2016; Taylor et al., 2009b).

Hence, it is worthy to study the stability of casein microparticles under varying pH over the storage period. Fig. 4-2 includes a representative micrograph of casein microparticles stored at 4°C for 30 days and the plots on particle size changes under different pH. The casein microparticles shrunk slightly in size at 4°C but the spherical shape was intact. Consequently, the integrity of casein microparticles could conceivably be securely maintained under conventional cold storage. As shown in Fig. 4-2 B) and C), the particle size of the microparticle was sensitive to pH. It appeared that the internal assembly of casein microparticles and the solubility of individual caseins could be altered by changing the pH leading to swelling or decomposing the particles.

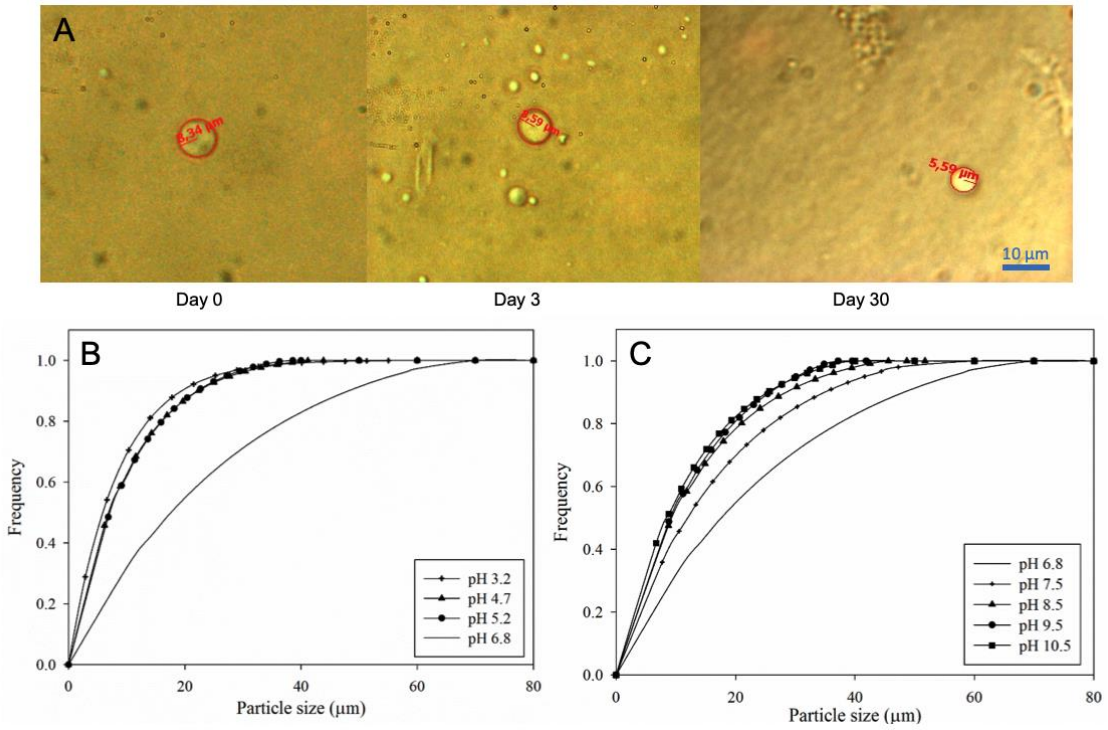

Fig. 4-2: A) representative optical micrographs on casein microparticle over a storage period of 30days. And particle size distribution of casein microparticle at B) low pH (<pH 6.8) and C) high pH (>pH 6.8). Data from Zhuang et al., 2016.

4.3 Demonstration of casein microparticles as carriers for biological substances

Casein microparticle could provide biological benefits by encapsulating bioactive substances (Głąb & Boratyński, 2017). Several processes could be applied for the encapsulation, such as high pressure homogenization, spray drying, emulsification, and pH shifting (Chu et al., 2007; Elzoghby et al., 2013; Mounsey et al., 2005; Roach et al., 2009). Generally, casein-based nano- or micro-particles are either a) individual capsules containing a solid shell with porous inner spaces to entrap biological components or b) spherical particles without outer layer (Głąb & Boratyński, 2017). In this work, casein microparticle did not fit either of the above definitions, as casein microparticle could deform to become a coat on an oil/water interface. The current approach could, therefore, be used to produce bio-functional products by enclosing bioactive substances, e.g., vitamin E, without treatment required in

microencapsulation or emulsification. One of the major benefits is energy conservation by bypassing spray drying to obtain a stable structure for the particles.

This work demonstrated that casein microparticles could accumulate and deform into a 'core-shell' structure with bioactive substances e.g., αT. It was hypothesized that the microparticles actively reacted to emulsion droplets and the interfacial structure were stabilized in dispersion. The preserved amphiphilic nature of casein in the microparticle demonstrates the natural affinity for hydrophobic substances as proposed previously (Semo et al., 2007). Microparticles, especially those are of small sizes, effectively move to αT/water interface to form a 5 μm-thick shell. Raman imaging reveals αT droplet forms an inner core with a surface of the spherical microparticle rather than entrapped by inner porous spaces. The particle sizes of the novel structure spread in a wide range up to 100 μm depending strongly on the droplet sizes of αT. It suggests above obtained casein microparticles are not able to fully cover large αT droplets (>50 μm) to stabilize the complex if surface/volume ratio of the emulsion droplet exceed a limit. Compared to conventional microparticle formed by cross-linking, the formed emulsion droplet could prolong the release of biological substances because of a casein based 'shell' (Głąb & Boratyński, 2017). Another interesting aspect for future investigation is to understand the potential structural transformation of casein microparticle especially during emulsion droplet establishment.

The current approach could produce casein microparticles from dried CM/pectin matrix films for use as a carrier to deliver functional components (such as bioactive substances). Nevertheless, further investigation is needed to understand the releasing mechanism of functional components and the durability of the polymeric matrix in a simulated digestion environment in order to broaden its application.

4.4 Outlook

Casein is an important source for a wide range of protein-based food products. To more fully exploit the potential of its functionality and improve processing operations, the molecular structure of CM was extensively discussed in the past, and several models were developed with new information or experimental data generated by using advanced techniques. Newly discovered interactions between CMs

and other colloidal macromolecules (e.g., polysaccharide and protein) could provide venues for creating novel structures and products. Understanding the fundamentals could benefit milk processing. For instance, by applying well-defined conditions, CM could be changed from its well-known hard sphere structure to a different physique that provides useful functionality unseen before. In the future, advanced analytical methodologies aided by in-situ apparatus can be applied to detect the structure, transformation, and interaction details on the intricate milk system that may lead to commercial applications utilizing CM colloids.

Biopolymers from different sources have been studied to identify CM's potentials for new structures adding bioactive benefits or to increase the techno-functional properties. Depending on the polymer type and surrounding conditions, CM could behave differently to arrive at either a conjunct complex or self-assembled microparticle or micro-gels. For future works, the stability of newly form structures is of great interest prior to incorporate additional functional benefits. Further study on the process parameters could help upgrade the yield of casein microparticles in large scale productions. Altering pH, temperature, and oxidation or applying UV radiation and hydrostatic pressure might be considered in a scale-up production for food and pharmaceutical industries. Fundamental understanding on structural transformation of the CM-based complex seemed to offer ample room for new applications and process improvements.

Further understanding on the encapsulation mechanism of other bioactive agents, initially to be gained through simulated experimentation, could, undoubtedly, usher in a new horizon for casein microparticles. Needless to say, the biodegradability and time-release capability of the encapsulated food and pharmaceutical products have already shown the market potential of the casein microparticles. It is, therefore, up to the scientists and professionals in the academic and industrial communities to explore and exploit the possibilities.

5 References

Adar, F. (2001). Evolution and Revolution of Raman Instrumentation - Application of Available Technologies to Spectroscopy and Microscopy. In I. R. Lewis & E. Howell (Eds.), *Handbook of Raman spectroscopy. From the research laboratory to the process line* (pp.11-40). New York: CRC press.

Alford, J.R., Kendrick, B.S., Carpenter, J.F., Randolph, T.W. (2008). Measurement of the second osmotic virial coefficient for protein solutions exhibiting monomer-dimer equilibrium, *Analytical Biochemistry*, *377*, 128-133.

Amidon, G. E., Meyer, P. J., & Mudie, D. M. (2017). Chapter 10 - Particle, Powder, and Compact Characterization. In Y. Qiu, Y. Chen, G. G. Z. Zhang, L. Yu, & R. V. Mantri (Eds.), *Developing Solid Oral Dosage Forms (Second Edition)* (pp. 271-293). Boston: Academic Press.

Anema, S. & Li, Y. (2003). Association of denatured whey proteins with casein micelles in heated reconstituted skim milk and its effect on casein micelle size. *Journal of Dairy Research*, 70(1), 73-83.

Antonov, Y. A., & Moldenaers, P. (2011). Structure formation and phase-separation behaviour of aqueous casein-alginate emulsions in the presence of strong polyelectrolyte. *Food Hydrocolloids*, *25*(3), 350-360.

Antonov, Y. A., Lashko, N. P., Glotova, Y. K., Malovikova, A., & Markovich, O. (1996). Effect of the structural features of pectins and alginates on their thermodynamic compatibility with gelatin in aqueous media. *Food Hydrocolloids*, *10*(1), 1-9.

Apenten, R. K. O., Khokhar, S., & Galani, D. (2002). Stability parameters for β-lactoglobulin thermal dissociation and unfolding in phosphate buffer at pH 7.0. *Food Hydrocolloids*, *16*(2), 95-103.

Asakura, S., & Oosawa, F. (1954). On Interaction between Two Bodies Immersed in a Solution of Macromolecules. *The Journal of Chemical Physics*, *22*(7), 1255-1256.

Baker, M. J., Trevisan, J., Bassan, P., Bhargava, R., Butler, H. J., Dorling, K. M., et al. (2014). Using Fourier transform IR spectroscopy to analyze biological materials. *Nature Protocols*, *9*, 1771 -1791.

Baranska, M., Baranski, R., Grzebelus, E., & Roman, M. (2011). In situ detection of a single carotenoid crystal in a plant cell using Raman microspectroscopy.

Vibrational Spectroscopy, *56*(2), 166-169.

Bastos, D. D. S., Gonçalves, M. D. P., Andrade, C. T. de, Araújo, K. G. de L., & Rocha Leão, M. H. M. D. (2012). Microencapsulation of cashew apple (Anacardium occidentale, L.) juice using a new chitosan-commercial bovine whey protein isolate system in spray drying. *Food and Bioproducts Processing*, *90*(4), 683-692.

Beattie, J. R., Maguire, C., Gilchrist, S., Barrett, L. J., Cross, C. E., Possmayer, F., et al. (2007). The use of Raman microscopy to determine and localize vitamin E in biological samples. *The FASEB Journal*, *21*(3), 766-776.

Belitz, H. D., Grosch, W., & Schieberle, P. (2009). Milk and Dairy Products. In H. D. Belitz, W. Grosch, & P. Schieberle (Eds.), *Food Chemistry* (pp. 498-545). Berlin, Heidelberg: Springer Berlin Heidelberg.

BeMiller, J. N. (2009). An Introduction to Pectins: Structure and Properties. In J. N. BeMiller (Eds.), *Chemistry and Function of Pectins* (pp. 2-12). Washington, DC: American Chemical Society.

Berk, Z. (2018). Chapter 9 - Centrifugation. In Z. Berk (Eds.), *Food Science and Technology* (pp. 243-259). Boston: Academic Press.

Bingham, E. W. (1971). Influence of Temperature and pH on the Solubility of α_{s1}-, β- and κ-Casein. *Journal of Dairy Science*, *54*(7), 1077-1080.

Bloomfield, V.A. & Mead, R.J. (1975). Structure and stability of casein micelles. *Journal of Dairy Science*, 58(4), 592-601.

Boland, M. (2011). 3 - Whey proteins. In M. Boland (Eds.), *Woodhead Publishing Series in Food Science, Technology and Nutrition* (pp. 30-55). Cambridge: Woodhead Publishing.

Bouchoux, A., Gésan-Guiziou, G., Pérez, J., & Cabane, B. (2010). How to Squeeze a Sponge: Casein Micelles under Osmotic Stress, a SAXS Study. *Biophysical Journal*, *99*(11), 3754-3762.

Bobe, G., Beitz, D. C., Freeman, A. E., & Lindberg, G. L. (1998). Sample Preparation Affects Separation of Whey Proteins by Reversed-Phase High-Performance Liquid Chromatography. *Journal of Agricultural and Food Chemistry*, *46*(4), 1321-1325.

Bonizzi, I., Buffoni, J.N., Feligini, M. (2009). Quantification of bovine casein fractions by direct chromatographic analysis of milk. Approaching the application to a real production context. *Journal of Chromatography A*, 1216(1), 165-168

Bonfatti, V., Grigoletto, L., Cecchinato, A., Gallo, L., & Carnier, P. (2008). Validation of a new reversed-phase high-performance liquid chromatography method for separation and quantification of bovine milk protein genetic variants. *Journal of Chromatography A*, *1195*(1-2), 101-106.

Bramanti, E., Sortino, C., Onor, M., Beni, F., & Raspi, G. (2003). Separation and determination of denatured α_{s1}-, α_{s2}-, β- and κ-caseins by hydrophobic interaction chromatography in cows', ewes' and goats' milk, milk mixtures and cheeses. *Journal of Chromatography A*, *994*(1), 59-74.

Bunaciu, A. A., Aboul-Enein, H. Y., & Hoang, V. D. (2015). Raman Spectroscopy for Protein Analysis. *Applied Spectroscopy Reviews*, *50*(5), 377-386.

Burdon, R. H., van Knippenberg, P. H., & Sharpe, P. T. (1988). Chapter 3: Centrifugation. In R. H. Burdon, P. H. V. Knippenberg, & P. T. Sharpe (Eds.), *Methods of Cell Separation* (Vol. 18, pp. 18-69). New York: Elsevier.

Bysell, H., Månsson, R., Hansson, P., & Malmsten, M. (2011). Microgels and microcapsules in peptide and protein drug delivery. *Advanced Drug Delivery Reviews*, *63*(13), 1172-1185.

Byler, M. D., Farrell, H. M., & Susi, H. (1988). Raman Spectroscopic Study of Casein Structure. *Journal of Dairy Science*, *71*(10), 2622-2629.

Capron, I., Costeux, S., & Djabourov, M. (2001). Water in water emulsions: phase separation and rheology of biopolymer solutions. *Rheologica Acta*, *40*(5), 441-456.

Cardell, C., & Guerra, I. (2016). An overview of emerging hyphenated SEM-EDX and Raman spectroscopy systems: Applications in life, environmental and materials sciences. *TrAC Trends in Analytical Chemistry*, *77*, 156-166.

Cesi, V., Katzbauer, B., Narodoslawsky, M., & Moser, A. (1996). Thermophysical properties of polymers in aqueous two-phase systems. *International Journal of Thermophysics*, *17*(1), 127-135.

Champagne, C.P. (2006). Starter Cultures Biotechnology: The Production of Concentrated Lactic Cultures in Alginate Beads and Their Applications in the Nutraceutical and Food Industrie. *Chemical Industry, Chemical Engineering Quarterly*, *12(*1), 11-17.

Champagne, C. P., & Fustier, P. (2007). Microencapsulation for the improved delivery of bioactive compounds into foods. *Plant Biotechnology / Food Biotechnology*, *18*(2), 184-190.

Chernova, V. V., Tuktarova, I. F., & Kulish, E. I. (2016). Enzymatic hydrolysis of chitosan films in water and physiological solution. *Applied Biochemistry and Microbiology*, *52*(5), 525-530.

Christianson, G., Jenness, R. & Coulter, S. T. (1954). Determination of Ionized Calcium and Magnesium in Milk. *Analytical Chemistry*. 26(12), 1923-1927.

Cho, Y., Singh, H., & Creamer, L. K. (2003). Heat-induced interactions of β-lactoglobulin A and κ-casein B in a model system. *Journal of Dairy Research*, *70*(1), 61-71.

Chu, B.-S., Ichikawa, S., Kanafusa, S., & Nakajima, M. (2007). Preparation of Protein-Stabilized β-Carotene Nanodispersions by Emulsification-Evaporation Method. *Journal of the American Oil Chemists' Society*, *84*(11), 1053-1062.

Clark, A. H. (2000). Direct analysis of experimental tie line data (two polymer-one solvent systems) using Flory-Huggins theory. *Carbohydrate Polymers*, *42*(4), 337-351.

Clarke, A. R., & Eberhardt, C. N. (2002). 5 - Complementary optical and EM imaging techniques. In A. R. Clarke & C. N. Eberhardt (Eds.), *Woodhead Publishing Series in Electronic and Optical Materials* (pp. 305-357). Cambridge: Woodhead Publishing.

Cook, M. T., Tzortzis, G., Charalampopoulos, D., & Khutoryanskiy, V. V. (2012). Microencapsulation of probiotics for gastrointestinal delivery. *Journal of Controlled Release*, *162*(1), 56-67.

Creamer, L., Berry, G. & Mills, O. (1977). A study of the dissociation of b-casein from the bovine casein micelle at low temperature [milk and cream], *New Zealand Journal of Dairy Science and Technology*, 12(1), 58-66.

Croak, S., & Corredig, M. (2006). The role of pectin in orange juice stabilization: Effect of pectin methylesterase and pectinase activity on the size of cloud particles. *Food Hydrocolloids*, *20*(7), 961-965.

Dai, J., Wu, Y., Chen, S.-W., Zhu, S., Yin, H.-P., Wang, M., & Tang, J. (2010). Sugar compositional determination of polysaccharides from Dunaliella salina by modified RP-HPLC method of precolumn derivatization with 1-phenyl-3-methyl-5-pyrazolone. *Carbohydrate Polymers*, *82*(3), 629-635.

Dalgleish, D. G. (1998). Casein Micelles as Colloids: Surface Structures and Stabilities. *Journal of Dairy Science*, *81*(11), 3013-3018.

Dalgleish, D. G. (2011). On the structural models of bovine casein micelles—review and possible improvements. *Soft Matter*, *7*(6), 2265-2272.

Dalgleish, D. G., & Corredig, M. (2012). The Structure of the Casein Micelle of Milk and Its Changes During Processing. *Annual Review of Food Science and Technology*, *3*(1), 449-467.

Dalgleish, D. G., & Hallett, F. R. (1995). Dynamic light scattering: applications to food systems. *DOF2015, 6th Edition of the International Symposium on Delivery of Functionality in Complex Food Systems: Physically Inspired Approaches From the Nano Scale to the Micro Scale*, *28*(3), 181-193.

Dalgleish, D. G., & Law, A. J. R. (1988). pH-Induced dissociation of bovine casein micelles. I. Analysis of liberated caseins. *Journal of Dairy Research*, *55*(4), 529-538.

Dalgleish, D. G., & Law, A. J. R. (1989). pH-Induced dissociation of bovine casein micelles. II. Mineral solubilization and its relation to casein release. *Journal of Dairy Research*, *56*(5), 727-735.

Dalgleish, D. G., & Parker, T. G. (1980). Binding of calcium ions to bovine αsl-casein and precipitability of the protein-calcium ion complexes. *Journal of Dairy Research*, *47*(1), 113-122.

Dalgleish, D. G., Paterson, E., & Horne, D. S. (1981). Kinetics of aggregation of α_{s1}-casein/ca2+ mixtures: charge and temperature effects. *Biophysical Chemistry*, *13*(4), 307-314.

Dalgleish, D. G., Spagnuolo. P, Douglas Goff, H. (2004). A possible structure of the casein micelle based on high-resolution field-emission scanning electron microscopy, *International Dairy Journal,* 14(12), 1025-1031

Dalgleish, D. G., van Mourik, L., & Corredig, M. (1997). Heat-Induced Interactions of Whey Proteins and Casein Micelles with Different Concentrations of α -Lactalbumin and β-Lactoglobulin. *Journal of Agricultural and Food Chemistry*, *45*(12), 4806-4813.

Dang, B., Huynh, T., & Le, V. (2012). Simultaneous treatment of acerola mash by ultrasound and pectinase preparation in acerola juice processing: Optimization of the pectinase concentration and pectolytic time by response surface methodology. *International Food Research Journal*, *19*, 509-513.

de Freitas, R. A., Nicolai, T., Chassenieux, C., & Benyahia, L. (2016). Stabilization of Water-in-Water Emulsions by Polysaccharide-Coated Protein Particles.

Langmuir, *32*(5), 1227-1232.

de Kruif, C. G. (1999). Casein micelle interactions. *International Dairy Journal*, *9*(3-6), 183-188.

de Kruif, C. G., & Holt, C. (2003). Casein micelle structure, functions and interactions. *Advanced Dairy Chemistry 3rd Ed.*, *1*(PART A), 233-276.

de Kruif, C. G., & Tuinier, R. (2001). Polysaccharide protein interactions. *Food Hydrocolloids*, *15*(4), 555-563.

de Kruif, C.G., Huppertz, T., Urban, V. S., Petukhov, A. V. (2012). Casein micelles and their internal structure. *Advances in Colloid and Interface Science*, 171-172, 36-52.

de Kruif, C. G., & Zhulina, E. B. (1996). κ-casein as a polyelectrolyte brush on the surface of casein micelles. *Colloids and Surfaces a: Physicochemical and Engineering Aspects*, *117*(1), 151-159.

Deabate, S., Fatnassi, R., Sistat, P., & Huguet, P. (2008). In situ confocal-Raman measurement of water and methanol concentration profiles in Nafion® membrane under cross-transport conditions. *Journal of Power Sources*, *176*(1), 39-45.

Debye, P. (1915). Zerstreuung von Röntgenstrahlen. *Annalen Der Physik*, *351*(6), 809-823.

Delben, F., & Stefancich, S. (1997). Interaction of food proteins with polysaccharides, I. Properties upon mixing. *Journal of Food Engineering*, *31*(3), 325-346.

Dewan, R. K., Chudgar, A., Mead, R., Bloomfield, V. A., & Morr, C. V. (1974). Molecular weight and size distribution of bovine milk casein micelles. *Biochimica Et Biophysica Acta (BBA) - Protein Structure*, *342*(2), 313-321.

Dickinson, E. (2015). Structuring of colloidal particles at interfaces and the relationship to food emulsion and foam stability. *Journal of Colloid and Interface Science*, *449*, 38-45.

Dickinson. E., & McClements. D.J. (1996). In *Advances in Food Colloids* (pp. 281-284), London: Blackie Academic & Professional.

Dinsmore, A. D., Hsu, M. F., Nikolaides, M. G., Marquez, M., Bausch, A. R., & Weitz, D. A. (2002). Colloidosomes: Selectively Permeable Capsules Composed of Colloidal Particles. *Science*, *298*(5595), 1006-1009.

Doi, H., Ibuki, F., & Kanamori, M. (1981). Effect of Carbohydrate Moiety of κ-Casein on the Complex Formation with β-Lactoglobulin TI . *Agricultural and Biological Chemistry*, *45*(10), 2351-2353.

Doublier, J. L., Garnier, C., Renard, D., & Sanchez, C. (2000). Protein-polysaccharide interactions. *Current Opinion in Colloid & Interface Science*, *5*(3), 202-214.

Douša, M., Reitmajer, J., Lustig, P., & Štefko, M. (2016). Effect of Chromatographic Conditions on Enantioseparation of Bedaquiline Using Polysaccharide-based Chiral Stationary Phases in RP-HPLC. *Journal of Chromatographic Science*, *54*(9), 1501-1507.

Dumpler, J., Wohlschläger, H., & Kulozik, U. (2017). Dissociation and coagulation of caseins and whey proteins in concentrated skim milk heated by direct steam injection. *Dairy Science & Technology*, *96*(6), 807-826.

Edwards, P.B., Creamer, L.K., & Jameson, G.B. (2009). Structure and stability of whey proteins, In A. Thompson, M. Boland, H. Singh (Eds*.), Milk Proteins: From Expression to Food*(pp. 163-203), Amsterdam: Academic Press/Elsevier.

Egerton, R. F. (2005). The Scanning Electron Microscope. In R. F. Egerton (Eds.), *Physical Principles of Electron Microscopy: An Introduction to TEM, SEM, and AEM* (pp. 125-153). Boston, MA: Springer US.

Einstein, A. (1905). Über einen die Erzeugung und Verwandlung des Lichtes betreffenden heuristischen Gesichtspunkt. *Annalen Der Physik*, *322*(6), 132-148.

Einstein, A. (1906). Zur Theorie der Brownschen Bewegung. *Annalen Der Physik*, *324*(2), 371-381.

Einstein, A. (1910). Theorie der Opaleszenz von homogenen Flüssigkeiten und Flüssigkeitsgemischen in der Nähe des kritischen Zustandes. *Annalen Der Physik*, *338*(16), 1275-1298.

Elkharraz, K., Dashevsky, A., & Bodmeier, R. (2003). Microparticles prepared by grinding of polymeric films. *Journal of Microencapsulation*, *20*(5), 661-673.

Elzoghby, A. O., Abo El-Fotoh, W. S., & Elgindy, N. A. (2011). Casein-based formulations as promising controlled release drug delivery systems. *Journal of Controlled Release*, *153*(3), 206-216.

Elzoghby, A. O., Helmy, M. W., Samy, W. M., & Elgindy, N. A. (2013). Spray-dried casein-based micelles as a vehicle for solubilization and controlled delivery of

flutamide: Formulation, characterization, and in vivo pharmacokinetics. *European Journal of Pharmaceutics and Biopharmaceutics*, *84*(3), 487-496.

Endreß, H. U., & Christensen, S. H. (2009). 12 - Pectins. In H. U. Endreß, S. H. Christensen (Eds.), *Woodhead Publishing Series in Food Science, Technology and Nutrition* (pp. 274-297). Cambridge: Woodhead Publishing.

Erokhin, V. (2002). Chapter 10 - Langmuir-Blodgett films of biological molecules. In H. S. Nalwa (Eds.), *Handbook of Thin Films* (pp. 523-557). Burlington: Academic Press.

Esquena, J. (2016). Water-in-water (W/W) emulsions. *Current Opinion in Colloid & Interface Science*, *25*, 109-119.

Fang, Y., Li, L., Inoue, C., Lundin, L., & Appelqvist, I. (2006). Associative and Segregative Phase Separations of Gelatin/κ-Carrageenan Aqueous Mixtures. *Langmuir*, *22*(23), 9532-9537.

Farkye, N. Y. (2017). Chapter 43 - Quark, Quark-like Products, and Concentrated Yogurts. In P. L. H. McSweeney, P. F. Fox, P. D. Cotter, & D. W. Everett (Eds.), *Cheese (Fourth Edition)* (pp. 1103-1110). San Diego: Academic Press.

Farrell, H., Brown, E., Malin, E., (2013). Higher Order Structures of the Caseins: A Paradox?. In P. L. H. McSweeney & P. F. Fox (Eds.), *Advanced dairy chemistry: Volume 1A: Proteins: Basic aspects* (pp.161-184), New York: Springer.

Feng, S., Gao, F., Chen, Z., Grant, E., Kitts, D. D., Wang, S., & Lu, X. (2013). Determination of α-Tocopherol in Vegetable Oils Using a Molecularly Imprinted Polymers-Surface-Enhanced Raman Spectroscopic Biosensor. *Journal of Agricultural and Food Chemistry, 61*(44), 10467-10475.

Ferreira, IM, Mendes, E. A. L., & Ferreira, M. A. (2001). HPLC/UV Analysis of Proteins in Dairy Products Using a Hydrophobic Interaction Chromatographic Column TI. *Analytical Sciences*, *17*(4), 499-501.

Finsy, R., de Groen, P., Deriemaeker, L., Geladé, E., & Joosten, J. (2004). Data Analysis of Multi-Angle Photon Correlation measurements without and with prior knowledge. *Particle & Particle Systems Characterization*, *9*(1-4), 237-251.

Firoozmand, H., Murray, B. S., & Dickinson, E. (2009). Interfacial Structuring in a Phase-Separating Mixed Biopolymer Solution Containing Colloidal Particles. *Langmuir*, *25*(3), 1300-1305.

Flutto, L. (2003). Pectin | Properties and Determination. In B. Caballero (Eds.), *Encyclopedia of Food Sciences and Nutrition (Second Edition)* (pp. 4440-4449).

Oxford: Academic Press.

Fontecha, J., Bellanato, J., & Juarez, M. (1993). Infrared and Raman Spectroscopic Study of Casein in Cheese: Effect of Freezing and Frozen Storage. *Journal of Dairy Science*, *76*(11), 3303-3309.

Foord, R., Jakeman, E., Oliver, C. J., Pike, E. R., Blagrove, R. J., Wood, E., & Peacocke, A. R. (1970). Determination of Diffusion Coefficients of Haemocyanin at Low Concentration by Intensity Fluctuation Spectroscopy of Scattered Laser Light. *Nature*, *227*(5255), 242-245.

Forgács, E., & Cserháti, T. (2003). Chromatography | Principles. In B. Caballero (Ed.), *Encyclopedia of Food Sciences and Nutrition (Second Edition)* (pp. 1259-1267). Oxford: Academic Press.

Fox, P. F. (1989). *Developments in Dairy Chemistry: 4-Function milk proteins* (pp.97-100). London: Elsevier Applied Science.

Fox, P. F. (2003). Milk Proteins: General and Historical Aspects. In P. F. Fox & P. L. H. McSweeney (Eds.), *Advanced Dairy Chemistry—1 Proteins: Part A / Part B* (pp. 1-48). Boston, MA: Springer US.

Fox, P. F. (2008). Chapter 1 - Milk: an overview. In A. Thompson, M. Boland, & H. Singh (Eds.), *Food Science and Technology* (pp. 1-54). San Diego: Academic Press.

Fox, P. F., & Brodkorb, A. (2008). The casein micelle: Historical aspects, current concepts and significance. *International Dairy Journal*, *18*(7), 677-684.

Fraeye, I., De Roeck, A., Duvetter, T., Verlent, I., Hendrickx, M., & Van Loey, A. (2007). Influence of pectin properties and processing conditions on thermal pectin degradation. *Food Chemistry*, *105*(2), 555-563.

Fraeye, I., Doungla, E., Duvetter, T., Moldenaers, P., Van Loey, A., & Hendrickx, M. (2009). Influence of intrinsic and extrinsic factors on rheology of pectin-calcium gels. *Food Hydrocolloids*, *23*(8), 2069-2077.

Gangidi, P.R. & Metzger, L. E. (2006) Ionic calcium determination in skim milk with molecular probes and front-face fluorescence spectroscopy: simple linear regression. *Journal of Dairy Science*, 89(11), 4105-13.

Gast, K., & Fiedler, C. (2012). Dynamic and static light scattering of intrinsically disordered proteins. *Methods in Molecular Biology (Clifton, N.J.)*, *896*, 137-161.

Gaucheron, F. (2005). The minerals of milk. *Reproduction Nutrition Development, 45*(4), 473-483.

Gebhardt, R., Doster, W., Friedrich, J., Kulozik, U. (2006). Size distribution of pressure-decomposed casein micelles studied by dynamic light scattering and AFM, *European Biophysics Journal*, *35*, 503-509.

Gebhardt, R., & Kulozik, U. (2011d). High pressure stability of protein complexes studied by static and dynamic light scattering. *High Pressure Research*, *31*(1), 243-252.

Gebhardt, R., & Kulozik, U. (2014). Simulation of the shape and size of casein micelles in a film state. *Food & Function*, *5*(4), 780.

Gebhardt, R., Holzmüller, W., Zhong, Q., Müller-Buschbaum, P., & Kulozik, U. (2011c). Structural ordering of casein micelles on silicon nitride micro-sieves during filtration. *Colloids and Surfaces. B, Biointerfaces*, *88*(1), 240-245.

Gebhardt, R., Steinhauer, T., Meyer, P., Sterr, J., Perlich, J., & Kulozik, U. (2012b). Structural changes of deposited casein micelles induced by membrane filtration. *Faraday Discussions*, *158*, 77-88.

Gebhardt, R., Toro-Sierra, J., & Kulozik, U. (2012a). Pressure dissociation of [small beta]-lactoglobulin oligomers near their isoelectric point, *Soft Matter*, *8*, 11654-11660

Gebhardt, R., Takeda, N., Kulozik, U., & Doster, W. (2011a). Structure and Stabilizing Interactions of Casein Micelles Probed by High-Pressure Light Scattering and FTIR. *J. Phys. Chem. B*, *115*(10), 2349-2359.

Gebhardt, R., Teulon, J.-M., Pellequer, J.-L., Burghammer, M., Colletier, J.-P., & Riekel, C. (2014). Virus particle assembly into crystalline domains enabled by the coffee ring effect. *Soft Matter*, *10*(30), 5458-5462.

Gebhardt, R., Vendrely, C., & Kulozik, U. (2011b). Structural characterization of casein micelles: shape changes during film formation. *Journal of Physics: Condensed Matter*, *23*(44), 444201.

Gebhardt, R., Vendrely, C., Burghammer, M., & Riekel, C. (2009). Characterization of the Boundary Zone of a Cast Protein Drop: Fibroin β-Sheet and Nanofibril Formation. *Langmuir*, *25*(11), 6307-6311.

Giridhar, G., Manepalli, R. R. K. N., & Apparao, G. (2017). Chapter 7 - Confocal Raman Spectroscopy. In S. Thomas, R. Thomas, A. K. Zachariah, & R. K. Mishra (Eds.), *Micro and Nano Technologies* (pp. 141-161). New York: Elsevier.

Goldstein, J. I., Newbury, D. E., Echlin, P., Joy, D. C., Fiori, C., & Lifshin, E. (1981). Image Formation in the Scanning Electron Microscope. In J. I. Goldstein, D. E.

Newbury, P. Echlin, D. C. Joy, C. Fiori, & E. Lifshin (Eds.), *Scanning Electron Microscopy and X-Ray Microanalysis: A Text for Biologist, Materials Scientist, and Geologists* (pp. 123-204). Boston, MA: Springer US.

Goldstein, J. I., Newbury, D. E., Echlin, P., Joy, D. C., Lyman, C. E., Lifshin, E., et al. (2003). Specimen Preparation of Hard Materials: Metals, Ceramics, Rocks, Minerals, Microelectronic and Packaged Devices, Particles, and Fibers. In J. I. Goldstein, D. E. Newbury, P. Echlin, D. C. Joy, C. E. Lyman, E. Lifshin, et al. (Eds.), *Scanning Electron Microscopy and X-ray Microanalysis: Third Edition* (pp. 537-564). Boston, MA: Springer US.

Gomes da Costa, S., Richter, A., Schmidt, U., Breuninger, S., & Hollricher, O. (2019). Confocal Raman microscopy in life sciences. *Morphologie*, *103*(341), 11-16.

Gonzalez-Jordan, A., Thomar, P., Nicolai, T., & Dittmer, J. (2015). The effect of pH on the structure and phosphate mobility of casein micelles in aqueous solution. *Food Hydrocolloids*, *51*, 88-94.

Grimley, H. J., Grandison, A., & J Lewis, M. (2010). The effect of calcium removal from milk on casein micelle stability and structure. *Milchwissenschaft*, *65*, 151-154.

Griffin, M. C. A., & Anderson, M. (1983). The determination of casein micelle size distribution in skim milk by chromatography and photon correlation spectroscopy. *Biochimica Et Biophysica Acta (BBA) - Protein Structure and Molecular Enzymology*, *748*(3), 453-459.

Griffiths, P. (1983). Fourier transform infrared spectrometry. *Science*, *222*(4621), 297-302.

Grinberg, V. Y., & Tolstoguzov, V. B. (1997). Thermodynamic incompatibility of proteins and polysaccharides in solutions. *Food Hydrocolloids*, *11*(2), 145-158.

Grodecki, K., Jozwik, I., Baranowski, J. M., Teklinska, D., & Strupinski, W. (2016). SEM and Raman analysis of graphene on SiC(0001). *Micron*, *80*, 20-23.

Gupta, V. P. (2016). 8 - Vibrational Frequencies and Intensities. In V. P. Gupta (Eds.), *Principles and Applications of Quantum Chemistry* (pp. 247-289). Boston: Academic Press.

Głąb, T. K., & Boratyński, J. (2017). Potential of Casein as a Carrier for Biologically Active Agents. *Topics in Current Chemistry (Cham)*, *375*(4), 71.

Hall, D. B., Underhill, P., & Torkelson, J. M. (2004). Spin coating of thin and ultrathin

polymer films. *Polymer Engineering & Science*, *38*(12), 2039-2045.

Haque, Z., & Kinsella, J. E. (1987). Interaction between κ-Casein and β-Lactoglobulin: Effect of Calcium TI . *Agricultural and Biological Chemistry*, *51*(7), 1997-1998.

Harding, SE. (1999) Protein hydrodynamics. In: G. Allen (Ed.), *Protein: a comprehensive treatise* (pp. 271-135), Stamford: JAI Press.

Heidebach, T., Först P., Kulozik U. (2009). Microencapsulation of probiotic cells by means of rennet-gelation of milk proteins. Food hydrocolloids, *23*(7), 1670-1677.

Heinrich, M., & Kulozik, U. (2011). Study of chymosin hydrolysis of casein micelles under ultra high pressure: Effect on re-association upon pressure release. *International Dairy Journal*, *21*(9), 664-669.

Henry, G., Mollé, D., Morgan, F., Fauquant, J., & Bouhallab, S. (2002). Heat-Induced Covalent Complex between Casein Micelles and β-Lactoglobulin from Goat's Milk: Identification of an Involved Disulfide Bond. *Journal of Agricultural and Food Chemistry, 50*(1), 185-191.

Hernández Sánchez, M. D. R., Cuvelier, M. E., & Turchiuli, C. (2016). Effect of α-tocopherol on oxidative stability of oil during spray drying and storage of dried emulsions. *DOF2015, 6th Edition of the International Symposium on Delivery of Functionality in Complex Food Systems: Physically Inspired Approaches From the Nano Scale to the Micro Scale*, *88*, 32-41.

Herzberg, G., & Spinks, J. W. T. (1939). In G. Herzberg, J. W. T. Spinks (Eds.), *Molecular Spectra and Molecular Structure: Infrared and Raman spectra of polyatomic molecules* (pp. 13-22). Upper Saddle River: Prentice-Hall.

Hill, T., (1960). Polymer and Polylelctrolyte Solutions and Gels. In T. Hill（Eds.), An Introduction to Statistical Thermodynamics (pp. 398-423). New York: Dover Publication, Inc..

Holmér, J., Zeng, L., Kanne, T., Krogstrup, P., Nygård, J., de Knoop, L., & Olsson, E. (2018). An STM - SEM setup for characterizing photon and electron induced effects in single photovoltaic nanowires. *Nano Energy*, *53*, 175-181.

Holt, C. (1992). Structure and Stability of Bovine Casein Micelles. In C. B. Anfinsen, F. M. Richards, J. T. Edsall, & D. S. Eisenberg (Eds.), *Advances in Protein Chemistry* (pp. 63-151). Massachusetts: Academic Press.

Holt, C. (1998). Casein Micelle Substructure and Calcium Phosphate Interactions Studied by Sephacryl Column Chromatography. *Journal of Dairy Science*, *81*(11), 2994-3003.

Holt, C., & Horne, D. (1996). The hairy casein micelle: Evolution of the concept and its implications for dairy process. *Netherlands Milk & Dairy Journal*, *50*, 85-1.

Holt, C., de Kruif, C. G. K., Tuinier, R., & Timmins, P. A. (2003). Substructure of bovine casein micelles by small-angle X-ray and neutron scattering. *Colloids and Surfaces A: Physicochemical and Engineering Aspects, 213*(2-3), 275-284.

Hollricher, O. (2010) Raman Instrumentation for Confocal Raman Microscopy. In T. Dieing,O. Hollricher, J. Toporski (Eds), *Confocal Raman Microscopy* (pp. 43-60). Springer:Heidelberg

Horne, D. S. (1998). Casein Interactions: Casting Light on the Black Boxes, the Structure in Dairy Products. *International Dairy Journal*, *8*(3), 171-177.

Horne, D. S. (2002). Casein structure, self-assembly and gelation. *Current Opinion in Colloid & Interface Science*, *7*(5), 456-461.

Horne, D. S. (2006). Casein micelle structure: Models and muddles. *Current Opinion in Colloid & Interface Science*, *11*(2-3), 148-153.

Horne, D. S., & Dalgleish, D. G. (1985). A photon correlation spectroscopy study of size distributions of casein micelle suspensions. *European Biophysics Journal*, *11*(4), 249-258.

Hu, M., Li, Y., Decker, E. A., Xiao, H., & McClements, D. J. (2010). Impact of Layer Structure on Physical Stability and Lipase Digestibility of Lipid Droplets Coated by Biopolymer Nanolaminated Coatings. *Food Biophysics*, *6*(1), 37-48.

Huen, J., Weikusat, C., Bayer-Giraldi, M., Weikusat, I., Ringer, L., & Lösche, K. (2014). Confocal Raman microscopy of frozen bread dough. *Journal of Cereal Science*, *60*(3), 555-560.

Huppertz, T., & de Kruif, C. G. (2008). Structure and stability of nanogel particles prepared by internal cross-linking of casein micelles. *International Dairy Journal*, *18*(5), 556-565.

Huppertz, T., Fox, P. F., & Kelly, A. L. (2018). 3 - The caseins: Structure, stability, and functionality. In R. Y. Yada (Eds.), *Woodhead Publishing Series in Food Science, Technology and Nutrition* (pp. 49-92). Cambridge: Woodhead Publishing.

Huppertz, T., Smiddy, M. A., & de Kruif, C. G. (2007). Biocompatible Micro-Gel

Particles from Cross-Linked Casein Micelles. *Biomacromolecules*, *8*(4), 1300-1305.

Huppertz, T., Vaia, B., & Smiddy, M. A. (2008). Reformation of casein particles from alkaline-disrupted casein micelles. *Journal of Dairy Research*, *75*(1), 44-47.

Lametti, S., Scaglioni, L., Mazzini, S., Vecchio, G., & Bonomi, F. (1998). Structural Features and Reversible Association of Different Quaternary Structures of β-Lactoglobulin. *Journal of Agricultural and Food Chemistry*, *46*(6), 2159-2166.

Ikeda, S., & Morris, V. J. (2002). Fine-Stranded and Particulate Aggregates of Heat-Denatured Whey Proteins Visualized by Atomic Force Microscopy. *Biomacromolecules*, *3*(2), 382-389.

Irene Boye, J., Kalab, M., Alli, I., & Ma, C. Y. (2000). Microstructural Properties of Heat-set Whey Protein Gels: Effect of pH. *LWT - Food Science and Technology*, *33*(3), 165-172.

Jachimska, B., Wasilewska, M., & Adamczyk, Z. (2008). Characterization of Globular Protein Solutions by Dynamic Light Scattering, Electrophoretic Mobility, and Viscosity Measurements. *Langmuir*, *24*(13), 6866-6872.

Jandera, P. (2013). Liquid chromatography | Normal Phase. In P. Worsfold, C. Poole, A. Townshend, & M. Miró (Eds.), *Encyclopedia of Analytical Science (Third Edition)* (pp. 162-173). Oxford: Academic Press.

Jenkins, P., & Snowden, M. (1996). Depletion flocculation in colloidal dispersions. *Advances in Colloid and Interface Science*, *68*(1-3), 57-96.

Jenness, R., Wong, N. P., Marth, E. H., & Keeney, M. (1988). Composition of Milk. In R. Wong (Eds.), *Fundamentals of Dairy Chemistry(pp. 1-38)*. New York: Springer.

Jensen, S., Rolin, C., & Ipsen, R. (2010). Stabilisation of acidified skimmed milk with HM pectin. *Food Hydrocolloids*, *24*(4), 291-299.

Jeschek, D., Lhota, G., Wallner, J., & Vorauer-Uhl, K. (2016). A versatile, quantitative analytical method for pharmaceutical relevant lipids in drug delivery systems. *Journal of Pharmaceutical and Biomedical Analysis*, *119*, 37-44.

Jeyarajah, S., Allen, J.C. (1994) Calcium binding and salt-induced structural changes of native and preheated beta-lactoglobulin, *Journal of Agricultural and Food Chemistry*, *42*, 80-85.

Ji, Y., Lee, S. K., & Anema, S. G. (2016). Characterisation of heat-set milk protein gels. International Dairy Journal, *54*, 10-20.

Karmowski, J., Hintze, V., Kschonsek, J., Killenberg, M., & Böhm, V. (2015). Antioxidant activities of tocopherols/tocotrienols and lipophilic antioxidant capacity of wheat, vegetable oils, milk and milk cream by using photochemiluminescence. *Food Chemistry*, *175*, 593-600.

Karnchanajindanun, J., Srisa-ard, M., Srihanam, P., & Baimark, Y. (2010). Preparation and characterization of genipin-cross-linked chitosan microparticles by water-in-oil emulsion solvent diffusion method. *Natural Science*, *02*(10), 1061.

Kasapis, S., Morris, E. R., Norton, I. T., & Gidley, M. J. (1993). Phase equilibria and gelation in gelatin/maltodextrin systems — Part II: polymer incompatibility in solution. *Carbohydrate Polymers*, *21*(4), 249-259.

Kavukcuoglu, N. B., & Pleshko, N. (2011). 3.322 - Infrared and Raman Microscopy and Imaging of Biomaterials. In P. Ducheyne (Eds.), *Comprehensive Biomaterials* (pp. 365-378). Oxford: Elsevier.

Keen, P. H. R., Slater, N. K. H., & Routh, A. F. (2012). Encapsulation of Lactic Acid Bacteria in Colloidosomes. *Langmuir*, *28*(46), 16007-16014.

Kessler, H. G. (2002). Centrifugation - separation - cylone separation in H.G. Kessler, *Food and bio process engineering: dairy technology* (pp.41-52). Munich: Verlag A. Kessler.

Kimpel, F., & Schmitt, J. J. (2015). Review: Milk Proteins as Nanocarrier Systems for Hydrophobic Nutraceuticals. *Journal of Food Science*, *80*(11), R2361-R2366.

Kirchmeier, O. (1973). Arrangement of components, electric charge and interaction energies of casein particles. *Nederlands Milk Dariy Journal, 27,*191-198

Klemmer, K. J., Waldner, L., Stone, A., Low, N. H., & Nickerson, M. T. (2012). Complex coacervation of pea protein isolate and alginate polysaccharides. *Food Chemistry*, *130*(3), 710-715.

Knoop, A.-M., Knoop, E., & Wiechen, A. (1979). Sub-structure of synthetic casein micelles. *Journal of Dairy Research*, *46*(2), 347-350.

Koppel, D. E. (1972). Analysis of Macromolecular Polydispersity in Intensity Correlation Spectroscopy: The Method of Cumulants. *The Journal of Chemical Physics*, *57*(11), 4814-4820.

Korhonen, H. J. (2011). 20 - Bioactive milk proteins, peptides and lipids and other

functional components derived from milk and bovine colostrum. In M. Saarela (Eds.), *Woodhead Publishing Series in Food Science, Technology and Nutrition* (pp. 471-511). Cambridge: Woodhead Publishing CY.

Kontopidis, G., Holt, G., Sawyer, L. (2004). Invited review: beta-lactoglobulin: binding properties, structure, and function, *Journal of Dairy Science*. *87*, 785-796.

König, A. M., Weerakkody, T. G., Keddie, J. L., & Johannsmann, D. (2008). Heterogeneous Drying of Colloidal Polymer Films: Dependence on Added Salt. *Langmuir*, *24*(14), 7580-7589.

Krzeminski, A., Prell, K. A., Busch-Stockfisch, M., Weiss, J., & Hinrichs, J. (2014). Whey protein-pectin complexes as new texturising elements in fat-reduced yoghurt systems. *International Dairy Journal*, *36*(2), 118-127.

la Fuente, de, M. A., Singh, H., & Hemar, Y. (2002). Recent advances in the characterisation of heat-induced aggregates and intermediates of whey proteins. *Trends in Food Science and Technology*, *13*(8), 262-274.

Lam, M., Shen, R., Paulsen, P., & Corredig, M. (2007). Pectin stabilization of soy protein isolates at low pH. *Food Research International*, *40*(1), 101-110.

Laurent, M. A., & Boulenguer, P. (2003). Stabilization mechanism of acid dairy drinks (ADD) induced by pectin. *Food Hydrocolloids*, *17*(4), 445-454.

Lazidis, A., Hancocks, R., Spyropoulos, F., Kreuß, M., Berrocal, R., & Norton, I. (2016). Whey protein fluid gels for the stabilisation of foams. *Food hydrocolloids*, *53*, 209-217.

Lenthe, W. C., Stinville, J. C., Echlin, M. P., Chen, Z., Daly, S., & Pollock, T. M. (2018). Advanced detector signal acquisition and electron beam scanning for high resolution SEM imaging. *Ultramicroscopy*, *195*, 93-100.

Leroy, M., Labbé, J.-F., Ouellet, M., Jean, J., Lefèvre, T., Laroche, G., et al. (2014). A comparative study between human skin substitutes and normal human skin using Raman microspectroscopy. *Acta Biomaterialia*, *10*(6), 2703-2711.

Li, RN., Clough, A., Yang, Z., & Tsui, O. K. C. (2012). Equilibration of Polymer Films Cast from Solutions with Different Solvent Qualities. *Macromolecules*, *45*(2), 1085-1089.

Li-Chan, E., Nakai, S., & Hirotsuka, M. (1994). Raman spectroscopy as a probe of protein structure in food systems. In R. Y. Yada, R. L. Jackman, & J. L. Smith (Eds.), *Protein Structure-Function Relationships in Foods* (pp. 163-197). Boston, MA: Springer US.

Lin, S. H. C., Dewan, R. K., Bloomfield, V. A., & Morr, C. V. (2002). Inelastic light-scattering study of the size distribution of bovine milk casein micelles. *Biochemistry*, *10*(25), 4788-4793.

Liu, Y., & Guo, R. (2008). pH-dependent structures and properties of casein micelles. *Biophysical Chemistry*, *136*(2), 67-73.

Liu, G., Jæger, T.C., Nielsen, S.B., Ray, C.A., Ipsen, R. (2017). Interactions in heated milk model systems with different ratios of nanoparticulated whey protein at varying pH, *International Dairy Journal*, *74*, 57-62.

Livesey, A. K., Licinio, P., & Delaye, M. (1986). Maximum entropy analysis of quasielastic light scattering from colloidal dispersions. *The Journal of Chemical Physics*, *84*(9), 5102-5107.

Livney, Y. D. (2010) Milk proteins as vehicles for bioactives. *Current Opinion in Colloid & Interface Science, 15*(1-2), 73-83

Livney, Y. D., Corredig, M., & Dalgleish, D. G. (2003). Influence of thermal processing on the properties of dairy colloids. *Current Opinion in Colloid & Interface Science*, *8*(4), 359-364.

Loiseleux, T., Rolland-Sabaté, A., Garnier, C., Croguennec, T., Guilois, S., Anton, M., Riaublanc, A. (2018). Determination of hydro-colloidal characteristics of milk protein aggregates using asymmetrical flow field-flow fractionation coupled with multiangle laser light scattering and differential refractometer (AF4-MALLS-DRi), *Food Hydrocolloid*, 74, 197-206.

Lozano, J. M., Giraldo, G. I., & Romero, C. M. (2008). An improved method for isolation of β-lactoglobulin. *International Dairy Journal*, *18*(1), 55-63.

Lozano-Sánchez, J., Borrás-Linares, I., Sass-Kiss, A., & Segura-Carretero, A. (2018). Chapter 13 - Chromatographic Technique: High-Performance Liquid Chromatography (HPLC). In D. W. Sun (Ed.), *Modern Techniques for Food Authentication (Second Edition)* (pp. 459-526). Academic Press.

Luo, Y., Pan, K., & Zhong, Q. (2015). Casein/pectin nanocomplexes as potential oral delivery vehicles. *International Journal of Pharmaceutics*, *486*(1-2), 59-68.

Luo, Y., Zhang, B., Whent, M., Yu, L. L., & Wang, Q. (2011). Preparation and characterization of zein/chitosan complex for encapsulation of α-tocopherol, and its in vitro controlled release study. *Colloids and Surfaces. B, Biointerfaces*, *85*(2), 145-152.

Madadlou, A., Floury, J., Pezennec, S., & Dupont, D. (2018). Encapsulation of β-

lactoglobulin within calcium carbonate microparticles and subsequent in situ fabrication of protein microparticles. *Food Hydrocolloids*, *84*, 38-46.

Manderson, G. A., Creamer, L. K., & Hardman, M. J. (1999). Effect of Heat Treatment on the Circular Dichroism Spectra of Bovine β-Lactoglobulin A, B, and C. *Journal of Agricultural and Food Chemistry*, *47*(11), 4557-4567.

Ma, L., Yang, Y., Chen, J., Wang, J., & Bu, D. (2017). A rapid analytical method of major milk proteins by reversed-phase high-performance liquid chromatography. *Animal Science Journal*, *88*(10), 1623-1628.

Mao, L., Boiteux, L., Roos, Y. H., & Miao, S. (2014). Evaluation of volatile characteristics in whey protein isolate-pectin mixed layer emulsions under different environmental conditions. *Food Hydrocolloids*, *41*, 79-85.

Mao, L., Roos, Y. H., O'Callaghan, D. J., & Miao, S. (2013). Volatile Release from Whey Protein Isolate-Pectin Multilayer Stabilized Emulsions: Effect of pH, Salt, and Artificial Salivas. *Journal of Agricultural and Food Chemistry*, *61*(26), 6231-6239.

Mao, Y., Krischke, M., Hengst, C., & Kulozik, U. (2018). Comparison of the influence of pH on the selectivity of free and immobilized trypsin for β-lactoglobulin hydrolysis. *Food Chemistry*, *253*, 194-202.

Marchin, S., Putaux, J.-L., Pignon, F., & Léonil, J. (2007). Effects of the environmental factors on the casein micelle structure studied by cryo transmission electron microscopy and small-angle x-ray scattering/ultrasmall-angle x-ray scattering. *The Journal of Chemical Physics*, *126*(4), 045101.

Maroziene, A., & de Kruif, C. G. (2000). Interaction of pectin and casein micelles. *Food Hydrocolloids*, *14*(4), 391-394.

Marreto, R. N., Ramos, M. F. S., Silva, E. J., de Freitas, O., & de Freitas, L. A. P. (2013). Impact of Cross-linking and Drying Method on Drug Delivery Performance of Casein-Pectin Microparticles. *AAPS PharmSciTech*, *14*(3), 1227-1235.

Marziali, A. (2000). Nucleic acids | Centrifugation. In I. D. Wilson (Eds.), *Encyclopedia of Separation Science* (pp. 3517-3524). Oxford: Academic Press.

Matés, J. M., & Pérez-Gómez, C. (2000). POLYSACCHARIDES | Liquid Chromatography. In I. D. Wilson (Ed.), *Encyclopedia of Separation Science* (pp. 3929-3937). Oxford: Academic Press.

Mehalebi, S., Nicolai, T., Durand, D. (2008). Light scattering study of heat-denatured globular protein aggregates, *International Journal of Biological Macromolecules, 43*, 129-135.

McClements, D. J. (2006). Non-covalent interactions between proteins and polysaccharides. *Biotechnology Advances*, *24*(6), 621-625.

McGann, T. C. A., Donnelly, W. J., Kearney, R. D., & Buchhemm, W. (1980). Composition and size distribution of bovine casein micelles. *Biochimica Et Biophysica Acta (BBA) - General Subjects*, *630*(2), 261-270.

McMullan, D. (2006). Scanning electron microscopy 1928-1965. *Scanning*, *17*(3), 175-185.

Menéndez-Aguirre, O., Kessler, A., Stuetz, W., Grune, T., Weiss, J., & Hinrichs, J. (2014). Increased loading of vitamin D2 in reassembled casein micelles with temperature-modulated high-pressure treatment. *Food Research International*, *64*, 74-80.

Meyer, A., Raba, C., & Fischer, K. (2001). Ion-Pair RP-HPLC Determination of Sugars, Amino Sugars, and Uronic Acids after Derivatization with p-Aminobenzoic Acid. *Analytical Chemistry, 73*(11), 2377-2382.

Meyer, V. R. (2004). Introduction In V.R. Meyer (Eds.), *Practical High-Performance Liquid Chromatography*. (pp. 5-16). New York: John Wiley & Sons.

Mie, G. (1908). Beiträge zur Optik trüber Medien, speziell kolloidaler Metallösungen. *Annalen Der Physik*, *330*(3), 377-445.

Miller, J., Schätzel, K., & Vincent, B. (1991). The Determination of Very Small Electrophoretic Mobilities in Polar and Nonpolar Colloidal Dispersions Using Phase-Analysis Light-Scattering. *Journal of Colloid and Interface Science*, *143*, 532-554.

Mimouni, A., Deeth, H. C., Whittaker, A. K., Gidley, M. J., & Bhandari, B. R. (2009). Rehydration process of milk protein concentrate powder monitored by static light scattering. *Food Hydrocolloids*, *23*(7), 1958-1965.

Morrison, I. D., Grabowski, E. F., & Herb, C. A. (1985). Improved techniques for particle size determination by quasi-elastic light scattering. *Langmuir*, *1*(4), 496-501.

Moreno-Arribas, M. V., & Polo, M. C. (2003). CHROMATOGRAPHY | High-performance Liquid Chromatography. In B. Caballero (Ed.), *Encyclopedia of Food*

Sciences and Nutrition (Second Edition) (pp. 1274-1280). Oxford: Academic Press.

Mojsov, K. D. (2016). Chapter 16 - Aspergillus Enzymes for Food Industries. In V. K. Gupta (Ed.), *New and Future Developments in Microbial Biotechnology and Bioengineering* (pp. 215-222). Amsterdam: Elsevier.

Movasaghi, Z., Rehman, S., & ur Rehman, D. I. (2008). Fourier Transform Infrared (FTIR) Spectroscopy of Biological Tissues. *Applied Spectroscopy Reviews*, *43*(2), 134-179.

Mounsey, J., O'Kennedy, B., & Kelly, P. (2005). Comparison of re-micellised casein prepared from acid casein with micellar casein prepared by membrane filtration. *Lait*, *85*, 419-430.

Mukherjee, P. K. (2019). Chapter 10 - High-Performance Liquid Chromatography for Analysis of Herbal Drugs. In P. K. Mukherjee (Ed.), *Quality Control and Evaluation of Herbal Drugs* (pp. 421-458). New York: Elsevier.

Muller-Buschbaum, P., Gebhardt, R., Roth, S. V., Metwalli, E., & Doster, W. (2007). Effect of Calcium Concentration on the Structure of Casein Micelles in Thin Films. *Biophysical Journal*, *93*(3), 960-968.

Nakamura, A., Yoshida, R., Maeda, H., & Corredig, M. (2006). The stabilizing behaviour of soybean soluble polysaccharide and pectin in acidified milk beverages. *International Dairy Journal*, *16*(4), 361-369.

Naumann, D., Helm, D., & Labischinski, H. (1991). Microbiological characterizations by FT-IR spectroscopy. *Nature*, *351*, 81-82.

Neue, U. D., Alden, B. A., Iraneta, P. C., Méndez, A., Grumbach, E. S., Tran, K., & Diehl, D. M. (2005). 4 - HPLC Columns for Pharmaceutical Analysis. In S. Ahuja, S. & M. W. Dong (Eds.), *Bioseparation of Proteins* (Vol. 6, pp. 77-122). New York: Academic Press.

Nicolai, T., & Murray, B. (2017). Particle stabilized water in water emulsions. *Food Hydrocolloids*, *68*, 157-163.

Norton, J. E., Gonzalez Espinosa, Y., Watson, R. L., Spyropoulos, F., & Norton, I. T. (2015). Functional food microstructures for macronutrient release and delivery. *Food & Function*, *6*(3), 663-678.

Ntazinda, A., Cheserek, M. J., Sheng, L.-X., Meng, J., & Lu, R.-R. (2014). Combination effect of sodium carboxymethyl cellulose and soybean soluble polysac-

charides on stability of acidified skimmed milk drinks. *Dairy Science & Technology*, *94*(3), 283-295.

Nyeo, S. L., & Chu, B. (1989). Maximum-entropy analysis of photon correlation spectroscopy data. *Macromolecules*, *22*(10), 3998-4009.

Oakenfull, D.G. (1991). Chapter 5 - The Chemistry of High Methoxyl Pectins. In R. H. Walter (Ed.) *The Chemistry and Technology of Pectin* (pp. 87-108). Oxford: Academic Press.

Oakenfull, D., & Scott, A. (1984). Hydrophobic Interaction in the Gelation of High Methoxyl Pectins. *Journal of Food Science*, *49*(4), 1093-1098.

Oldfield, D. J., Singh, H., & Taylor, M. W. (1998). Association of β-Lactoglobulin and β-Lactalbumin with the Casein Micelles in Skim Milk Heated in an Ultra-high Temperature Plant. *International Dairy Journal*, *8*(9), 765-770.

Oldfield, D. J., Singh, H., Taylor, M. W., & Pearce, K. N. (2000). Heat-induced interactions of β-lactoglobulin and α-lactalbumin with the casein micelle in pH-adjusted skim milk. *International Dairy Journal*, *10*(8), 509-518.

Otoni, C. G., Avena-Bustillos, R. J., Azeredo, H. M. C., Lorevice, M. V., Moura, M. R., Mattoso, L. H. C., & McHugh, T. H. (2017). Recent Advances on Edible Films Based on Fruits and Vegetables-A Review. *Comprehensive Reviews in Food Science and Food Safety*, *16*(5), 1151-1169.

Otter, D. (2003). Protein | Determination and Characterization. In B. Caballero (Eds.), *Encyclopedia of Food Sciences and Nutrition (Second Edition)* (pp. 4824-4830). Oxford: Academic Press.

Panouillé, M., Durand, D., Nicolai, T., Larquet, E., & Boisset, N. (2005). Aggregation and gelation of micellar casein particles. *Journal of Colloid and Interface Science*, *287*(1), 85-93.

Papiz, M.Z., Sawyer, L., Eliopoulos, E.E., North, A.C., Findlay, J.B., Sivaprasadarao, R., Jones, T.A, Newcomer, M.E., Kraulis, P.J. (1986). The structure of beta-lactoglobulin and its similarity to plasma retinol-binding protein, *Nature*, *324*, 383-385.

Pavlath, A. E., & Orts, W. (2009). Edible Films and Coatings: Why, What, and How? In K. C. Huber & M. E. Embuscado (Eds.), *Edible Films and Coatings for Food Applications* (pp. 1-23). New York: Springer.

Pecora, R. (1964). Doppler Shifts in Light Scattering from Pure Liquids and Polymer Solutions. *The Journal of Chemical Physics*, *40*(6), 1604-1614.

Petit, J., Herbig, A.-L., Moreau, A., Delaplace, G. (2011). Influence of calcium onb-lactoglobulin denaturation kinetics: implications in unfolding and aggregation mechanisms, *Journal of Dairy Science, 94*, 5794-5810.

Phan-Xuan, T., Durand, D., Nicolai, T., Donato, L., Schmitt, C., & Bovetto, L. (2011). On the Crucial Importance of the pH for the Formation and Self-Stabilization of Protein Microgels and Strands. *Langmuir*, *27*(24), 15092-15101.

Philippe, M., Le Graët, Y., & Gaucheron, F. (2005). The effects of different cations on the physicochemical characteristics of casein micelles. *Food Chemistry*, *90*(4), 673-683.

Pomastowski, P., Walczak-Skierska, J., Gawin, M., Bocian, S., Piekoszewski, W., & Buszewski, B. (2014). HPLC separation of casein components on a diol-bonded silica column with MALDI TOF/TOF MS identification. *Analytical Methods*, *6*, 5236.

Poortinga, A. T. (2008). Microcapsules from Self-Assembled Colloidal Particles Using Aqueous Phase-Separated Polymer Solutions. *Langmuir*, *24*(5), 1644-1647.

Pouliot, Y., Boulet, M., & Paquin, P. (1989). Observations on the heat-induced salt balance changes in milk I. Effect of heating time between 4 and 90°C. *Journal of Dairy Research*, *56*(2), 185-192.

Price, C. A. (1982). 2 - Origins of Density Gradient Centrifugation. In C. A. Price (Eds.), *Centrifugation in Density Gradients* (pp. 12-31). Massachusetts: Academic Press.

Pusey, P. N. (1972). Correlation and light beating spectroscopy. In: H. Z. Cummings, E. R. Pike (Eds.). *Photon correlation and light beating spectroscopy* (pp.387-428). New York: Plenum.

Puthli S., Vavia, P. (2008). Gamma irradiated micro system for long-term parenteral contraception. An alternative to synthetic polymers. *European Journal of Pharmaceutical Sciences*, *35*, 307-317.

Qi, P. X. (2007). Studies of casein micelle structure: the past and the present. *Le Lait*, *87*(4-5), 363-383.

Reimer, L. (1998). Emission of Backscattered and Secondary Electrons. In L. Reimer (Eds.), *Scanning Electron Microscopy: Physics of Image Formation and Microanalysis* (pp. 135-169). Berlin: Springer.

Rickwood, D., Ford, T., & Steensgaard, J. (1994). In *Centrifugation: Essential Data.* New York: Wiley.

Roach, A., Dunlap, J., & Harte, F. (2009). Association of Triclosan to Casein Proteins Through Solvent-Mediated High-Pressure Homogenization. *Journal of Food Science*, *74*(2), N23-N29.

Robuschi, L., Tomba, J. P., & Busalmen, J. P. (2017). Proving Geobacter biofilm connectivity with confocal Raman microscopy. *SI:Professor Antonio Aldaz*, *793*, 99-103.

Rodrigues M., Simioni A., Primo F., Siqueira-Moura M., Morais P., Tedesco A. (2009). Preparation, characterization and in vitro cytotoxicity of BSA-based nanospheres containing nanosized magnetic particles and/or photosensitizer. *Journal of Magnetism and Magnetic Materials*, *321(10)*, 1600-1603.

Rolin, C. (1993). CHAPTER 10 - PECTIN. In R. L. Whistler & J. N. Bemiller (Eds.), *Industrial Gums (Third Edition)* (pp. 257-293). London: Academic Press.

Ronningen, T. J., Schuetter, J. M., Wightman, J. L., Murdock, A., & Bartko, A. P. (2014). Raman spectroscopy for biological identification. In R. P. Schaudies (Ed.), *Biological Identification* (pp. 313-333). New York: Elsevier.

Roth, R., Schoelkopf, J., Huwyler, J., & Puchkov, M. (2018). Functionalized calcium carbonate microparticles for the delivery of proteins. *European Journal of Pharmaceutics and Biopharmaceutics*, *122*, 96-103.

Robards, K., Haddad, P. R., & Jackson, P. E. (2004). 6 - High-performance Liquid Chromatography—Separations. In Robards K., Haddad, P. R., & Jackson, P. E. (Eds.), *Principles and Practice of Modern Chromatographic Methods* (pp. 305-380). Boston: Academic Press.

Rygula, A., Majzner, K., Marzec, K. M., Kaczor, A., Pilarczyk, M., & Baranska, M. (2013). Raman spectroscopy of proteins: a review. *Journal of Raman Spectroscopy*, *44*(8), 1061-1076.

Rygula, A., Oleszkiewicz, T., Grzebelus, E., Pacia, M. Z., Baranska, M., & Baranski, R. (2018). Raman, AFM and SNOM high resolution imaging of carotene crystals in a model carrot cell system. *Festschrift in Honor of Prof. Yukihiro Ozaki*, *197 IS* -, 47-55.

Sadana, A. (1998). 5 - Protein Inactivations During Chromatographic Methods of Separation. In A. Sadana (Ed.), *Bioseparation of Proteins* (Vol. 1, pp. 135-176). Academic Press.

Sadegh Pourshahab, P., Gilani, K., Moazeni, E., Eslahi, H., Fazeli, M., & Jamalifar, H. (2011). Preparation and characterization of spray dried inhalable powders

containing chitosan nanoparticles for pulmonary delivery of isoniazid. *Journal of Microencapsulation*, *28*, 605-613.

Sagis, L. M. C. (2008a). Dynamics of controlled release systems based on water-in-water emulsions: A general theory. *Journal of Controlled Release*, *131*(1), 5-13.

Sagis, L. M. C. (2008b). Dynamics of Encapsulation and Controlled Release Systems Based on Water-in-Water Emulsions: Negligible Surface Rheology. *The Journal of Physical Chemistry B*, *112*(43), 13503-13508.

Sağlam, D., Venema, P., van der Linden, E., & de Vries, R. (2014). Design, properties, and applications of protein micro- and nanoparticles. *Current Opinion in Colloid and Interface Science*, *19*(5), 428-437.

Salvatore, E., Pirisi, A., & Corredig, M. (2011). Gelation properties of casein micelles during combined renneting and bacterial fermentation: Effect of concentration by ultrafiltration. *International Dairy Journal*, *21*(11), 848-856.

Sano, Y. (1992). Drying of polymer solution. *Drying Technology*, *10*(3), 591-622.

Sant'Ana, A. S. (2014). Physical removal of microfloras | Centrifugation. In C. A. Batt & M. L. Tortorello (Eds.), *Encyclopedia of Food Microbiology (Second Edition)* (pp. 30-35). Oxford: Academic Press.

Santos, A. C., Cunha, J., Veiga, F., Cordeiro-Da-Silva, A., & Ribeiro, A. J. (2013). Ultrasonication of insulin-loaded microgel particles produced by internal gelation: Impact on particle's size and insulin bioactivity. *Carbohydrate Polymers*, *98*(2), 1397-1408.

Saveyn, H., Thu, T. L., Govoreanu, R., Van der Meeren, P., & Vanrolleghem, P. A. (2006). In-line Comparison of Particle Sizing by Static Light Scattering, Time-of-Transition, and Dynamic Image Analysis. *Particle & Particle Systems Characterization*, *23*(2), 145-153.

Semo, E., Kesselman, E., Danino, D., & Livney, Y. (2007). Casein micelle as a natural nano-capsular vehicle for nutraceuticals. *Food Hydrocolloids*, *21*(5-6), 936-942.

Schachman, H. K. (1959). II - General Considerations. In H. K. Schachman (Eds.), *Ultracentrifugation in Biochemistry* (pp. 5-12). Massachusetts: Academic Press.

Schmidt, D. G. (1982). Association of caseins and casein micelle structure. In P. F. Fox (Eds.). D*evelopments in Dairy Chemistry* (pp. 61-85). London: Applied Science Publishers.

Schmidt, U. K. (2015). *Citrus pectin as a hydrocolloid emulsifier: Emulsifying and emulsion stabilizing properties*. Dissertation: Karlsruher Institiut für Technologie (KIT), Karlsruher.

Schokker, E. P., Singh, H., Pinder, D. N., Norris, G. E., & Creamer, L. K. (1999). Characterization of intermediates formed during heat-induced aggregation of β-lactoglobulin AB at neutral pH. *International Dairy Journal*, *9*(11), 791-800.

Schrader, B. (1995). General survey of vibrational spectroscopy. In P. Schrader (Eds.) *Infrared and Raman Spectroscopy(pp7-61),* Weinheim: VCH.

Sedlmeyer, F., Brack, M., Rademacher, B., & Kulozik, U. (2004). Effect of protein composition and homogenisation on the stability of acidified milk drinks. *International Dairy Journal*, *14*(4), 331-336.

Selamat, S. N., Muhamad, I. I., & Sarmidi, M. (2009). Encapsulation of a-tocopherol and tocotrienol in vitamin-E using spray drying technique. *South East Asian Technical Universities Consortium (SEATUC) - 3rd SEATUC Symposium Proceeding. Johor Bahru, Malaysia*.

Selo, C., Bernard, C., Creminon, P., & Wal, JM. (1999). Allergy to bovine beta-lactoglobulin: specificity of human IgE to tryptic peptides. *Clinical Experimental Allergy*, *29*(8), 1055-1063.

Semo, E., Kesselman, E., Danino, D., & Livney, Y. (2007). Casein micelle as a natural nano-capsular vehicle for nutraceuticals. *Food Hydrocolloids*, *21*(5-6), 936-942.

Serfert, Y., Schröder, J., Mescher, A., Laackmann, J., Rätzke, K., Shaikh, M. Q. (2013). Spray drying behaviour and functionality of emulsions with β-lactoglobulin/pectin interfacial complexes. *Food Hydrocolloids*, *31*(2), 438-445.

Shapira, A., Markman, G., Assaraf, Y. G., & Livney, Y. D. (2010). β-casein-based nanovehicles for oral delivery of chemotherapeutic drugs: drug-protein interactions and mitoxantrone loading capacity. *Nanomedicine: Nanotechnology, Biology, and Medicine*, *6*(4), 547-555.

Shi, Q., Roux, S., Latourte, F., Hild, F., Loisnard, D., & Brynaert, N. (2018). Measuring topographies from conventional SEM acquisitions. *Ultramicroscopy*, *191*, 18-33.

Shilpi, S., Jain, A., Gupta, Y., & Jain, S. (2007). Colloidosomes: An Emerging Vesicular System in Drug Delivery. *Critical Reviews™ in Therapeutic Drug Carrier Systems*, *24*(4), 361-391.

Singh, H., & Fox, P. F. (1987). Heat stability of milk: influence of colloidal and soluble salts and protein modification on the pH-dependent dissociation of micellar κ-casein. *Journal of Dairy Research*, *54*(4), 523-534.

Singh, S., & Gupta, R. (2004). Apple juice clarification using fungal pectinolytic enzyme and gelatin. *Indian Journal of Biotechnology*, *3*, 573-576.

Sirijariyawat, A., Charoenrein, S., & Barrett, D. M. (2012). Texture improvement of fresh and frozen mangoes with pectin methylesterase and calcium infusion. *Journal of the Science of Food and Agriculture*, *92*(13), 2581-2586.

Smits, P., & Brouwershaven, J. H. V. (1980). Heat-induced association of β-lactoglobulin and casein micelles. *Journal of Dairy Research*, *47*(3), 313-325.

Snyder, R. G., Scherer, J. R., & Gaber, B. P. (1980). Effects of chain packing and chain mobility on the raman spectra of biomembranes. *Biochimica Et Biophysica Acta (BBA) - Biomembranes*, *601*, 47-53.

Soares, M. M. C. N., Da Silva, R., Carmona, E. C., & Gomes, E. (2001). Pectinolytic enzyme production by Bacillus species and their potential application on juice extraction. *World Journal of Microbiology and Biotechnology*, *17*(1), 79-82.

Sobel, R., Versic, R., & Gaonkar, A. G. (2014). Chapter 1 - Introduction to Microencapsulation and Controlled Delivery in Foods. In A. G. Gaonkar, N. Vasisht, A. R. Khare, R. Sober (Eds.), *Microencapsulation in the Food Industry* (pp. 3-12). San Diego: Academic Press.

Solar, O., & Gunasekaran, S. (2010). Rheological properties of rennet casein-whey protein gels prepared at different mixing speeds. *Journal of Food Engineering*, 99, 338-343.

Somchue, W., Sermsri, W., Shiowatana, J., & Siripinyanond, A. (2009). Encapsulation of α-tocopherol in protein-based delivery particles. *Food Research International*, *42*(8), 909-914.

Spiegel, T. (1999). Whey protein aggregation under shear conditions -effects of lactose and heating temperature on aggregate size and structure. *International Journal of Food Science and Technology*, *34*(5-6), 523-531.

Sriamornsak, P. (1999). Effect of calcium concentration, hardening agent and drying condition on release characteristics of oral proteins from calcium pectinate gel beads. *European Journal of Pharmaceutical Sciences*, *8*(3), 221-227.

Sriamornsak, P. (2003). Chemistry of pectin and its pharmaceutical uses: a review. *Silpakorn University International Journal, 3(*1-2*), 226-228.*

Stetefeld, J., McKenna, S. A., & Patel, T. R. (2016). Dynamic light scattering: a practical guide and applications in biomedical sciences. *Biophysical Reviews*, *8*(4), 409-427.

Steinhauer, T., Kulozik, U. Gebhardt, R. (2014) Structure of milk protein deposits formed by casein micelles and b-lactoglobulin during frontal microfiltration, *Journal of Membrane Science*, 468, 126-132.

Steinhauer, T., Hanély, S., Bogendörfer, K., Kulozik, U. (2015) Temperature dependent membrane fouling during filtration of whey and whey proteins, *Journal of Membrane Science*, *492*, 364-370.

Sturaro, A., De Marchi, M., Masi, A., & Cassandro, M. (2016). Quantification of whey proteins by reversed phase-HPLC and effectiveness of mid-infrared spectroscopy for their rapid prediction in sweet whey. *Journal of Dairy Science*, *99*(1), 68-76.

Sutherland, W. (2009). LXXV. A dynamical theory of diffusion for non-electrolytes and the molecular mass of albumin. *The London, Edinburgh, and Dublin Philosophical Magazine and Journal of Science*, *9*(54), 781-785.

Syrbe, A., Bauer, W.J., Klostermeyer, H. (1998). Polymer science concepts in dairy systems - an overview of milk protein and food hydrocolloid interaction. *International Dairy Journal*, *8*(3), 179-193.

Synytsya, A. (2003). Fourier transform Raman and infrared spectroscopy of pectins. *Carbohydrate Polymers*, *54*(1), 97-106.

Takka, S., & Acarturk, F. (1999). Calcium alginate microparticles for oral administration. I: Effect of sodium alginate type on drug release and drug entrapment efficiency. *Journal of Microencapsulation*, *16*, 275-290.

Taulbee, D. N., & Mercedes Maroto-Valer, M. (2000). Centrifugation. In I. D. Wilson (Eds.), *Encyclopedia of Separation Science* (pp. 17-40). Oxford: Academic Press.

Taylor, J., Taylor, J. R. N., Belton, P. S., & Minnaar, A. (2009a). Kafirin Microparticle Encapsulation of Catechin and Sorghum Condensed Tannins. *Journal of Agricultural and Food Chemistry*, *57*(16), 7523-7528.

Taylor, J., Taylor, J. R. N., Belton, P. S., & Minnaar, A. (2009b). Preparation of Free-Standing Films from Kafirin Protein Microparticles: Mechanism of Formation and Functional Properties. *Journal of Agricultural and Food Chemistry*, *57*(15), 6729-6735.

Thakur, B. R., Singh, R. K., Handa, A. K., & Rao, M. A. (2009). Chemistry and uses of pectin — A review. *Critical Reviews in Food Science and Nutrition*, *37*(1), 47-73.

Taulier, N. & Chalikian, T.V. (2001) Characterization of pH-induced transitions of b-lactoglobulin: ultrasonic, densimetric, and spectroscopic studies, *Journal of Molecular Biology*, *314*, 873-889.

Thomar, P., & Nicolai, T. (2016). Heat-induced gelation of casein micelles in aqueous suspensions at different pH. *Colloids and Surfaces. B, Biointerfaces*, *146*, 801-807.

Thompson, K. L., Williams, M., & Armes, S. P. (2015). Colloidosomes: Synthesis, properties and applications. *Journal of Colloid and Interface Science*, *447*, 217-228.

Tirumkudulu, M. S., & Russel, W. B. (2004). Role of Capillary Stresses in Film Formation. *Langmuir*, *20*(7), 2947-2961.

Toro-Sierra, J., Tolkach, A., Kulozik, U. (2013). Fractionation of a-lactalbumin and b-lactoglobulin from whey protein isolate using selective thermal aggregation, an optimized membrane separation procedure and resolubilization techniques at pilot plant scale, *Food Bioprocess Technology*, *6*, 1032-1043.

Tosato, M. G., Orallo, D. E., Ali, S. M., Churio, M. S., Martin, A. A., & Dicelio, L. (2015). Confocal Raman spectroscopy: In vivo biochemical changes in the human skin by topical formulations under UV radiation. *Journal of Photochemistry and Photobiology B: Biology*, *153*, 51-58.

Tourrette, A., De Geyter, N., Jocic, D., Morent, R., Warmoeskerken, M. M. C. G., & Leys, C. (2009). Incorporation of poly(N-isopropylacrylamide)/chitosan microgel onto plasma functionalized cotton fibre surface. *Colloids and Surfaces a: Physicochemical and Engineering Aspects*, *352*(1-3), 126-135.

Tran Le, T., Saveyn, P., Hoa, H.D., van der Meeren, P. (2008). Determination of heat-induced effects on the particle size distribution of casein micelles by dynamic light scattering and nanoparticle tracking analysis, *International Dairy Journal*, *18*, 1090-1096.

Tuinier, R., & de Kruif, C. G. (2002). Stability of casein micelles in milk. *The Journal of Chemical Physics*, *117*(3), 1290-1295.

Tyndall, J. (1869). IV. On the blue colour of the sky, the polarization of skylight, and on the polarization of light by cloudy matter generally. *Proceedings of the*

Royal Society of London, *17*, 223-233.

Van Buggenhout S, Sila, D. N., Duvetter, T., Van Loey A, & Hendrickx, M. (2009). Pectins in Processed Fruits and Vegetables: Part III-Texture Engineering. *Comprehensive Reviews in Food Science and Food Safety*, *8*(2), 105-117.

Veloso, A. C. A., Teixeira, N., & Ferreira, IM (2002). Separation and quantification of the major casein fractions by reverse-phase high-performance liquid chromatography and urea-polyacrylamide gel electrophoresis: Detection of milk adulterations. *Journal of Chromatography A*, *967*(2), 209-218.

Vittayanont, M., Steffe, J. F., Flegler, S. L., & Smith, D. M. (2002). Gelling Properties of Heat-Denatured β-Lactoglobulin Aggregates in a High-Salt Buffer. *Journal of Agricultural and Food Chemistry, 50*(10), 2987-2992.

Walstra, P. (1990). On the Stability of Casein Micelles. *Journal of Dairy Science*, *73*(8), 1965-1979.

Walstra, P. (1999). Casein sub-micelles: do they exist? *International Dairy Journal*, *9*(3), 189-192.

Ware, B. R., & Flygare, W. H. (1971). The simultaneous measurement of the electrophoretic mobility and diffusion coefficient in bovine serum albumin solutions by light scattering. *Chemical Physics Letters*, *12*(1), 81-85.

Wellner. N. (2013). Fourier transform infrared (FTIR) and Raman Microscopy: Principles and Applications to Food Microstructures. In T. J. Morris & K. Groves. (Eds.) *Food Microstructures - Microscopy, measurement and Modelling* (pp.163-188). Oxford: Woodhead Publishing.

Wieking, W. (2002). Centrifuges. In H. Roginski (Eds.), *Encyclopedia of Dairy Sciences* (pp. 244-251). Oxford: Elsevier.

Williams, J. W. (1972). Chapter II - Size Distribution Analysis by Ultracentrifugal Methods. In J. W. Williams (Ed.), *Ultracentrifugation of Macromolecules* (pp. 21-35). London: Academic Press.

Winzor, D.J., Deszczynski, M., Harding, S.E., Wills, P.R. (2007). Nonequivalence of second virial coefficients from sedimentation equilibrium and static light scattering studies of protein solutions, Biophysical Chemistry, *128*, 46-55.

Wu, J., Liu, J., Dai, Q., & Zhang, H. (2013). The stabilisation of acidified whole milk drinks by carboxymethylcellulose. *International Dairy Journal*, *28*(1), 40-42.

Wu, Q., & Zhang, L. (2001). Structure and properties of casting films blended with starch and waterborne polyurethane. *Journal of Applied Polymer Science*,

79(11), 2006-2013.

Zhang, F., Brinck, T., Brandner, B. D., Claesson, P. M., Dedinaite, A., & Pan, J. (2013). In situ confocal Raman micro-spectroscopy and electrochemical studies of mussel adhesive protein and ceria composite film on carbon steel in salt solutions. *Electrochimica Acta*, *107*, 276-291.

Zhuang, Y., Sterr, J., Kulozik, U., & Gebhardt, R. (2015). Application of confocal Raman microscopy to investigate casein microparticles in blend casein/pectin films. *International Journal of Biological Macromolecules*, *74*, 44-48.

Zhuang, Y., Sterr, J., Schulte, A., Kulozik, U., Gebhardt, R. (2016). Casein microparticles from blend films forming casein/α-tocopherol emulsion droplets in solution. *Food Biophysics*, *11*, 332-338.

Zimet, P., Rosenberg, D., & Livney, Y. D. (2011). Re-assembled casein micelles and casein nanoparticles as nano-vehicles for ω-3 polyunsaturated fatty acids. *Food Hydrocolloids*, *25*(5), 1270-1276.

Zimm, B. H. (1945). Molecular Theory of the Scattering of Light in Fluids. *The Journal of Chemical Physics*, *13*(4), 141-145.

Zimm, B. H. (1948). Apparatus and Methods for Measurement and Interpretation of the Angular Variation of Light Scattering; Preliminary Results on Polystyrene Solutions. *The Journal of Chemical Physics*, *16*(12), 1099-1116.

Zittle, C.A., DellaMonica, E.S., Rudd, R.K., Custer, J.H. (1957) The binding of calcium ions by b-lactoglobulin both before and after aggregation by heating in the presence of calcium ions, Journal of the American Chemical Society, *79*, 4661-4666.

6 Summary

Casein micelle (CM) is a convenient source of hydrocolloids with unique physio-chemical functionalities. It could be found in various technical applications in the food and pharmaceutical industries. Its structure has been discussed extensively in order to predict its behavior under varying process conditions. Casein monomers, α_{S1}-, α_{S2}- , β- and κ-caseins, self-assemble into micellar form known as CM aided by CCP, which gives CM a stable structure against environmental stress, e.g., temperature, pressure or shear force. Interesting new structures could be generated when CM interacts with other hydrocolloids, such as proteins or polysaccharides. Depending upon the pre-defined pH in the system, it can form either associative complexes with other polymers or segregative complexes among themselves. Associative complex of CM is often studied and reported when surface charges between CM and co-polymers are altered by low pH. Co-polymer type, pH, and polymer concentration are key contributors to the structure of the resulting complex leading to varied functionalities for specific applications. On the other hand, the segregative interaction/complex was less studied due to the depletion flocculation or aggregation of the formed complexes rendering the system unstable for a reliable investigation.

The main objective of this work was to understand the structural changes of CM triggered by interaction with other hydrocolloids such as protein or polysaccharide. Firstly, the structural changes of CM were examined with the presence of ß-Lg and salts containing calcium via SLS. It aimed to create a better understanding of the interaction between individual CMs with the presence of other natural milk components. ß-Lg concertation was shown to impact the colloidal stability of CM. With 0.5 wt% ß-Lg and 10mM $CaCl_2$, the M_w of CM was reduced and R_g increased, according to an observation under static and dynamic light scattering. The structural changes were mainly attributed to the release of α_{S2}- and κ-caseins as found under elevated concentration in solution. Similarly, it was also observed when a high concentration of calcium chloride was present, irrespective of the presence of ß-Lg. Two mechanisms were proposed to explain the phenomena: a) the increased ß-Lg concentration competed with CM for micellar calcium which mitigated the contact for casein. This led to a decrease on the M_w of CM due to dissociation of α_{S2}-

and κ-caseins. And b) the elevated calcium concentration induced new intermolecular interaction among different caseins suggesting the structural changes mainly occurred in the core of CM. On the other hand, the intermolecular interaction among CMs remained unaffected despite the release of κ-caseins.

Secondly, we determine if and how a process by which CMs could self-assemble into microparticles with addition of polysaccharide (HM-pectin as an example in this study) via film formation. In solution, spherical CMs were surrounded by HM-pectin. The mixture was not stable and could easily lose its integrity if surrounding conditions became unfriendly. However, by spreading the solution on a solid surface and subsequent film drying, casein microparticles were immobilized. Then, detail structure of the microparticles could be examined under confocal Raman microscopy. The images revealed the casein microparticle remained a soft matter like its predecessor CM but was vertically deformed into elliptical shape by the drying procedure. Physically, however, because of the elasticity or semi-rigidity of the microparticles, gaps were found in the film matrix between casein microparticles and rigid HM-pectin.

Ultimately, casein microparticles were isolated and released from the dried film matrix by means of enzymatic hydrolysis using pectinase. The enzyme was introduced onto the film to break down the matrix built with HM-pectin. The process released the casein microparticles into solution and collected for cleaning washes. The spherical casein microparticles thus obtained could remain stable for up to 3 weeks under cool storage at 4°C. They sized between 10 and 50 μm in diameter, which were similar to what were found in the films. The IR and Raman spectra indicated that the microparticle mainly consisted of caseins, with an increased amount of α_{S2}-casein over the native caseins. To carry a biological functionality, α-tocopherol was incorporated into casein microparticles by mixing them in a solution with constant stirring. The Raman images on the resulting matrix showed αT in the core as an emulsion droplet covered by a casein microparticle ‘shell’. The complex was much larger in size than the original casein microparticle. It was speculated that the casein microparticles traveled to the interface in the aqueous solution owing to their amphiphilicity. The deformability of the casein microparticles afforded the formation of a ‘core-shell’ like structure with αT. These phenomena offered a new approach for creating protein-based complexes carrying bio-functionalities.

Better understanding on the structure of CM would not only benefit the optimization of milk product processing but also the creation of novel functional foods using protein-based hydrocolloids. Naturally, it would not limit on heat- or pressure-sensitive bio-functional products either. In fact, besides energy conservation, casein microparticles might well help to meet a certain specific requirement in food processing, such as pH- and viscosity-control, as well as providing a means for product shelf-life monitoring through color change, for instance. Consequently, further research on parameters relating to the structural changes of CM in a scale-up processing environment would be of particular interest to the food and pharmaceutic industries.

7 Zusammenfassung

Die Casein-Mizelle (CM) ist eine gute Quelle für Hydrokolloide mit einzigartigen physikalisch-chemischen Funktionen. Es kann in verschiedenen technischen Anwendungen in der Lebensmittelindustrie gefunden werden. Seine Struktur wurde ausführlich untersucht, um das Verhalten von CM unter vielen Prozessbedingungen vorherzusagen. Einzelne Caseine, α_{S1}-, α_{S2}-, β- und κ-Casein, bauen sich mittels CCP zu Mizellen zusammen, wodurch eine stabile Struktur gegen Umweltstress, wie z. B. Temperatur, Druck oder Scherkraft, entsteht. Es ergeben sich interessante, neue Strukturen, wenn CM mit anderen Hydrokolloiden wie Proteinen oder Polysacchariden interagiert. Je nach vordefinierten pH-Wert im System, bilden sich daraus entweder assoziative Komplexe mit anderen Polymeren, oder segregative Komplexe. Die Bedingungen für die assoziative Komplex-Bildung von CM wurde bereits sehr ausführlich untersucht, wie z.B. Typ der Co-polymeren, pH-Wert und Polymer-Konzentration. Auf der anderen Seite wurde die segregative Wechselwirkung weniger untersucht, da ein Verlust durch Ausflockung oder Aggregation zu einem instabilen System führt.

Das Hauptziel dieser Arbeit ist es, die strukturellen Veränderungen von CM zu verstehen, die durch Wechselwirkung mit anderen Hydrokolloiden wie Protein oder Polysaccharid ausgelöst werden. Zunächst wurden die strukturellen Veränderungen von CM mit ß-Lg und salzhaltigen Salzen über SLS untersucht. Ziel ist es, die Wechselwirkung zwischen einzelnen CM mit dem Vorhandensein anderer natürlicher Milchkomponenten zu verstehen. Das Ergebnis zeigt, dass die ß-Lg Konzentration die kolloidale Stabilität von CM beeinflusst. Bei einer ß-Lg Konzentration von 0,5 wt% und 10 mM $CaCl_2$, zeigt CM eine Abnahme des Molekulargewichts und eine Zunahme des Drehungsradius, welche durch statische und dynamische Lichtstreuung gezeigt wird. Diese strukturellen Veränderungen sind hauptsächlich auf die Freisetzung von α_{S2} - und κ-Casein zurückzuführen, die mit einer erhöhten Konzentration in Lösung gefunden werden können. Eine ähnliche Beobachtung wird auch bei einer höheren Konzentration von Calciumchlorid beobachtet, unabhängig von der Anwesenheit von ß-Lg. Es werden zwei Mechanismen vorgeschlagen, um diese Phänomene zu erklären: a) Die erhöhte ß-Lg-Konzentration konkurrierte mit CM um mizellares Calcium, wodurch der Kontakt mit Casein gemindert wurde. Dies führte zu einer Abnahme

des M_w von CM aufgrund der Dissoziation von α_{S2}- und κ-Caseinen. Und b) die erhöhte Calciumkonzentration induzierte eine neue intermolekulare Wechselwirkung zwischen verschiedenen Caseinen, was darauf hindeutet, dass die strukturellen Veränderungen hauptsächlich im Kern von CM auftraten. Andererseits blieb die intermolekulare Wechselwirkung zwischen CMs trotz der Freisetzung von κ-Caseinen unberührt.

Zweitens bestimmen wir, ob und wie sich CMs durch Zugabe von Polysaccharid (HM-Pektin als Beispiel in dieser Studie) über die Filmbildung selbst zu Mikropartikeln zusammensetzen können. In HM-Pektin enthaltendem Lösungsmittel akkumuliert CM zuerst und bildet eine Runde Struktur. Diese Struktur ist nicht stabil und verliert leicht ihre Integrität, wenn sich die Reaktionsbedingungen ändern. Die Filmtrocknung wird deswegen durchgeführt, um neu gebildete CM-Mikropartikel zu stabilisieren, wodurch eine detaillierte Strukturanalyse ermöglicht wird. Ihre Struktur wurde durch konfokale Raman-Mikroskopie untersucht, um die innere Struktur der Mikropartikel im Film aufzudecken. Die Ergebnisse zeigen, dass durch die Trocknung die Casein-Mikropartikel vertikal in eine elliptische Form verformt werden, welche der Eigenschaften (als weiche Materie der) von CMs ähnelt. Die Elastizität der Mikropartikel führt zu einer Lücke zwischen den Mikropartikeln und der umgebenden starren HM-Pektin-Matrix im Film.

Letztendlich wurden Casein-Mikropartikel isoliert und aus der getrockneten Filmmatrix freigesetzt, was eine weitere strukturelle Charakterisierung und Zuordnung der biologischen Vorteile ermöglicht. In dieser Arbeit wurde die enzymatische Hydrolyse mit Hilfe von Pektinase durchführt, um die HM-Pektin enthaltene Filmmatrix abzubauen. Casein-Mikropartikel werden in Lösung freigesetzt und bleiben bei kühler Lagerung (4 °C) bis zu 3 Wochen stabil. Ihre Größe liegt im Bereich zwischen 10 bis 50 µm, was mit den nach mehreren Waschschritten untersuchten CMs im Film vergleichbar ist. IR- und Raman-Spektren zeigen, dass Mikropartikel hauptsächlich aus Caseinen bestehen. Interessanterweise wurde in den Mikropartikeln im Vergleich zur Zusammensetzung von nativen Caseinen eine erhöhte Menge an α_{S2}-Casein gefunden. Um die biologische Funktionalität herauszufinden, wurden Casein-Mikropartikel in einer gerührten Lösung mit α-Tocopherol gemischt. Raman-Bilder

zeigen, dass α-Tocopherol die innere Hülle des Casein-Mikropartikels auskleidet, was zu einem Emulsionströpfchen führt. Diese Tröpfchen sind im Vergleich zu den ursprünglichen Casein-Mikropartikel viel größer. Es wird vermutet, dass Casein-Mikropartikel aufgrund ihrer amphiphilen Eigenschaft an die Grenzoberfläche mit der wässrigen Lösung gelangen können. Die Verformbarkeit von Mikropartikeln führt beim Mischen mit α-Tocopherol zu einer "Kern-Schale" -artigen Struktur. Diese Methoden bieten einen neuen Weg für die Herstellung von auf Protein basierenden Mikropartikeln mit biofunktionellen Eigenschaften.

Die strukturelle Untersuchung von CM ist nicht nur relevant für die Optimierung der Milchprodukt-Herstellung, sondern auch für die Herstellung neuartiger funktioneller Lebensmittel unter Verwendung von Protein-basierten Hydrokolloiden. Natürlich würde es hitze- oder druckempfindliche biofunktionelle Produkte nicht einschränken. Neben der Energieeinsparung könnten Kasein-Mikropartikel durchaus dazu beitragen, eine bestimmte spezifische Anforderung in der Lebensmittelverfahren zu erfüllen, wie z. B. die Kontrolle des pH-Werts und der Viskosität, und beispielsweise ein Mittel zur Überwachung der Haltbarkeit von Produkten durch Farbwechsel bereitstellen. Dies wurde von besonderem Interesse für die Lebensmittel- und Pharmaindustrie sein, weiter die Auswirkungen unterschiedlicher Prozessparameter auf die strukturellen Veränderungen von CM in einem Scale-up Prozess aufzuklären.

8 Appendix

The following publications and presentations were generated in the period of this work. They are shown in chronological order.

8.1 Peer reviewed publications

Zhuang, Y., Sterr, J., Kulozik, U., & Gebhardt, R. (2015). Application of confocal Raman microscopy to investigate casein microparticles in blend casein/pectin films. *International Journal of Biological Macromolecules*, *74*, 44-48.

Zhuang, Y., Sterr, J., Schulte, A., Kulozik, U., & Gebhardt, R. (2016). Casein Microparticles from Blend Films Forming Casein/α-tocopherol Emulsion Droplets in Solution. *Food Biophysics*, *11*(4), 332-338.

Zhuang, Y., Ueda, I., Kulozik, U., & Gebhardt, R. (2018). Influence of β-lactoglobulin and calcium chloride on the molecular structure and interactions of casein micelles. *International Journal of Biological Macromolecules*, *107*, 560-566.

8.2 Non-peer reviewed publications

Zhuang, Y., Sterr, J., Kulozik, U., & Gebhardt, R. (2016a). Investigation of Casein Microparticles in Casein/Pectin Blend Film. In Gums and Stabilisers for the Food Industry 18: Hydrocolloid Functionality for Affordable and Sustainable Global Food Solutions (pp. 148-153). Cambridge: Royal Society of Chemistry.

Zhuang, Y., Sterr J., Schutle, A., Gebhardt, R. (2015): Isolation and characterization of casein microparticles as carrier for α-tocopherol; Jahresbericht zur Milchwissenschaftlichen Forschung am Zentralinstitut für Ernährungs- und Lebens-mittelforschung (ZIEL), ISBN: 978-3-939182-75-7, pp. 40-41

Zhuang, Y., Sterr J., Gebhardt, R. (2014): Investigation of casein microparticles in casein/pectin blend film; Jahresbericht zur Milchwissenschaftlichen Forschung am Zentralinstitut für Ernährungs- und Lebens-mittelforschung (ZIEL), ISBN: 978-3-939182-63-4, pp. 51-53

Zhuang, Y., Gebhardt, R. (2013): Effects of high-methyoxyl pectin on casein micelles; Jahresbericht zur Milchwissenschaftlichen Forschung am Zentralinstitut für Ernährungs- und Lebens-mittelforschung (ZIEL), ISBN: ISBN: 978-3-939182-52-8, pp. 49-51

8.3 Oral presentations

Zhuang, Y., Sterr, J., Kulozik, U., Gebhardt, R.: Casein microparticles as carriers for Vitamin E - a new approach for isolation and characterization., The 2nd Food Structure and Functionality Forum Symposium "From Molecules to Functionality" (FSFF), Singapore, March 2016

Zhuang, Y.: Casein microparticles as carriers for hydrophobic substances - new approach for preparation and characterization.,16th Food Colloids Conference: Structure beyond the colloidal scale, Wageningen, Netherlands, 10.-13. April 2016

Zhuang, Y., Sterr, J., Kulozik, U., Gebhardt, R.: Investigation of casein microparticle in blend casein/pectin films., 8th Gums and Stabilisers for Food Industry Conference, Wrexham, UK, June 2015

Zhuang, Y., Kulozik, U, Gebhardt, R: Effects of high-methoxyl pectin on assembly of casein micelles on films., 8th International Congress of Food Technologists, Biotechnologists and Nutritionists, Opatija / Croatia, October 2014

8.4 Poster presentations

Zhuang, Y., Sterr, J., Kulozik, U., Gebhardt, R.: Fabrication and characterization of casein microparticles in blend film., ICEF 12 - International Congress on Engineering and Food, Québec City, Canada, June 2015

Zhuang, Y., Sterr, J., Kulozik, U., Gebhardt, R.: Fabrication and characterization of casein microparticles for functional substance., 9th NIZO Dairy Conference, Papendal, Netherlands, October 2015

Zhuang, Y., Sterr, J, Kulozik, U, Yang C, Zhao, N, Bian, F, Tian, F, Gebhardt, R: Nano/mesoscale structures of protein-polysaccharide systems., Deutsche Tagung für Forschung mit Synchrotronstrahlung, Neutronen und Ionenstrahlen an Großgeräten 2014, Bonn, September 2014